HHS Public Access

Author manuscript

Coord Chem Rev. Author manuscript; available in PMC 2022 January 15.

Published in final edited form as:

Coord Chem Rev. 2021 January 15; 427: . doi:10.1016/j.ccr.2020.213560.

Supramolecular Fluorescent Sensors: An Historical Overview and Update

Chenxing Guo[a], **Adam C. Sedgwick**[a], **Takehiro Hirao**[b,*], **Jonathan L. Sessler**[a,*]

[a]Department of Chemistry, The University of Texas at Austin, 105 E. 24th Street, Stop A5300, Austin, Texas 78712, United States

[b]Department of Chemistry, Graduate School of Advanced Science and Engineering, Hiroshima University, 1-3-1 Kagamiyama, Higashi-Hiroshima 739-8526, Japan

Abstract

Since as early as 1867, molecular sensors have been recognized as being intelligent “devices” capable of addressing a variety of issues related to our environment and health (e.g., the detection of toxic pollutants or disease-related biomarkers). In this review, we focus on fluorescence-based sensors that incorporate supramolecular chemistry to achieve a desired sensing outcome. The goal is to provide an illustrative overview, rather than a comprehensive listing of all that has been done in the field. We will thus summarize early work devoted to the development of supramolecular fluorescent sensors and provide an update on recent advances in the area (mostly from 2018 onward). A particular emphasis will be placed on design strategies that may be exploited for analyte sensing and corresponding molecular platforms. Supramolecular approaches considered include, *inter alia*, binding-based sensing (BBS) and indicator displacement assays (IDAs). Because it has traditionally received less treatment, many of the illustrative examples chosen will involve anion sensing. Finally, this review will also include our perspectives on the future directions of the field.

Graphical Abstract

*Corresponding authors: Hirao, T. (thirao@hiroshima-u.ac.jp) and Sessler, J. L. (sessler@cm.utexas.edu).

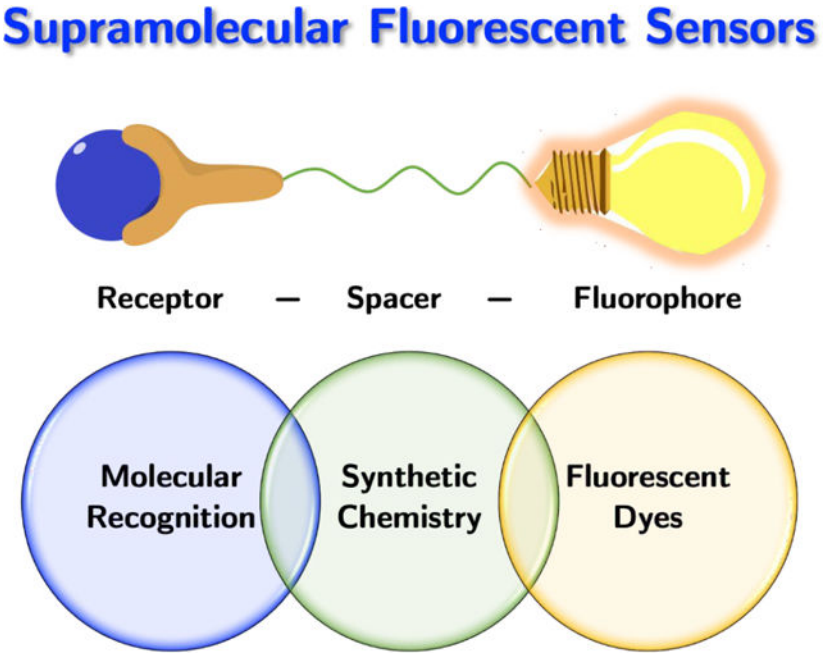

Keywords

Fluorescence; Supramolecular chemistry; Chemosensors; Binding-based sensing; Indicator displacement assays; Aggregation/Disaggregation-induced emission

1. Introduction

The crisis of COVID-19 underscores the importance, demand, and challenges in sensor development [1]. In a broad sense, sensors represent a class of “devices” that are capable of detecting specific chemical entities or monitoring changes to the surrounding environment by translating a certain chemical “event” (input) into a measurable “readout” (output). The significance of this area is underscored by the variety of sensors being applied across multiple facets of science, medicine, technology, and engineering. Among various sensing methods, fluorescence-based approaches are arguably among the most attractive due to their low cost, rapid response, excellent sensitivity, and high modularity [2]. For these reasons, chemists have explored and exploited various aspects of chemistry to develop a subset of fluorescence-based sensors called “chemosensors” (also known as chemical sensors, molecular sensors or optical sensors) [3,4].

Within the broad lexicon of chemosensors, fluorescent sensors that incorporate supramolecular chemistry to achieve sensing have begun to attract particular attention because of their ease of use and versatility. These so-called “supramolecular fluorescent sensors” are in general terms synthetic systems designed to bind to target analytes through non-covalent interactions (also known as supramolecular or host–guest interactions) so as to produce a discernible change in the emission profile of the incorporated fluorophores. The rise of supramolecular chemistry, particularly molecular recognition, has made the creation

of supramolecular fluorescent sensors possible. As we hope to make clear in this review, considerable progress has been made; however, much remains to be done.

The treatment in this review will be organized as follows: First, we will provide a brief introduction to the field of supramolecular fluorescent sensors. We will illustrate a number of core concepts by highlighting several pioneering studies carried out in the 1980s and 1990s. Next, we will review recent work on supramolecular fluorescent sensors for cationic, anionic, and neutral species, respectively. We will then conclude with a brief, yet hopefully informative, personal perspective on where we see the future of this field. It is to be noted that this review is by no means comprehensive. Rather, it is meant to be illustrative such that key design strategies can, we hope, be readily assimilated. The readers are encouraged to refer to other review papers related to this theme, including those referenced in the present review.

1.1 The Origins of Fluorescent Binding-Based Sensing (BBS)

The design of supramolecular fluorescent sensors requires knowledge of host–guest chemistry (molecular recognition), synthetic chemistry, and fluorescent dyes (e.g., fluorescent scaffolds and their corresponding photophysical properties) [5]. Typical supramolecular fluorescent sensors are created per the paradigmatic “fluorophore–spacer–receptor” design. As shown in Scheme 1a, the moiety capable of emitting light upon excitation is known as the fluorophore (or signaling unit), whereas the moiety capable of recognizing the target analyte(s) is called the receptor (or binding unit). In addition, a spacer (or linker) connecting the above two moieties is required to allow the fluorophore to produce detectable readouts in response to the analyte in question. A modification to this classic “fluorophore–spacer–receptor” design, shown in Scheme 1b, involves the use of a fluorophore that is itself a receptor. As a general rule, achieving selective interactions between a synthetic receptor and analyte requires a knowledge of the relevant binding affinities and specificities. Thus, most known supramolecular sensors are built on a foundation of host–guest chemistry. In this review, we adopt the term “binding-based sensing (BBS)” suggested by Chang et al. to refer to this sensing approach, which is distinguished from an emerging sensing approach termed “activity-based sensing (ABS)” in which the sensing primarily relies on irreversible chemical reactions [6,7]. Note: we do not intend to elaborate ABS since it is beyond the proposed scope of the present review. Nevertheless, some examples are highlighted in this review (cf. Sections 2.1–2.3). Also, our focus will be on fluorescent BBS, as opposed to ones where the signaling element relies on some other readout, such as a colorimetric or electrochemical response.

Depending on how the emission profiles of the fluorophores respond to the analytes, fluorescent sensors can be divided into three limiting classes, i.e., “turn-on”, “turn-off”, and ratiometric. As shown in Scheme 2, upon the addition of analytes, the fluorescence intensities of “turn-on” and “turn-off” sensors are enhanced or quenched, respectively. The current cannonical thinking in the field is that binding between the receptor and analyte and how that binding translates into changes in the fluorescence emission intensity of a fluorophore is what determines the performance of a given sensing system. From a mechanistic perspective, it is important to appreciate that the fluorescence “turn-on” and

"turn-off" features could reflect changes in the fluorescence quantum yields and lifetimes of the fluorophores in response to analytes [8]. Unfortunately, the requisite photophysical data has not been collected in the case of most fluorescent sensors reported to date. This stands in contrast to what is true for many synthetic dyes and light-emitting materials where measurements of fluorescence quantum yields and lifetimes, as well as other photophysical properties (e.g., Stokes shifts), are routine.

In general, "turn-on" sensors are preferred over "turn-off" sensors because the latter type of sensors may give false-positive results if the devices malfunction or the fluorophore is bleached; in addition, "turn-off" sensors are not usually suitable for cellular imaging where the background emission may be high. However, there are notable exceptions, such as the chloride-sensitive fluorescent "turn-off" probe, i.e., 6-methoxy-*N*-(3-sulfopropyl)quinolinium (SPQ), developed by Verkman in the late 1980s [9,10]. Ratiometric sensors differ from classic "turn-on" and "turn-off" sensors in that distinct changes in the intensities of two or more fluorescence emission bands in response to analytes are monitored. The resulting ratio allows for internal "ratiometric" referencing that increases the accuracy and reliability of quantitative analyses [11]. Hence, ratiometric sensors represent the state-of-the-art for many imaging applications.

In the 1980s, Tsien et al. reported pioneering efforts to develop binding-based fluorescent sensors that would allow for the selective detection of biologically relevant cations, including Ca^{2+} and Na^{+} [12–14]. This led to the synthesis of sensors **1**–**3** (Figure 1) wherein various fluorophores were linked to calcium-selective chelators, such as (aminophenoxy)ethane-*N,N,N',N'*-tetraacetic acid (BAPTA). These multi-component receptors proved capable of providing an appreciable "turn-on" or ratiometric fluorescent response for Ca^{2+} with decent selectivities for Ca^{2+} over Mg^{2+} in aqueous buffer solutions. A series of fluorescent sensors (e.g., **4**) for cytosolic sodium were also created by linking fluorophores and crown ethers [15]. The creation of these sensors by Tsien et al. not only laid the foundation for the field of supramolecular fluorescent sensors, but also set the stage for Tsien's later pioneering work on bioengineering the green fluorescent proteins (GFPs) [16]. Efforts along the latter lines eventually led him to be awarded the 2008 Nobel prize in chemistry jointly with Shimomura and Chalfie.

While Tsien's early work on calcium sensors conformed to the "fluorophore–spacer–receptor" paradigm, the generality of such designs was mainly codified in a series of pioneering studies conducted by de Silva and co-workers in the 1980s and 1990s. Specifically, this research team designed a series of fluorescent sensors for various cationic species. Among these sensors were the tertiary amine-appended anthracene **5** capable of acting as a pH indicator and the crown ether-appended anthracene **6** capable of sensing alkali metals [17,18]. These sensors were created on the basis of so-called "photoinduced electron transfer (PET)"; the "turn-on" response was ascribed to the fact that the binding of these analytes suppressed or blocked the intramolecular PET quenching that would otherwise occur as the result of the close proximity between the lone pair electrons of the receptors and the attached fluorophores [19].

Early on another pioneer in the field of chemosensing—Czarnik—developed a fluorescent "turn-on" sensor for Zn^{2+} ions **7** based on an anthracene-linked bis(tetramethylethylenediamine) (TMEDA), as shown in Figure 2c [20]. Although the authors ascribed the "turn-on" of fluorescence upon complexation of a Zn^{2+} center to a so-called "chelation-enhanced fluorescence (CHEF)" mechanism, the essence of the CHEF effect in this particular case was consistent with a PET process. In particular, interactions between the metal cations and the nitrogen atoms associated with the recognition event is expected to block the intramolecular PET that would otherwise quench the fluorescence of the anthracene subunit. In the event, the fluorescence of the anthracene reporter subunit is turned on in the presence of the Zn^{2+} cation [21].

To date, a number of supramolecular fluorescent sensors for cations have been developed [22], with many of these being presumed PET-based sensors (i.e., sensors that rely on the PET effect) [23–25]. Parallel efforts have also been devoted to developing binding-based sensors for anions. Not surprisingly, work along these latter lines has been motivated in part by the ubiquity and importance of anions (*vide infra*) [26].

In 1988, Lehn et al. reported an acridine-appended aza-crown ether **8** (Figure 3a) that acted not only as an anion receptor capable of recognizing adenosine triphosphate (ATP) but also as an artificial enzyme that promoted the hydrolysis of ATP in water [27]. In particular, these researchers found that the fluorescence of **8** was slightly enhanced upon the addition of ATP. It is worth noting that a prior report from the Lehn group had already revealed that the native aza-crown ether would effect the binding and hydrolysis of ATP [28]; the acridine subunit was introduced in an effort to improve the selectivity for ATP while enhancing the binding affinity via presumed **π**–**π** interactions between the acridine and adenine moieties (cf. Figure 3b). Although the authors did not elaborate the potential of receptor **8** as an anion sensor per se, this work nevertheless provided an early example of a formal fluorescent anion receptor.

A year after Lehn's report, Czarnik et al. detailed two tris(3-aminopropyl)amine-appended anthracene derivatives **9** and **10**. They found these two fluorogenic receptors were capable of producing a fluorescent "turn-on" response upon exposure to a variety of anions in water, including ATP, citrate, sulfate, acetate, and phosphate [29]. The authors ascribed the presumed CHEF effect seen in the case of phosphate sensing to the close proximity of the OH group on the phosphate to the free amine group close to the anthracene subunit. Notably, this seminal work served to underscore the potential of fluorescent anion sensors as possible analytical tools.

Since the pioneering studies of Lehn and Czarnik, increasing attention has been devoted to the development of supramolecular fluorescent anion sensors. This progress now spans almost three decades and is well-documented in the literature [30–36]. Nevertheless, anion sensing remains challenging and is generally appreciated as being more problematic than cation sensing in part due to the intrinsic difficulties associated with achieving anion recognition in water [37,38]. In fact, only a small number of anion sensors are known that operate successfully in pure water. Consistent with this notion is the fact that most of the anion sensors discussed in this review were studied in organic solvents or mixed aqueous

media containing some percentage of water, rather than in pure water (see Section 2.2 for more details).

Supramolecular fluorescent sensors for neutral species also have an appreciable history. Much of the early effort focused on carbohydrate sensing, an emphasis that reflects the importance of this class of metabolites in human physiology [39]. In the early 1990s, a number of pioneering studies on polyol sensing were reported in the literature. As a general rule, the underlying recognition event involved the formation of cyclic boronate esters via the reaction of boronic acids with diols. For instance, Yoon and Czarnik reported that 2-anthracene-boronic acid **11** could act as a "turn-off" sensor for polyols such as fructose. The authors ascribed the "turn-off" response to a chelation-enhanced quenching (CHEQ) process [40]. In separate work, James and Shinkai et al. reported a series of "turn-on" sensors for monosaccharides **12**–**14** (cf. Figure 5) [41–43].

In their initial reports, the "turn-on" response of the James–Shinkai sensors was ascribed to the formation of B–N dative bonds upon forming boronate esters, giving rise to the suppression of intramolecular PET quenching pathways. However, this postulated mechanism was later challenged by others; in the early 2000s, Wang and Franzen et al. conducted a series of experimental and computational studies, and proposed that an alternative pK_a switching mechanism accounts for the observed "turn-on" response [44,45]. In 2017, Anslyn and Larkin et al. performed further mechanistic study and ascribed the "turn-on" response to so-called "disaggregation-induced emission (DIE)" [46]. A more recent mechanistic study by Sun, James, and Anslyn led to the suggestion it is a so-called "loose bolt internal conversion" that underlies the "turn-on" response seen in this type of carbohydrate sensors [47]. The upshot of this debate is that a consensus agreement on the "correct" mechanism now appears to have been reached [48].

Boronate esters are noteworthy in that they constitute a well-studied class of dynamic covalent bonds [49]. Dynamic covalent bonds possess unique properties that lie at the nexus of covalent bonds and non-covalent bonds. They are particularly appealing to supramolecular chemists and have often been studied under the rubric of so-called "dynamic covalent chemistry" [50]. Because of the dynamic nature of the bonding interactions they support, sensors such as **11**–**14** discussed above can additionally be viewed as being binding-based sensors.

1.2 The Origins of Indicator Displacement Assays (IDAs)

Although the "fluorophore–spacer–receptor" paradigm for creating fluorescent sensors is appreciated being as a tried-and-true modality, functionalizing synthetic receptors with fluorophores requires additional synthetic effort and can pose preparative challenges. An elegant alternative strategy that circumvents this synthetic requirement, involves the use of so-called "indicator displacement assays (IDAs)" (*vide infra*).

Scheme 3a illustrates how a classic IDA-based sensor is created. The key feature of IDAs is that the paradigmatic spacers linking the receptor and fluorophore are replaced by supramolecular bonds that rely on non-covalent interactions (e.g., hydrogen bonding). This

substantially reduces the synthetic effort needed to create a functioning chemosensor since it allows appropriately chosen fluorophores to be introduced readily.

The term “indicator displacement assay” was introduced by Anslyn [51], and first elaborated in their 1998 seminal study on the fluorescent sensing for citrate based on a tripodal anion receptor-fluorophore complex **15·16** (cf. Figure 6a) [52]. Since then, tremendous efforts have been made by many groups, including that of Anslyn, to apply the IDA approach to the construction of sensor ensembles, as documented in a series of reviews [53–55]. It is notable that, four years prior to Anslyn’s seminal work on citrate sensing, Inouye et al. developed a host–guest complex **17·18** based on a calix[4]resorcinarene system that acted as a “turn-on” sensor for acetylcholine (cf. Figure 6b) [56]. However, due to the low acidity of phenol groups, Inouye’s IDA-based sensing system only operated under strongly basic conditions, which promoted the degradation of both the indicator and the acetylcholine. To address this issue, an improved sensing system was developed by Shinkai et al. in 1996, wherein the host was replaced by a calix[6]arene-*p*-sulfonate; this allowed the sensor to be functional under neutral conditions and precluded the undesired degradation [57]. In retrospect, these two sensing systems, both of which in essence relied on an IDA approach, antedated Anslyn’s seminal report in 1998. Nevertheless, Anslyn is recognized as being the one who codified and popularized the IDA concept, in part by making continuous contributions to this particular sub-field.

In fact, the base-promoted degradation issue mentioned above was noted in Inouye’s original work. In an attempt to solve this problem, Inouye and co-workers modified their sensing system by covalently attaching the fluorescent indicator to the upper rim of a calix[4]resorcinarene host. The resulting sensor, shown as **19** in Figure 7a, was found to give an acetylcholine-induced response under neutral condition.

Although the intramolecular sensor **19** shown in Figure 7a requires additional synthetic efforts to link the fluorophore and receptor together, this design differs in operational terms from the “fluorophore–spacer–receptor” design in that the attached fluorophore interacts with the receptor via non-covalent interactions. In contrast, the fluorophores of “fluorophore–spacer–receptor” sensors do not interact in a host–guest sense with the receptors to which they are bound.

The generalized design embodied in Inouye’s sensor **19** is shown in Scheme 3b. Analogous designs could be seen in even earlier work published in 1992 by Ueno et al. [58]. In spite of these precedents, it was not until recently that Anzenbacher, Kubo, and co-workers introduced the term “intramolecular indicator displacement assay (IIDA)” to refer to this type of design; this was done in the context of their seminal work on the fluorescent sensing of glyphosate using sensor **20** as shown schematically in Figure 7b [59]. More importantly, the authors underscored the advantages of sensors based on IIDAs over those based on IDAs, such as improved sensitivity and reversibility. These benefits are, however, balanced against the synthetic effort needed to create an IIDA-based sensor. Currently, the IIDA approach remains in its infancy in that only a few studies describing such sensors have appeared in the literature since the initial work by Anzenbacher et al. [60,61]. However, this

emerging sensing approach is ripe with promise; it is thus expected to receive continued attention in the years to come.

It is recognized that IDAs are generally not suitable for cellar imaging in that the released fluorescent indicators may diffuse to locales other than where the targeted analytes and sensor complexes originally interact [51]. Emerging IIDAs are likely free of this limitation in that the to-be-displaced fluorophores are covalently attached to the receptors. In fact, the imaging promise inherent in IIDAs has recently been demonstrated by Jolliffe and co-workers as discussed in Section 2.2 below.

2. Recent Advances in Supramolecular Fluorescent Sensors

2.1 Sensors for Cationic Species

In 2018, inspired by the design of conventional IDAs, Hof et al. developed a new sensing approach which they termed a “DimerDye disassembly assay (DDA)”. Initially, this research team applied the DDA approach to develop fluorescent “turn-on” sensors for trimethyllysine-bearing peptides viewed as being key post-translationally modified products [62]. On the basis of prior work from this same group [63], a water-soluble styryl merocyanine-appended calix[4]arene **21a** was created that proved capable of forming a self-assembled non-emissive homodimer, i.e., DimerDye (DD) (**21a**)$_2$ in water (cf. Figure 8a). The addition of strongly bound guests (e.g., trimethyllysine) was found to induce the disassembly of the DD (**21a**)$_2$; the resulting 1:1 **21a**–guest complexes, such as the **21a**–trimethyllysine complex, all proved fluorescent, which allowed for the real-time “turn-on” sensing of these types of analytes. Furthermore, the authors demonstrated that this sensing system was capable of sensing H3K4me3, i.e., the epigenetic modification product of the enzymatic methylation of H3K4 catalyzed by the methyltransferase PRDM9 (Figure 8b). Of particular note is that this DDA-based sensor proved tolerant of the various salts, metal ions, and co-factors involved in the enzymatic reaction. This allowed their sensing system to remain functional even in competitive biological milieus.

In 2019, Hof et al. reported a DDA-based sensing system for illicit drugs wherein a variety of fluorescent dyes were attached covalently to the calix[4]arene scaffold (Figure 9) [64]. The resulting library of DDs, consisting of **21a**–**21o**, was prepared via parallel synthesis whereby each fluorescent dye in question was reacted with the calix[4]arene precursor. The resulting crude products, containing a mixture of the starting materials, products, and side products, were directly subjected to initial high-throughput screening in 96-well plates without further purification. By using nicotine as the model analyte, all crude DD sensors exhibiting potential sensing capability (i.e., **21a**, **21d**, **21h**, **21l**, and **21m**) were resynthesized, purified, and analyzed individually. Among these lead sensors, DD **21h** was found to show the highest sensitivity toward nicotine, wherein the limits of detection (LODs) in water and saliva were determined to be 3.4 μM and 18.6 μM, respectively. Furthermore, inspired by the pioneering work of Anslyn et al., involving the creation of so-called “sensor arrays” [65], the authors combined multiple DDs into sensor arrays that proved capable of discriminating between drugs (e.g., opioids) and structurally analogous metabolites. The authors also envisioned that the parallel sensing approach described in their study could be exploited to create DD-based sensors suitable for the analysis of other classes of analytes.

Given the limitation of IDAs in cellular imaging (cf. Section 1.2) and the merits of DDA discussed by the authors, we also envision DDA systems emerging as new tools useful in a range of imaging applications.

In recent years, supramolecular polymers and so-called supramolecular organic frameworks (SOFs), particularly those based on macrocycles, have emerged as novel functional materials with a variety of applications [66–68]. Pillar[*n*]arenes are a class of macrocyclic hosts that have received considerable attention in the context of SOFs (as well as a variety of other areas) owing to their unique properties [69–71]. Recently, Lin, Liu, and Wei et al. reported the construction of a stimuli-responsive pillar[5]arene-based SOF capable of sensing and separating various species including metal cations, anions, and amino acids [72]. Specifically, as shown in Figure 10, the pillar[5]arene-based two-dimensional sheet-like SOF $(\mathbf{22}\cdot\mathbf{23})_n$ was constructed via the self-assembly of **22** and **23** driven by hydrogen bonding interactions between a pair of self-complementary thioacetylhydrazine moieties in **23** and CH–π interactions between the pillar[5]arene cavity of **22** and the alkyl chain of **23**. SOF $(\mathbf{22}\cdot\mathbf{23})_n$ was found to form a self-supported gel in cyclohexanol that could act as a fluorescent "turn-off" sensor for metal ions such as Hg^{2+}, Cr^{3+}, Cu^{2+}, and Fe^{3+}. In addition, the volatiles could be removed from $(\mathbf{22}\cdot\mathbf{23})_n$ to form a xerogel that allowed for the near-quantitative separation of these metal ions from water. This same set of test cations (Hg^{2+}, Cr^{3+}, Cu^{2+}, and Fe^{3+}) was used to prepare metal-ion-incorporated SOFs (MSOFs). The MOSF-Fe and MSOF-Hg were found to act as fluorescent "turn-on" sensors selective for F^- and Br^- in water with LODs of 69 nM and 48 nM, respectively. The addition of L-Cys also served to enhance selectively the emission intensities of MOSF-Fe and MSOF-Cu, for which the L-Cys LODs were determined to be 61 nM and 54 nM, respectively. In contrast, no change in the emission intensity was seen upon treating MSOF-Fe or MSOF-Hg with other competing amino acids. Finally, as depicted in Figure 10, these SOFs not only allowed for selective detection and efficient separation of multiple guests, they also could be readily recycled upon proper treatment.

It is recognized that certain fluorescent molecules are capable of emitting light strongly upon the formation of aggregates in concentrated solutions while showing negligible emission intensity in dilute solutions. This phenomenon is widely known as "aggregation-induced emission (AIE)", while fluorophores showing AIE features are referred to as AIEgens [73–76]. The concept of AIE was first introduced by Tang et al. in 2001 [77] and led to a paradigm shift in photoluminescence. Prior to Tang's seminal report it was widely accepted that most available fluorophores were planar and rigid (e.g., pyrene), and thus prone to so-called "aggregation-caused quenching (ACQ)", wherein the fluorescence is quenched in the aggregated state (i.e., highly concentrated solutions or solid state). In contrast, AIEgens are non-planar and conformationally flexible molecules; the non-radiative decay processes that would normally serve to deactivate the excited states of these unconventional fluorophores is largely suppressed by the restriction of intramolecular motion (RIM) in the aggregated state, leading to a turn-on in the fluorescence [78]. Since 2001, the field of AIE has seen explosive growth, with a number of AIE-based sensing and imaging agents now known [79,80].

Among the AIEgens reported to date, tetraphenylethylene (TPE) and its derivatives have received particular attention owing to their high modularity [81,82]. Recently, Yang et al.

fabricated a stimuli-responsive fluorescent supramolecular polymer that allowed for the selective detection and rapid removal of Hg^{2+} [83]. Their system consists of an AABB-type supramolecular polymer $(\mathbf{24}\cdot\mathbf{25})_n$ prepared via the self-assembly of thymine-appended [2]biphenyl-extended pillar[6]arene **24** and TPE-bridged bis(ammonium) **25** driven by presumed cation–**π** interactions (cf. Figure 11). As prepared, polymer $(\mathbf{24}\cdot\mathbf{25})_n$ proved weakly fluorescent in a mixed solvent system, i.e., $CHCl_3$/acetone/H_2O (v/v/v = 1:4:495). Once an aqueous solution of $HgCl_2$ was added to the solution containing $(\mathbf{24}\cdot\mathbf{25})_n$, spherical aggregates, stabilized by presumed thymine–Hg–thymine (T–Hg^{2+}–T) bonds [84], were formed. The fluorescence of the resulting Hg^{2+}-incorporated supramolecular polymer was significantly enhanced. As such, $(\mathbf{24}\cdot\mathbf{25})_n$ was found capable of acting as a fluorescent sensor selective for Hg^{2+} with a LOD of 0.3 μM. Moreover, the addition of Na_2S to the Hg^{2+}-incorporated supramolecular polymer resulted in the formation of HgS as a black precipitate, allowing the initial supramolecular polymer $(\mathbf{24}\cdot\mathbf{25})_n$ to be regenerated.

In 2019, Shao et al. reported the synthesis of chalcogen- and phosphorus(V)-doped sumanenes **26**–**28** and their optical response toward Ag^+ ion (Figure 12) [85]. In particular, a dichloromethane solution containing sumanene **26** was found to produce a “turn-on” response upon coordination with Ag^+ in a 2:1 (ligand/metal) fashion. The fluorescence emission of the solution changed from blue to green as the wavelength of the maximum emission peak (λ_{max}) varied from 470 nm to 510 nm. On the other hand, little change in the emission intensity or profile was seen in the presence of various other metal cations, including Co^{2+}, Ni^{2+}, Cu^{2+}, Zn^{2+}, Fe^{3+}, Cr^{3+}, Pb^{2+}, Hg^{2+}, Mn^{2+}, and Pd^{2+}. Since fluorescent sensors for Ag^+ are generally prone to interference from other competing metal ions, the remarkable selectivity toward Ag^+ allowed **26** to act as a novel sumanene-based ratiometric sensor for Ag^+. Notably, the LOD of **26** for Ag^+ was determined to be 0.21 μM, which surpasses the LOD for Ag^+ in drinking water (i.e., 0.5 μM) established by World Health Organization (WHO).

2.2 Sensors for Anionic Species

Silsesquioxanes (SQs) represent a class of organosilicon compounds that can act as building blocks for inorganic–organic hybrid materials containing a variety of peripheral groups. Among the SQs currently known, the so-called “T_8 cages”, cubic oligosilsesquioxanes possessing eight silicon vertices, have received particular attention in a variety of contexts [86,87]. In 2003, a seminal study by Bassindale et al. revealed that T_8 cages are capable of encapsulating fluoride within their central cavities [88]. Recently, Ervithayasuporn et al. successively developed two fluorescent anion sensors, i.e., **29** and **30** (cf. Figure 13), wherein pyrene and anthracene were attached as fluorophores onto T_8 cages, respectively [89,90]. In the first of two reports, they noted that **29** could act as a fluorescent “turn-on” sensor selective for fluoride [as its tetrabutylammonium (TBA^+) salt] in DMSO with a low LOD of 1.61 ppb [89]. The second report from this team consisted of a more comprehensive investigation regarding the sensing ability of **30** [90]. In contrast to what was seen in the case of **29**, sensor **30** produced a distinct fluorescent response upon the addition of various anions such as F^-, OH^-, CN^-, and PO_4^{3-} in a highly solvent-dependent manner. These features not only permitted the discrimination of the anions in question using a principal component analysis (PCA), but also allowed the authors to develop a workflow whereby an

unknown anion could be identified on the basis of the anion-responsive behavior in different solvents. In both studies, the authors ascribed the changes in fluorescence emission to the fluoride-induced geometrical reorganization of the T_8 cage that changed the ratio between the intensity of the monomer emission and that of excimer emission. The polarities of the solvents also played a critical role in affecting the overall fluorescent response to anionic salts.

It is worth noting that **29** and **30** were found to be the most abundant species among all possible congeneric products of the Heck coupling reaction based on the mass spectrometric analyses of the product mixtures. While not highlighted by the authors, compounds **29** and **30** as depicted in Figure 13 represent "Janus-type" silsesquioxane cages since the four fluorophore pendant groups are all located in the same face of the T_8 cage [91,92]. It should be noted, however, that the preparation of "Janus-type" silsesquioxane cages typically relies on the cross-coupling of "half-cubes". However, the reaction scheme shown in Figure 13 should not favor the formation of specific "Janus-type" silsesquioxane cages. Rather it is expected to afford a mixture of all tetrasubstituted products along with other multisubstituted products. Therefore, the chemical structures of **29** and **30** shown in Figure 13 may not represent fully the products the authors actually obtained. Corresponding caveats associated with the use of likely mixtures of compounds to perform the reported sensing studies should thus be noted. Nevertheless, these two studies demonstrated how T_8 cages could provide a novel hybrid platform that permits anion sensing. As such, this work is expected to sow the seeds for future research.

Over the past decade, the Nitschke group has developed so-called "subcomponent self-assembly" that has allowed many complex self-assembled supramolecular architectures to be created readily from simple precursors. These elegant systems have seen use in a variety of applications ranging from guest binding and release to catalysis, extraction, and sensing, among others [93,94]. In 2019, Nitschke et al. reported the creation of a subcomponent self-assembled cationic cage **31** that could function as a fluorescent sensor capable of detecting selectively biologically relevant anionic guests in water [95]. As shown in Figure 14, the cationic cage **31** was prepared by mixing its three constituent subcomponents, i.e., Zn^{2+}, tris(2-aminoethyl)amine (TREN), and fluorescent triazatriangulenium ($TATA^+$). Cage **31** proved water-soluble in the form of its sulfate salt (**31**–SO_4) and appreciably fluorescent. Initial ^1H NMR spectroscopic studies carried out in D_2O revealed that cage **31**–SO_4 was capable of encapsulating 2-naphthyl phosphate along with a wide range of anionic nucleotides, including UMP, AMP, GMP, ATP, and NAD^+ (all as their sodium salts) with binding constants ranging from $10^{2.7}$ to 10^3 M^{-1}. On the other hand, little appreciable interaction was seen between **31**–SO_4 and various neutral guests, such as nucleosides, representative polyaromatic hydrocarbons and fullerenes (cf. Figure 14). The binding selectivity for the former set of analytes was ascribed in part to the electrostatic interactions between the cationic cage and the anionic guests. Notably, the authors found that treating **31**–SO_4 with Na_2AMP led to considerable quenching of the fluorescence such that **31**–SO_4 could act as a "turn-off" sensor selective for Na_2AMP in water. This work highlights how suitably designed self-assembled molecular containers may be exploited as anion sensors.

In recent years, Sessler and co-workers have developed a series of non-cyclic formylated dipyrromethanes [96,97]. Several of these oligopyrrolic anion receptors display high binding affinities (typically $>10^6$ M^{-1}) for dihydrogen phosphate ($H_2PO_4^-$) and high selectivities over other anions in organic media. In 2018, Sessler and co-workers reported a pyrene-linked formylated bis(dipyrromethane) **32** that was prepared in an effort to create a fluorescent probe that was selective for $H_2PO_4^-$ [98]. The authors found that the fluorescence of **32** was quenched or turned off upon treatment with dihydrogen phosphate (as its TBA^+ salt) in chloroform, presumably via a PET quenching mechanism. This feature allowed **32** to act as a "turn-off" sensor for $H_2PO_4^-$ with the LOD proving to be 46 nM in this solvent system. Other oxyanions (as their TBA^+ salts), such as pyrophosphate ($HP_2O_7^{3-}$), acetate ($CH_3CO_2^-$), and hydrogen sulfate (HSO_4^-), were also seen to quench the fluorescence of probe **32**; however, the associated binding affinities revealed interactions that were reduced as compared to that between **32** and $H_2PO_4^-$. Interestingly, the fluorescence of **32** was turned on upon exposure to the benzoate anion ($PhCO_2^-$), a finding ascribed to the putative interactions between the phenyl group of the $TBAPhCO_2$ analyte and the pyrene subunit of **32** in the excited state. Further evidence that **32** could interact with $H_2PO_4^-$ came from a single crystal X-ray diffraction analysis of a formal 1:3 host–guest complex, i.e., $[\mathbf{32}\cdot 3H_2PO_4^-]_2$, wherein one of the three $H_2PO_4^-$ molecules was found directly bound to the receptor via hydrogen bonding (cf. Figure 15b).

Over the past several years, Kataev and co-workers have reported several fluorescent sensors capable of recognizing anions in buffered aqueous solutions containing various quantities of organic solvents (e.g., DMSO) [99–105]. Presumably encouraged by the versatility of azacryptand-based anion receptors [106], this research team created two novel anthracene-functionalized azacryptands **33** and **34** and tested their respective fluorescent response upon treating with various anions (as their sodium salts) in buffered aqueous solutions (cf. Figure 16) [101]. It was found that the changes in the fluorescent response induced by the anionic guests were not always correlated with the corresponding binding constants. For instance, even though the greatest fluorescent enhancement was seen when sensor **33** was treated with sodium nitrate, the associated binding constant proved only modest (log $K = 3.25$) and much lower than that for the interaction between **33** and the oxalate anion (log $K = 6.52$). In the case of sensor **34**, the greatest fluorescence enhancement was seen with the fluoride anion. On the basis of their results, the authors concluded that **33** and **34** could act as fluorescent "turn-on" sensors for the nitrate and fluoride anions, respectively, in buffered aqueous media.

More recently, Kataev et al. reported the creation of sensor **35** shown in Figure 17. This species displayed good selectivity for inorganic phosphate (as a presumed mixture of $H_2PO_4^-$ and HPO_4^{2-}) over other mono- and dianions in aqueous buffer solution at pH = 7.2 (all anions were studied as their sodium salts) [104]. Although sensor **35** was presumed to encapsulate only one $H_2PO_4^-$ anion in its cavity, it was found that the fluorescence intensity of **35** was at first quenched slightly but then significantly enhanced upon adding incremental quantities of NaH_2PO_4. Such behavior, in conjunction with a Job's plot analysis, led the authors to propose that the binding stoichiometry between **35** and NaH_2PO_4 was 1:2 instead of 1:1. Fitting the binding isotherm using a 1:2 binding profile allowed the stepwise binding

constants K_{11} and K_{12} to be determined as 4.5×10^3 M^{-1} and 1.5×10^2 M^{-1}, respectively. In addition, the authors found that sensor **35** provided a "turn-on" response upon treatment with oxalate, fumarate, maleate, and malonate. Thus, **35** could also be used as a sensor for these carboxylate dianions.

Bisantrene is a promising anticancer drug candidate originally developed in an effort to reduce the cardiotoxicity associated with commonly used anthracycline-based chemotherapeutic agents (e.g., doxorubicin) [107]. Recently, Anzenbacher et al. repurposed bisantrene dihydrobromide **36** as a fluorescent "turn-on" sensor capable of detecting ATP in DMSO-containing aqueous media [108]. As illustrated in Figure 18, they hypothesized that electrostatic and hydrogen bonding interactions between the two 4,5-dihydroimidazolium moieties present in **36** and the triphosphate moiety of ATP, in conjunction with presumed **π**–**π** interactions between the anthracene subunit of **36** and the adenosine moiety of ATP, would enhance the binding selectivity of **36** toward ATP. Indeed, sensor **36** was found to produce a significant CHEF effect upon exposure to ATP (30 equivalents) in Tris buffer (10 mM):DMSO (90:10) at pH 7; in contrast, sensor **36** produced a significantly smaller or negligible "turn-on" response upon treatment with other phosphorylated molecules, including AMP, ADP, GTP, CTP, and UTP under otherwise identical conditions. This was also true for a range of simple anions, such as F^-, Cl^-, AcO^-, $PhCO_2^-$, $H_2PO_4^-$, and $HP_2O_7^{3-}$ (as their TBA^+ salts). On the other hand, the latter simple anions could induce a CHEQ effect in acetonitrile, presumably as the result of some combination of binding and anion-induced deprotonation effects.

The advantages of AIE have also encouraged the creation of fluorescent "turn-on" anion sensors where anion binding is used to restrict the non-radiative decay associated with constituent AIE-active fluorophores [109]. A seminal contribution to AIEgen-containing anion sensors came from Wu et al. wherein a tetrakis(bisurea)-appended TPE ligand was prepared and found to produce a significant fluorescence enhancement upon exposure to various anions (as their TBA^+ salts) in DMSO [110]. This system, shown in Figure 19a, proved particularly effective for oxyanions (e.g., PO_4^{3-} and SO_4^{2-}). To draw analogy to AIE, the authors suggested that such approach could be referred to as "anion-coordination-induced emission (ACIE)".

In 2019, inspired by Wu's seminal work, Zheng et al. reported the use of a TPE-linked dimethylformamidine hydrochloride salt **37a** (Figure 19b) to realize the fluorescent "turn-on" sensing of Na_3PO_4 in water [111]. The authors first demonstrated that **37a** was soluble in water but not soluble in nonpolar solvents, such as hexanes. In fact, salt **37a** only produced a negligible fluorescence emission when dissolved in water. In contrast, upon deprotonation of **37a**, the resulting neutral species **37b** was no longer soluble in water and thus became strongly fluorescent, presumably due to the formation of aggregates in water. Although the authors originally postulated that electrostatic interactions between the cationic species **37a** and various anions in water would give rise to decrease in the solubility of **37a**, only the phosphate anion (PO_4^{3-}) proved capable of inducing significant "turn-on" in the fluorescence of the system. Other anionic guests tested did not enhance the fluorescence or even led to fluorescence quenching in the case of NaH_2PO_4. In addition, the authors noticed that several common transition metal ions, including Zn^{2+}, Cu^{2+}, Fe^{2+}, Pb^{2+}, and Hg^{2+}, all

quenched the fluorescence of the system, presumably owing to CHEQ effects. Despite apparently relying on a deprotonation mechanism, rather than anion binding per se, this TPE-based sensing system still highlights how AIEgens could be used to create easy-to-prepare “turn-on” anion sensors, particular ones where differences in the basicity of target anions are exploited to produce a discernable fluorescent response.

Dicarboxylic acids and their conjugated bases, i.e., dicarboxylic anions, are vital metabolites involved in various metabolic pathways, such as the citric acid cycle [112]. Not surprisingly, a number of hosts and sensors capable of binding and sensing dicarboxylic acids and the corresponding anions have been reported to date [113]. Nevertheless, it remains a challenge to discriminate between structurally analogous dicarboxylic acids, such as members of a homologous series. In 2018, Miljanić and co-workers repurposed **38** (Figure 20a), a trigonal fluorinated trispyrazole first developed in the context porous materials [114], as a fluorescent sensor for dicarboxylic acids [115]. Specifically, the fluorescence of sensor **38** was selectively turned on upon treatment with dicarboxylic acids such as **39a**, **39e**, **39g**, and **39h**, whereas a negligible change or even a decrease in emission intensity was seen upon the addition of all other dicarboxylic acids making up the test series (i.e., **39b**, **39c**, **39f**, and **39i**); this also proved true in the case of the control monocarboxylic acids (i.e., **39d**, **39j**–**39m**). These observations in conjunction with other mechanistic studies led the authors to suggest that the fluorescence “turn-on” of **38** was due to the formation of a dimer bridged by three dicarboxylate anions (cf. Figure 20c). The associated RIM was then thought to give rise to a fluorescent enhancement.

The use of RIM as a means of creating fluorescent “turn-on” sensors was also showcased in a recent study by Yokoyama and co-workers [116]. These authors postulated that the bis(cyanostyryl)pyrrole compound **40**, a conformationally flexible molecule previously investigated by their team [117], would show fluorescence enhancement upon exposure to anions since strongly bound anions would lock the rotation of the single bonds (cf. Figure 21) thereby suppressing non-radiative decay pathways. Consistent with this design expectation, the addition of 1000 equivalents of TBACl to a CH_2Cl_2 solution containing receptor **40** led to a 60% increase in the quantum yield from a baseline of 19%. The addition of other anions (1000 equivalents), such as $TBANO_3$, $TBABF_4$, $TBAClO_4$, and $TBAPF_6$, was also found to enhance the fluorescence of **40**, whereas the addition of TBABr and TBAI led to quenching. Control experiments with configurational isomers revealed no appreciable changes in fluorescence when **41a** was treated with the test anions in question, and a less significant change in the fluorescence of **41b** as compared to **40**. This work thus highlights the role RIM can play in creating anion-responsive fluorescence-tunable receptors and thus bears on efforts to create “turn-on” anion sensors based on other **π**–conjugated acyclic oligopyrroles and anion-responsive foldamers [118,119].

In general, ACQ is not a desirable feature for fluorescent sensors since it can limit their utility at higher concentrations. However, if one were able to design sensors bearing one or more ACQ-active fluorophores, and the analytes of interest could break up the aggregates formed in the solution, it might allow for the creation of fluorescent “turn-on” sensor by overcoming the effects of ACQ [120]. This strategy, where the reverse process of “undesirable” aggregation is leveraged, is often referred to as “disaggregation-induced

emission (DIE)". An early example of a DIE-based anion sensor came from Sessler et al., wherein the addition of phosphate anions (as the sodium salts) in buffered aqueous solution was used to promote the disaggregation of a series of water-soluble sapphyrins (such as the one shown in Figure 22a), thus providing a potential "turn-on" fluorescence response [121].

Recently, Yoon et al. applied the DIE strategy to develop an ATP sensor based on **42-Zn^{2+}** (Figure 22b) [122]. This complex proved highly emissive in pure DMSO but completely non-emissive in aqueous media, presumably due to ACQ in combination with PET. In the presence of ATP, a significant enhancement in the emission intensity at 485 nm was seen that was ascribed to the formation of a 2:1 host–guest complex. As shown schematically in Figure 22c, electrostatic interactions between the Zn^{2+} cation and ATP serve to break up the aggregates of **42-Zn^{2+}** that would normally be formed in water, thus giving rise to an appreciable "turn-on" in the fluorescence emission intensity. Sensor **42-Zn^{2+}** exhibited decent selectivity for ATP over other test anions with only pyrophosphate ($HP_2O_7^{3-}$ / $P_2O_7^{4-}$; PPi) being found to act as modest interferant. Of note is that sensor **42-Zn^{2+}** could be used to effect the fluorescent imaging of cellular ATP in melanoma cells.

In 2019, Gong, Sessler, and co-workers proposed a novel anion sensing approach based on so-called "excimer-disaggregation-induced emission (EDIE)" [123]. As shown in Figure 23, they prepared a hybrid macrocycle **43** bearing electron-rich pyridine moieties and electron-deficient imidazolium moieties. The emission intensity of **43** proved concentration-dependent, wherein 0.02 mM of **43** in acetonitrile showed the highest emission intensity; either decreasing or increasing the concentration of **43** led to an overall decrease in emission intensity. Under this condition, no appreciable aggregation of **43** was seen in the ground state, leading the authors to suggest it was the formation of a non-emissive excimer that led to such behavior. Upon treatment with oxyanions, such as $H_2PO_4^{3-}$and $HP_2O_7^{3-}$ (as their TBA^+ salts), considerable fluorescence enhancement was seen (up to ca. 200-fold in the case of $(TBA)_3HP_2O_7$). Other salts, including $TEAHCO_3$ (tetraethylammonium (TEA^+) bicarbonate) and $TBAHSO_4$, also induced only a slight increase in the fluorescence emission intensity. On this basis, it was proposed that **43** could act as a "turn-on" sensor selective for the above two inorganic phosphates. An elaborate monomer–dimeric excimer equilibrium model was provided in support of the proposed mechanism of EDIE. This work highlights the potential of exploiting mechanisms that break up excited-state aggregates as means to creating "turn-on" sensors.

Calix[4]pyrroles (C4Ps) and their derivatives represent a class of recognized macrocyclic oligopyrrolic receptors capable of binding anions and ion pairs [124–128]. Since the initial efforts made by Sessler et al. to create colorimetric and fluorescent C4P-based anion sensors [129,130], important progress has been made in terms of using this class of receptor to create sensing systems [131–133]. The contributions from the Anzenbacher group are particularly noteworthy. For instance, in a recent study summarized in Figure 24, Anzenbacher et al. attached fluorophores **a**–**c** onto the β-pyrrolic positions of octamethylcalix[4]pyrrole **44** and calix[2]benzo[4]pyrrole **45**, i.e., a so-called "expanded calix[4]pyrrole" [134]. The five fluorescent anion sensors in question, i.e., **44a**–**44c**, **45a**, and **45b**, were all found to give rise to fluorescent "turn-off" responses characterized by bathochromic shifts in the emission bands upon exposure to various anions (as their TBA^+

salts), including inorganic small anions (e.g., halides) and organic anions (e.g., non-steroidal anti-inflammatory drugs) in CH_3CN. Presumably, this response reflects anion-binding-induced changes in the intramolecular charge transfer interactions between the pyrrole moiety and the electron-deficient fluorophore used to create each sensor. Although sensors **45a** and **45b** based on expanded C4Ps with larger cavities were expected to display relatively enhanced selectivities for large anions over small anions compared to their C4P-based congeners **44a**–**44c**, to the surprise of these researchers, sensors **45a** and **45b** displayed higher binding selectivities for small anions over large anions as inferred from fluorescent spectroscopic titrations.

Once the basic features of these five sensors were understood, a sensor array was fabricated. As shown in Figure 24b, this array allowed 18 anionic analytes to be identified qualitatively with 100% correct classification accuracy by means of linear discrimination analysis (LDA). The authors also showed that this sensor array could be used to effect quantitative analyses for several dicarboxylate dianions, including the oxalate, malonate, glutamate, aspartate, and phthalate dianions.

So-called “vibration-induced emission (VIE)” is an emerging photophysical phenomenon proposed by Tian et al. in 2015 to account for the dual emission features and large Stokes shifts associated with a series of phenazine-derived fluorophores [135]. Since their seminal report, a number of luminescence-tunable systems relying on VIE have been developed [136,137]. For instance, inspired by a previous mechanistic study [138], Sessler and Tian et al. designed the VIE-active fluorescent anion sensor **46** (Figure 24) [139]. Here, the goal was to develop a sensing system comprised of a single fluorophore that was nevertheless capable of differentiating structurally analogous dicarboxylate dianions ($\mathbf{DC}^{2-}$). Sensor **46** was prepared by appending two C4P subunits onto a recognized VIE-active fluorophore, i.e., 9,14-diphenyl-9,14-dihydrodibenzo[*a*,*c*]phenazine (DPAC). The authors hypothesized that the fluorescent emission of sensor **46** would be tuned upon the addition of a homologous series of $\mathbf{DC}^{2-}$ guests in a length-dependent manner (cf. Figure 25b). Indeed, as shown in Figure 25c, they found that sensor **46** produced a unique fluorescent signature for each aliphatic $\mathbf{DC}^{2-}$ guest (as its TBA^+ salts) in acetonitrile with the λ_{max} increasing as a function of the chain length. The changes in emission color upon exposure to each dianion could be monitored both quantitatively and qualitatively (cf. Figure 25c,d). Sensor **46** could also be used to distinguish between the three regioisomeric phthalate dianion isomers. The authors thus suggested that fluorescent sensor **46** could be regarded as a “molecular caliper” capable of discriminating various $\mathbf{DC}^{2-}$ guests by translating their lengths and geometries into distinct fluorescent readouts. This work underscores the potential use of VIE-active fluorophores to create novel fluorescent sensors that allow for structure-based discrimination.

Bicarbonate (HCO_3^-), a hydrated anionic form of CO_2, is a vital catabolite that plays a critical role in maintaining the acid–base homeostasis and regulating blood pH [140]. In 2017, Sessler, Kim, and Lee et al. applied the IDA approach to create a “turn-on” sensor for bicarbonate (HCO_3^-) in an effort to address the need for bicarbonate sensing [141]. As shown in Figure 26, a sensor complex **47**·**48** was developed, wherein a *meso*-bis(benzimidazolium) C4P **47** and a coumarin derivative **48** served as the receptor and

fluorescent indicator, respectively. Upon the addition of HCO_3^- (as its TEA^+ salt) to an acetonitrile solution containing the sensor complex **47**·**48**, an appreciable increase in fluorescence intensity was seen as the result of the fluorescent dye **48** bound to **47** being replaced by HCO_3^-. The LOD for $TEAHCO_3$ was determined to be 4 nM in this organic solvent. In addition, the sensor complex showed high binding selectivities for $TEAHCO_3$ over other anionic guests, such as Cl^-, $H_2P_2O_7^{3-}$, $H_2PO_4^-$, SO_4^{2-}, and NO_3^- (as their TBA^+ salts). Notably, the authors also discovered that **47** could act as a catalyst to transform the bicarbonate salt to otherwise unstable alkyl carbonate esters, rendering it capable of not only sensing but also trapping bicarbonate anions.

The rapid determination of enantiomeric excess (ee) is of demand particularly in the pharmaceutical industry owing to the lessons we have learned from the thalidomide tragedy [142] and the need to market in many instances only a single enantiomer. In this context, supramolecular fluorescent sensors could also act as molecular tools capable of determining the ee of chiral mixtures and thus performing so-called “chirality sensing” [143,144]. In particular, Anslyn et al. pioneered so-called “enantioselective indicator displacement assay (eIDA)”, wherein the typical IDA strategy is applied to the creation of chirality sensors [145]. Recently, Anzenbacher et al. developed an eIDA-based fluorescent chirality sensing system for a series of chiral carboxylates (CCs) that functions in a mixed solvent system (CH_3CN:H_2O = 7:3, v/v) containing the MES buffer (50 mM) [146]. As shown in Figure 27a, the system consisted of a chiral sensor complex **49**·**50**, wherein the fluorescent indicator **50** acts as an apical ligand and is bound to the chiral Cu^{2+} complex **49**. The chiral sensor complex **49**·**50** was found to be weakly fluorescent, which was ascribed to the PET quenching of **50** by the Cu^{2+} ion. Upon the addition of the CCs in question (cf. Figure 27b) at a pseudo pH of 6, competitive binding of each CC led to the fluorescent dye **50** being displaced, resulting in a clear “turn-on” of fluorescence emission. The binding affinities between each enantiopure **49**, i.e., (*R*,*R*)-**49** or (*S*,*S*)-**49**, and each enantiopure CC guest were determined. It was found that **49** showed the largest enantioselectivity for ibuprofen (ca. 10-fold), whereas ca. 2-fold enantioselectivity was seen for naproxen, 2-phenylpropanoate, and atorvastatin. This allowed the ee of an unknown mixture containing both CC enantiomers to be determined with errors less than ±3%. In contrast, receptor **49** showed little enantioselectivity for lactate, mandelate, or 3-phenyllactate.

Phosphatidylserine (PS) externalization, wherein the anionic PS molecules that otherwise reside on the inner leaflet of the cell membrane are exposed to the cell surface, is recognized for being indicative of apoptosis [147]. In light of the potential of PS sensing for cancer diagnosis, Jolliffe et al. recently developed an IIDA-based fluorescent “turn-on” probe **51** capable of selectively and effectively detecting and imaging externalized PS [61]. The peptide backbone of sensor **51** was prepared by means of solid-phase peptide synthesis (SPPS), wherein a bis(Zn^{2+}-DPA) motif capable of binding PS was appended to the middle of the peptide backbone and a 6,7-dihydroxycoumarin indicator was “clicked” on near the N-terminus of the peptide backbone. As shown in Figure 28, probe **51** proved weakly emissive in a HEPES buffer solution (10 mM, pH = 7.4), presumably because coordination of the indicator to the Zn^{2+} center serves to quench the fluorescence. Upon treatment with anionic vesicles composed of 50% 1-palmitoyl-2-oleoyl-*sn*-glycero-3-phosphocholine

(POPC) and 50% 1-palmitoyl-2-oleoyl-*sn*-glycero-3-phospho-L-serine (POPS), probe **51** exhibited a ca. 4-fold increase in fluorescence intensity, which was ascribed to the displacement of the fluorescence-suppressed dye from the Zn^{2+}-DPA binding site. Confocal microscopy in conjunction with flow cytometry revealed that probe **51** also allowed for the detection of externalized PS, thereby enabling the differentiation of living, apoptotic, and necrotic cells. Under the same conditions, the imaging capability of probe **51** for PS compared favorably to that of annexin V (AnV) probe—a biosensor used to infer PS externalization. More importantly, probe **51** proved effective under certain conditions (i.e., no added Ca^{2+}, absence of a washing step, and low temperatures) where the use of AnV could prove problematic. It was thus suggested that probe **51** could act as a powerful molecular tool for detecting cell surface PS.

The Beer group is recognized for pioneering the use of interlocked systems (i.e., rotaxanes or catenanes) to realize anion recognition and sensing [148]. In the latter context, the introduction of electroactive moieties allowed certain appropriately chosen interlocked systems to function as electrochemical anion sensors [149]. Photoactive moieties (e.g., fluorophores) have also been introduced to these systems in an effort to create optical anion sensors. Recently, Beer et al. reported a series of metal complexes, including the acyclic hosts **52a·Pt** and **52a·Ru·PF$_6$**, the macrocyclic hosts **52b·Pt** and **52b·Ru·PF$_6$**, and the rotaxane-based hosts **53a·Pt** and **53a·Ru·PF$_6$** that function as fluorescent anion sensors (cf. Figure 29a) [150]. All these metal complexes exhibited typical luminescent emission properties in aerated organic media and were found to provide a distinct luminescent response upon the addition of a range of halides and oxyanions (as their TBA^+ salts). As shown in Figure 29b, **52a·Pt** gave rise to the greatest change (a ca. 60% increase) in emission upon adding Cl^- and SO_4^{2-}, and a modest change (a ca. 10% increase) in emission upon adding Br^-. In both cases, the fluorescence enhancement was ascribed to the RIM mechanism. In contrast, I^- and $H_2PO_4^-$ quenched the fluorescence of **52a·Pt**, presumably due to heavy atom and PET quenching effects, respectively. Macrocyclic congener **52b·Pt** provided a less pronounced change in fluorescence upon treatment with these anionic guests. Such a finding is in good agreement with the presumed RIM mechanism. This is because the macrocyclic effect renders the anion binding site of **52b·Pt** less flexible than that of **52a·Pt**. The congeneric complexes, **52a·Ru·PF$_6$** and **52b·Ru·PF$_6$**, only exhibited fluorescence quenching in response to various test anions, and higher cross-reactivity was seen in both cases. It was also found that the fluorescence of **52c·Ru·PF$_6$** was slightly quenched upon the addition of TBACl, presumably because both the interlocked cavity and the metal center of rotaxane **52c·Ru·PF$_6$** could serve as binding sites for Cl^-.

In parallel with the efforts by Beer and coworkers to create anion-binding interlocked systems, Jolliffe and Goldup et al. reported a fluorescent ditopic rotaxane **53** capable of acting as an ion pair receptor [151]. Rotaxane **53** was prepared readily via the modified active-template CuAAC reaction developed by Leigh and Goldup et al. [152,153]. Notably, the anion binding site of **53** (i.e., the urea moiety) is different from the position where the mechanical bond is formed (i.e., the triazole moiety); this stands in contrast to most of the anion-binding rotaxanes reported by Beer (e.g., **52c·Ru·PF$_6$**), wherein formation of the mechanical bonds generates the anion recognition site. As illustrated in Figure 30, no

binding was seen when the neutral rotaxane **53** was titrated with various test anions (as their TBA^+ salts) in $CH_3CN/CHCl_3$ (1:1, v/v) owing to the competitive binding of bipyridine moiety with the urea moiety. In contrast, the protonated form of **53**, obtained upon treatment with HBF_4, allowed various anions to be bound to the urea moiety. It is notable that **53**·HBF_4 produced a fluorescent "turn-on" response upon the addition of anions. It should be noted that the axle component of **53**, i.e., **54**, also proved capable of binding anions. However, fluorescent spectroscopic titrations revealed that **54** only produced a fluorescent "turn-off" response when treated with anions. The fluorescent "turn-on" response of **53**·HBF_4 was ascribed to a RIM mechanism, where presumed **π**–**π** interactions between the naphthalimide and bipyridine moieties serve to rigidify the framework and thus reduce the non-radiative decay; in contrast, the fluorescent "turn-on" response of **54** was ascribed to a PET quenching pathway. In addition, a comparison of the binding constants corresponding to the interaction of **53**·HBF_4 and **54** with anions revealed clear difference in terms of binding selectivities. These distinctions in terms of the fluorescent response and the binding affinities serve to highlight how mechanical bonds can serve to alter the inherent binding selectivities and fluorescent response of interlocked anion sensors relative to their non-interlocked counterparts.

In addition to various small-molecule-based approaches, such as those described above, polymeric materials can also serve as platforms for fluorescent anion sensing [154]. In 2018, Sessler et al. designed a novel fluorescent supramolecular polymeric gel capable of sensing chloride, wherein the readouts relied on so-called "3D code" patterns [155]. A series of fluorescent supramolecular organogels **55a–d** and **56a–d** were prepared (Figure 31a); the polymeric backbone of each organogel comprised a fluorophore (**a**, **b** or **c**), a C4P moiety, and an imidazolium anion salts (anion = F^- or Br^-). The non-fluorescent ("black") organogels **55d** and **56d** were readily prepared by treating **55c** and **56c** with $Cu(OAc)_2$, respectively. Figure 31b illustrates the proposed anion sensing mechanism for this system, which is based on the use of a double-layered fluorescent organogel arrangement. Specifically, a mechanically assembled 5×5 array of organogels **56a–c** with encoded information B (Code B) was prepared and designed to function as the top layer. This top layer was stacked onto a bottom layer composed of a different 5×5 array of organogels **55a–c** with encoded information A (Code A). Ion pair binding interactions between the C4P moieties and the imidazolium anion salts served to adhere the two gel arrays. Exposing the double-layered gels to a chloroform solution containing TBACl caused the top layer to disassemble, a finding ascribed to the fact that TBACl outcompetes the ion pair binding interactions of C4P with the imidazolium bromide salt. However, TBACl does not outcompete the interactions associated with the imidazolium fluoride salt (bottom layer). The binding-induced delamination of the double-layered organogels that occurs upon treatment with TBACl allows the information encoded by Code A to be read out by a smart phone "app" (COLORCODE™). The LOD of this system for TBACl was found to be ≥ 6 mM. This work remains relatively unique, but does show that stimuli-responsive supramolecular polymeric materials with encoded information may have a role to play in the context of fluorescent sensing [156].

Polyvinylpyrrolidone (PVP) is a commercially available water-soluble polymer recognized for its biomedical utility (e.g., povidone-iodine (PVP-I) as an over-the-counter broad-spectrum antiseptic) [157]. While the anion binding properties of PVP have been known for some time [158,159], it was only until recently that Wang et al. noticed the strong inherent fluorescence of PVP in water and ascribed this unexpected phenomenon to AIE [160]. Against this backdrop, in 2019, Dodani and co-workers repurposed PVP (i.e., compound **57**) as a polymeric fluorescent sensor for chaotropic anions such as NO_2^-, NO_3^-, I^-, and SCN^- (as their sodium salts) in water (cf. Figure 32) [161]. Specifically, buffered aqueous solutions containing 1 wt% **57** produced "turn-off" responses upon treatment with these chaotropic anions, wherein the extent of fluorescence quenching and binding affinities proved dependent on not only the identities of the anionic analytes, but also the pH and the molecular weight of **57**. The trend seen in the fluorescent response proved in good agreement with what would be expected based on the Hofmeister series (i.e. chaotropic being most effective) [162]. The authors ascribed the fluorescence quenching to inhibition of an AIE effect, wherein the interactions between the chaotropic anions and **57** served to break up aggregates of **57** that would otherwise form in water. The proposed sensing mechanism was also supported by the molecular dynamics (MD) simulations. In spite of being a "turn-off" anion sensor, the off-the-shelf nature of PVP means that it may have a role to play as a readily accessible fluorescent anion sensor that is amenable to use in aqueous media.

Metal−organic frameworks (MOFs) are porous materials that have seen use in a wide range of applications, including luminescent sensing [163–168]. Porphyrins, a class of tetrapyrrolic macrocycles, along with their congeners, are also recognized for enabling various applications, including luminescent sensing [169–171]. In 2018, Mohammed et al. reported that the tetracationic Pt^{2+}-porphyrin **58** could act as an ultrasensitive "turn-off" sensor for iodide (I^-) in aqueous media with the quenching attributed to a PET pathway, wherein a LOD at the picomolar (pM) level was seen [172]. The authors later noticed that the fluorescence of **58** could be quenched by other anions (e.g., sulfide) [173]. In an effort to improve the anion selectivity of sensor **58**, **58** was incorporated into a rho-type zeolite-like MOF (**rho**-ZMOF). The resulting system, **58**/**rho**-ZMOF, did not show any discernible fluorescent response even in the presence an excess of I^- (Figure 33), a finding that stands in contrast to what was observed in the case of the free sensor **58**. The difference in fluorescent response was rationalized in terms of electrostatic interactions between the cationic metalloporphyrin **58** and the anionic **rho**-ZMOF preventing anionic framework/I^- exchange such that no PET quenching occurs. On the other hand, **58**/**rho**-ZMOF was found to produce a "turn-on" response upon the addition of S^{2-} in aqueous media with a LOD of 27 nM. This study stands at the vanguard of efforts to exploit MOFs as frameworks for the construction of anion sensors based on organic guest encapsulation.

Lanthanides are known for their applications in the creation of luminescent anion sensors [174]. In 2020, Wu and Hou et al. reported a series of mixed lanthanide MOF-based sensors capable of detecting fluoride anions in water [175]. These mixed lanthanide MOFs were prepared using a 4,4′,4′′-*s*-triazine-2,4,6-triyltribenzoate (TATB) ligand and mixtures of the lanthanide ions (Tb^{3+} and Eu^{3+}). The fluorescence properties of these MOFs could be tuned by varying the Tb^{3+}:Eu^{3+} ratios. Sensor **59**, characterized by a 97:3 Tb:Eu ratio, was found

to exhibit a ratiometric response when exposed to fluoride anions in water. Specifically, the intensity ratio ($I_{547\ nm}/I_{617\ nm}$) was found to decrease upon the addition of F^-, allowing the fluoride to be detected with the a LOD of 96 ppb. Sensor **59** showed appreciable selectivities for F^- over other anions, including Cl^-, Br^-, I^-, NO_3^-, $H_2PO_4^-$, SO_4^{2-}, and HCO_3^-. (Note: The counter cations present in the anion salts used in this work were not mentioned by the authors.) Mechanistic studies revealed that the ratiometric response was primarily due to the displacement of water molecules bound to the Tb^{3+} center by F^-; anion–**π** interactions between the TATB ligand and F^- may also contribute to the observed changes in fluorescence. The authors also demonstrated that the fluorescent detection of F^- could be realized using a smartphone in conjunction with a handheld UV lamp, thus highlighting the potential practicality of this particular sensing platform.

Also in 2020, Zhou et al. described a multicomponent MOF, **60**, that proved capable of detecting cyanide (CN^-) *in vitro* [176]. As shown in Figure 35, the synthesis of sensor **60** was based on post-synthetic modifications of a previously reported Zr-MOF, known as PCN-700 [177]. Specifically, an anthracene-bearing fluorescent linker and a hemicyanine-bearing cyanide-responsive linker were installed in PCN-700 to serve as the signaling and recognition subunits, respectively. Sensor **60** proved weakly fluorescent, a finding ascribed to fluorescence (or Förster) resonance energy transfer (FRET) between the constituent anthracene and hemicyanine moieties [178]. Upon treating a suspension of **60** in water with CN^-, the hemicyanine subunits reacted with CN^-. (Note: the counter cation of the cyanide salt used in this work was not mentioned by the authors.) The resulting adduct, **61**, proved highly fluorescent, presumably as the result of energy transfer pathways being blocked. In the event, sensor **60** produced a discernible fluorescent “turn-on” response to CN^- with a LOD of 0.05 μM. The authors also showed that sensor **60** could be used to monitor intracellular cyanide concentrations in HeLa cells pre-incubated with cyanide salts. This work further underscores how MOFs can be used to create novel luminescent sensing materials.

2.3 Sensors for Neutral Species

Water-soluble calix[4]arene-based sensors for biologically relevant analytes have received considerable attention in light of their low cytotoxicity [179,180]. In 2019, Guo et al. reported the detection of hypoxia in living cells using the host–guest complex formed between azocalix[4]arene **63** and rhodamine 123 (**Rho123**) (Figure 36) [181]. This sensing system may be considered as being a combination of IDA and ABS. Specifically, the fluorescence of **Rho123** was quenched upon being encapsulated inside the cavity of the azocalix[4]arene host **63**. When **63·Rho123** was subjected to a hypoxic environment, the azo groups were reduced and converted to amino groups. This led to the displacement of the indicator, allowing the inherent fluorescence emission of **Rho123** to be restored. The authors suggested three intrinsic merits associated with this supramolecular sensing system: 1) no elaborate synthesis; 2) highly reliable sensing system selective for hypoxia; 3) easy adaptability in that this specific design strategy could be generalized into a universal sensing platform.

In 2020, Rosi et al. developed a MOF-based sensor for gossypol (**Gsp**), i.e., a well-known toxic chemical entity of particular concern to the cotton industry [182]. As shown in Figure 37, the MOF platform (**Yb-NH_2-TPDC**) was constructed by metal complexation between $YbCl_3 \cdot 6H_2O$ and ligand **64** (**H_2-NH_2-TPDC**). Upon treating the activated **Yb-NH_2-TPDC** with **Gsp** in acetone, a "turn-on" in the fluorescence emission intensity in the near-infrared (NIR) region was seen, while **Gsp** was absorbed by **Yb-NH_2-TPDC**. A LOD of 25 μg/mL was calculated for this system. The "turn-on" response was ascribed to the **Gsp** being either directly coordinated to the Ln^{3+} center or reacting with ligand **64** by forming, e.g., Schiff base complexes that ultimately led to fluorescence enhancement in the NIR region via energy transfer pathways. High selectivity for **Gsp** was inferred from the fact that a wide range of possible interferents, such as cottonseed oil, palmitic acid, linoleic acid, and α-tocopherol, did not give rise to any appreciable change in the fluorescence of **Yb-NH_2-TPDC**. This work highlights how lanthanide-based MOFs can be exploited to provide effective sensors for aromatic substrates with detection windows in the NIR region.

In 2020, Pischel and Ballester et al. reported an IDA-based sensor complex **65·BHQ** for creatinine (**Cr**) and its lipophilic congener **CrHex** that functions in chloroform. Here, the sensor complex comprised a dansyl-appended C4P **65** and a so-called "black-hole quencher (**BHQ**)" based on a pyridyl-*N*-oxide derivative (cf. Figure 38) [183]. The binding of **65** with **BHQ** quenched the inherent fluorescence of the dansyl group via a presumed FRET pathway [184]. When a creatinine analyte (either **Cr** or **CrHex**; Figure 38) was added to the solution containing the sensor complex **65·BHQ**, the **BHQ** was displaced by the creatinine guest as the result of competitive binding, thereby leading to the restoration of the inherent fluorescence of the dansyl fluorophore. Of particular note is that sensor **65** could detect creatinines at submicromolar concentrations (LOD = ca. 110 nM).

In recent years, Hooley and Zhong have developed collaboratively a cavitand-based fluorescent sensing platform based on an IDA strategy that allows the detection of diverse metabolic biomarkers, such as trimethylated and phosphorylated peptides [185,186]. In a recent work, Hooley et al. demonstrated the detection of cannabinoid metabolites based on an IDA approach that relies on the use of a cavitand host **66** in conjunction with a pair of fluorescent indicators, **67** and **68** (cf. Figure 39a) [187]. Cavitand **66** proved capable of encapsulating the fluorescent dye **67** to form the sensor complex **66·67**, wherein the fluorescence of **67** was quenched via a presumed PET pathway. In contrast, the ostensibly analogous sensor complex **66·68** was found to emit an enhanced fluorescence. Early work by Hooley and Rebek et al. had served to demonstrate that cavitand **66** was capable of encapsulating *n*-alkanes within its deep cavity with high binding affinity in water [188]. On this basis, the Hooley team envisioned that **66** could bind to cannabinoids **69**–**74** since these neutral metabolites all contain a constituent *n*-pentyl moiety. Indeed, when these two sensor complexes were treated with the six test metabolites **69**–**74** in aqueous media, discernible changes in the fluorescence intensity were seen in all cases as the result of presumed indicator displacement. The fluorescent response patterns could be modulated readily not only by altering the fluorescent indicators (**67** or **68**) but also by using other heavy metal salts. Such features enabled the creation of a series of sensor arrays, whereby the cannabinoids in question could be selectively discriminated in aqueous media with LODs at

the micromolar (μM) level. In addition, the authors demonstrated that these sensor arrays allowed for the effective sensing of cannabinoid present in actual samples taken from saliva or urine.

3. Conclusions and Perspectives

In this review we have tried to provide an historical perspective of the early development of supramolecular fluorescent sensors, as well as an illustrative discussion of selected work published within the past three years. In choosing this presentation approach, the goal was to give the readers a sense of how this field has evolved and where it may be heading. In particular, our hope was to illustrate both well-established sensing mechanisms and approaches, such as photoinduced electron transfer (PET), aggregation-induced emission (AIE), and indicator displacement assays (IDAs), as well as newer strategies embodied in neologisms such as DimerDye disassembly assay (DDA), excimer-disaggregation-induced emission (EDIE), and vibration-induced emission (VIE). It is our aspirational desire that this combination of the old and new will allow readers, whether new to the field or established practitioners, to create new sensing systems that can address currently unmet challenges associated with detecting complex biologically relevant species (e.g., biomarkers), as well as improving our capacity to detect classic small molecule analytes with greater fidelity.

Making this area of further timely interest from our perspective is that the fluorescent sensing strategies elaborated in this review are not limited to their specific settings; rather, they should be generalizable and thus applicable to other detection schemes and sensing platforms. In other words, a “mix-and-match” of these sensing approaches, mechanisms, and strategies, coupled with judicious designs, should inspire future developments in the generalized area of supramolecular fluorescent chemosensors. For instance, while a number of macrocycle-based and MOF-based fluorescent anion sensors have been reported (*vide supra*), to our knowledge, only limited efforts have been made to incorporate macrocyclic anion receptors into MOFs [189,190], and further exploiting them as anion sensors. Also, it would be appealing to see some of the new sensing methods (DDA, VIE, *etc.*) applied to classes of analytes not considered in the original research reports. Last but not least, we expect continued efforts will be made to promote the development of more reliable, versatile sensors or sensing platforms that address an ever-widening scope of real-world problems, such as the detection of infectious diseases, e.g., SARS-CoV-2 (i.e., the virus underlying COVID-19), as well as classic scourges such as cancer and neurodegenerative diseases. We hope the present contribution provides a useful foundation for these and other future contributions to the sensing field.

Acknowledgement

The work in Austin was supported by the National Institutes of Health (grant R01 GM 103790 to J.L.S.) and the Robert A. Welch Foundation (F-0018 to J.L.S.). The work in Hiroshima was supported by a Grants-in-Aid for Young Scientists, JSPS KAKENHI (20K15335 to T.H.). C.G. would like to thank the UT Austin for a Harold Thomas Hahn Endowed Presidential Fellowship.

Dedicated to Professor Eric V. Anslyn on the occasion of his 60th birthday.

Abbreviations:

ADP	adenosine diphosphate
AMP	adenosine monophosphate
COVID-19	coronavirus disease 2019
CTP	cytidine triphosphate
CuAAC	copper-catalyzed azide–alkyne cycloaddition
DMSO	dimethyl sulfoxide
DPA	dipicolylamine
GMP	guanosine monophosphate
GTP	guanosine triphosphate
HEPES	2-(4-(2-hydroxyethyl)-1-piperazineethanesulfonic acid
MES	2-(*N*-morpholino)ethanesulfonic acid
NAD^+	nicotinamide adenine dinucleotide
SARS-CoV-2	severe acute respiratory syndrome coronavirus 2
Tris	tris(hydroxymethyl)aminomethane
UMP	uridine monophosphate
UTP	uridine triphosphate

5. References

[1]. Udugama B, Kadhiresan P, Kozlowski HN, Malekjahani A, Osborne M, Li VYC, Chen H, Mubareka S, Gubbay JB, Chan WCW, ACS Nano, 14 (2020) 3822–3835. [PubMed: 32223179]

[2]. Demchenko AP, Introduction to Fluorescence Sensing, Springer, Berlin, Germany, 2009.

[3]. Chemosensors: Principles, Strategies, and Applications, Wang B, Anslyn EV (Eds.), Wiley, Hoboken, NJ, 2011.

[4]. Wu D, Sedgwick AC, Gunnlaugsson T, Akkaya EU, Yoon J, James TD, Chem. Soc. Rev, 46 (2017) 7105–7123. [PubMed: 29019488]

[5]. Mako TL, Racicot JM, Levine M, Chem. Rev, 119 (2019) 322–477. [PubMed: 30507166]

[6]. Iovan DA, Jia S, Chang CJ, Inorg. Chem, 58 (2019) 13546–13560. [PubMed: 31185541]

[7]. Bruemmer KJ, Crossley SWM, Chang CJ, Angew. Chem., Int. Ed, 59 (2019) 13734–13762.

[8]. Lakowicz JR, Principles of Fluorescence Spectroscopy, 3rd ed., Springer, New York, 2010.

[9]. Illsley NP, Verkman AS, Biochemistry, 26 (1987) 1215–1219. [PubMed: 3567167]

[10]. Verkman AS, Am. J. Physiol, 259 (1990) 375–388.

[11]. Lee MH, Kim JS, Sessler JL, Chem. Soc. Rev, 44 (2015) 4185–4191. [PubMed: 25286013]

[12]. Tsien RY, Biochemistry, 19 (1980) 2396–2404. [PubMed: 6770893]

[13]. Grynkiewicz G, Poenie M, Tsien RY, J. Biol. Chem, 260 (1985) 3440–3450. [PubMed: 3838314]

[14]. Minta A, Kao JP, Tsien RY, J. Biol. Chem, 264 (1989) 8171–8178. [PubMed: 2498308]

[15]. Minta A, Tsien RY, J. Biol. Chem, 264 (1989) 19449–19457. [PubMed: 2808435]

[16]. Heim R, Cubitt AB, Tsien RY, Nature, 373 (1995) 663–664.
[17]. de Silva AP, Rupasinghe RADD, J. Chem. Soc., Chem. Commun, (1985) 1669–1670.
[18]. de Silva AP, de Silva SA, J. Chem. Soc., Chem. Commun, (1986) 1709–1710.
[19]. Bissell RA, de Silva AP, Gunaratne HQN, Lynch PLM, Maguire GEM, Sandanayake KRAS, Chem. Soc. Rev, 21 (1992) 187–195.
[20]. Huston ME, Haider KW, Czarnik AW, J. Am. Chem. Soc, 110 (1988) 4460–4462.
[21]. Czarnik AW, Acc. Chem. Res, 27 (1994) 302–308.
[22]. Yeung MC-L, Yam VW-W, Chem. Soc. Rev, 44 (2015) 4192–4202. [PubMed: 25588608]
[23]. Valeur B, Leray I, Coord. Chem. Rev, 205 (2000) 3–40.
[24]. Carter KP, Young AM, Palmer AE, Chem. Rev, 114 (2014) 4564–4601. [PubMed: 24588137]
[25]. Daly B, Ling J, de Silva AP, Chem. Soc. Rev, 44 (2015) 4203–4211. [PubMed: 25695939]
[26]. Sessler JL, Gale PA, Cho W-S, Anion Receptor Chemistry, The Royal Society of Chemistry, Cambridge, 2006.
[27]. Hosseini MW, Blacker AJ, Lehn J-M, J. Chem. Soc., Chem. Commun, (1988) 596–598.
[28]. Hosseini MW, Lehn J-M, Mertes MP, Helv. Chim. Acta, 66 (1983) 2454–2466.
[29]. Huston ME, Akkaya EU, Czarnik AW, J. Am. Chem. Soc, 111 (1989) 8735–8737.
[30]. Fabbrizzi L, Licchelli M, Rabaioli G, Taglietti A, Coord. Chem. Rev, 205 (2000) 85–108.
[31]. Martínez-Máñez R, Sancenón F, Chem. Rev, 103 (2003) 4419–4476. [PubMed: 14611267]
[32]. Anion Sensing, Stibor I (Ed.), Springer-Verlag, Berlin Heidelberg, 2005.
[33]. Gunnlaugsson T, Glynn M, Tocci GM, Kruger PE, Pfeffer FM, Coord. Chem. Rev, 250 (2006) 3094–3117.
[34]. Gale PA, Caltagirone C, Chem. Soc. Rev, 44 (2015) 4212–4227. [PubMed: 24975326]
[35]. Serpell CJ, Beer PD, 8.16 - Anion Sensors, in: Atwood JL (Ed.) Comprehensive Supramolecular Chemistry II, Elsevier, Oxford, 2017, pp. 351–385.
[36]. Gale PA, Caltagirone C, Coord. Chem. Rev, 354 (2018) 2–27.
[37]. Kubik S, Chem. Soc. Rev, 39 (2010) 3648–3663. [PubMed: 20617241]
[38]. Langton MJ, Serpell CJ, Beer PD, Angew. Chem., Int. Ed, 55 (2016) 1974–1987.
[39]. Sun X, James TD, Chem. Rev, 115 (2015) 8001–8037. [PubMed: 25974371]
[40]. Yoon J, Czarnik AW, J. Am. Chem. Soc, 114 (1992) 5874–5875.
[41]. James TD, Sandanayake KRAS, Shinkai S, J. Chem. Soc., Chem. Commun, (1994) 477–478.
[42]. James TD, Sandanayake KRAS, Shinkai S, Angew. Chem., Int. Ed, 33 (1994) 2207–2209.
[43]. James TD, Samankumara Sandanayake KRA, Shinkai S, Nature, 374 (1995) 345–347.
[44]. Franzen S, Ni W, Wang B, J. Phys. Chem. B, 107 (2003) 12942–12948.
[45]. Ni W, Kaur G, Springsteen G, Wang B, Franzen S, Bioorg. Chem, 32 (2004) 571–581. [PubMed: 15530997]
[46]. Chapin BM, Metola P, Vankayala SL, Woodcock HL, Mooibroek TJ, Lynch VM, Larkin JD, Anslyn EV, J. Am. Chem. Soc, 139 (2017) 5568–5578. [PubMed: 28358506]
[47]. Sun X, James TD, Anslyn EV, J. Am. Chem. Soc, 140 (2018) 2348–2354. [PubMed: 29360350]
[48]. Sun X, Chapin BM, Metola P, Collins B, Wang B, James TD, Anslyn EV, Nat. Chem, 11 (2019) 768–778. [PubMed: 31444486]
[49]. Nishiyabu R, Kubo Y, James TD, Fossey JS, Chem. Commun, 47 (2011) 1124–1150.
[50]. Rowan SJ, Cantrill SJ, Cousins GRL, Sanders JKM, Stoddart JF, Angew. Chem., Int. Ed, 41 (2002) 898–952.
[51]. Wiskur SL, Ait-Haddou H, Lavigne JJ, Anslyn EV, Acc. Chem. Res, 34 (2001) 963–972. [PubMed: 11747414]
[52]. Metzger A, Anslyn EV, Angew. Chem., Int. Ed, 37 (1998) 649–652.
[53]. Nguyen BT, Anslyn EV, Coord. Chem. Rev, 250 (2006) 3118–3127.
[54]. Anslyn EV, J. Org. Chem, 72 (2007) 687–699. [PubMed: 17253783]
[55]. Wu J, Kwon B, Liu W, Anslyn EV, Wang P, Kim JS, Chem. Rev, 115 (2015) 7893–7943. [PubMed: 25965103]

[56]. Inouye M, Hashimoto K.-i., Isagawa K, J. Am. Chem. Soc, 116 (1994) 5517–5518.
[57]. Koh KN, Araki K, Ikeda A, Otsuka H, Shinkai S, J. Am. Chem. Soc, 118 (1996) 755–758.
[58]. Ueno A, Kuwabara T, Nakamura A, Toda F, Nature, 356 (1992) 136–137.
[59]. Minami T, Liu Y, Akdeniz A, Koutnik P, Esipenko NA, Nishiyabu R, Kubo Y, Anzenbacher P, J. Am. Chem. Soc, 136 (2014) 11396–11401. [PubMed: 25051138]
[60]. Liu X, Smith DG, Jolliffe KA, Chem. Commun, 52 (2016) 8463–8466.
[61]. Zwicker VE, Oliveira BL, Yeo JH, Fraser ST, Bernardes GJL, New EJ, Jolliffe KA, Angew. Chem., Int. Ed, 58 (2019) 3087–3091.
[62]. Beatty MA, Borges-González J, Sinclair NJ, Pye AT, Hof F, J. Am. Chem. Soc, 140 (2018) 3500–3504. [PubMed: 29461821]
[63]. Garnett GAE, Daze KD, Peña Diaz JA, Fagen N, Shaurya A, Ma MCF, Collins MS, Johnson DW, Zakharov LN, Hof F, Chem. Commun, 52 (2016) 2768–2771.
[64]. Beatty MA, Selinger AJ, Li Y, Hof F, J. Am. Chem. Soc, 141 (2019) 16763–16771. [PubMed: 31577900]
[65]. Wright AT, Anslyn EV, Chem. Soc. Rev, 35 (2006) 14–28. [PubMed: 16365639]
[66]. Tian J, Chen L, Zhang D-W, Liu Y, Li Z-T, Chem. Commun, 52 (2016) 6351–6362.
[67]. Wang H, Ji X, Li Z, Huang F, Adv. Mater, 29 (2017) 1606117.
[68]. Xia D, Wang P, Ji X, Khashab NM, Sessler JL, Huang F, Chem. Rev, 120 (2020) 6070–6123. [PubMed: 32426970]
[69]. Song N, Yang Y-W, Sci. China Chem, 57 (2014) 1185–1198.
[70]. Ogoshi T, Yamagishi T.-a., Nakamoto Y, Chem. Rev, 116 (2016) 7937–8002. [PubMed: 27337002]
[71]. Zhang H, Liu Z, Xin F, Zhao Y, Coord. Chem. Rev, 420 (2020) 213425.
[72]. Lin Q, Fan Y-Q, Mao P-P, Liu L, Liu J, Zhang Y-M, Yao H, Wei T-B, Chem. - Eur. J, 24 (2018) 777–783. [PubMed: 29165843]
[73]. Hong Y, Lam JWY, Tang BZ, Chem. Soc. Rev, 40 (2011) 5361–5388. [PubMed: 21799992]
[74]. Mei J, Hong Y, Lam JWY, Qin A, Tang Y, Tang BZ, Adv. Mater, 26 (2014) 5429–5479. [PubMed: 24975272]
[75]. Mei J, Leung NLC, Kwok RTK, Lam JWY, Tang BZ, Chem. Rev, 115 (2015) 11718–11940. [PubMed: 26492387]
[76]. He Z, Ke C, Tang BZ, ACS Omega, 3 (2018) 3267–3277. [PubMed: 31458583]
[77]. Luo J, Xie Z, Lam JWY, Cheng L, Chen H, Qiu C, Kwok HS, Zhan X, Liu Y, Zhu D, Tang BZ, Chem. Commun, (2001) 1740–1741.
[78]. Leung NLC, Xie N, Yuan W, Liu Y, Wu Q, Peng Q, Miao Q, Lam JWY, Tang BZ, Chem. - Eur. J, 20 (2014) 15349–15353. [PubMed: 25303769]
[79]. Gao M, Tang BZ, ACS Sens., 2 (2017) 1382–1399. [PubMed: 28945357]
[80]. Li X, Li M, Yang M, Xiao H, Wang L, Chen Z, Liu S, Li J, Li S, James TD, Coord. Chem. Rev, 418 (2020) 213358.
[81]. La DD, Bhosale SV, Jones LA, Bhosale SV, ACS Appl. Mater. Interfaces, 10 (2018) 12189–12216. [PubMed: 29043778]
[82]. Feng H-T, Yuan Y-X, Xiong J-B, Zheng Y-S, Tang BZ, Chem. Soc. Rev, 47 (2018) 7452–7476. [PubMed: 30177975]
[83]. Dai D, Li Z, Yang J, Wang C, Wu J-R, Wang Y, Zhang D, Yang Y-W, J. Am. Chem. Soc, 141 (2019) 4756–4763. [PubMed: 30807128]
[84]. Miyake Y, Togashi H, Tashiro M, Yamaguchi H, Oda S, Kudo M, Tanaka Y, Kondo Y, Sawa R, Fujimoto T, Machinami T, Ono A, J. Am. Chem. Soc, 128 (2006) 2172–2173. [PubMed: 16478145]
[85]. Wang S, Yan C, Shang J, Wang W, Yuan C, Zhang H-L, Shao X, Angew. Chem., Int. Ed, 58 (2019) 3819–3823.
[86]. Du Y, Liu H, Dalton Trans., 49 (2020) 5396–5405. [PubMed: 32232247]
[87]. Cordes DB, Lickiss PD, Rataboul F, Chem. Rev, 110 (2010) 2081–2173. [PubMed: 20225901]

[88]. Bassindale AR, Pourny M, Taylor PG, Hursthouse MB, Light ME, Angew. Chem., Int. Ed, 42 (2003) 3488–3490.

[89]. Chanmungkalakul S, Ervithayasuporn V, Hanprasit S, Masik M, Prigyai N, Kiatkamjornwong S, Chem. Commun, 53 (2017) 12108–12111.

[90]. Chanmungkalakul S, Ervithayasuporn V, Boonkitti P, Phuekphong A, Prigyai N, Kladsomboon S, Kiatkamjornwong S, Chem. Sci, 9 (2018) 7753–7765. [PubMed: 30429984]

[91]. Oguri N, Egawa Y, Takeda N, Unno M, Angew. Chem., Int. Ed, 55 (2016) 9336–9339.

[92]. Uchida T, Egawa Y, Adachi T, Oguri N, Kobayashi M, Kudo T, Takeda N, Unno M, Tanaka R, Chem. - Eur. J, 25 (2019) 1683–1686. [PubMed: 30511778]

[93]. Ronson TK, Zarra S, Black SP, Nitschke JR, Chem. Commun, 49 (2013) 2476–2490.

[94]. Zhang D, Ronson TK, Nitschke JR, Acc. Chem. Res, 51 (2018) 2423–2436. [PubMed: 30207688]

[95]. Plajer AJ, Percástegui EG, Santella M, Rizzuto FJ, Gan Q, Laursen BW, Nitschke JR, Angew. Chem., Int. Ed, 58 (2019) 4200–4204.

[96]. Deliomeroglu MK, Lynch VM, Sessler JL, Chem. Commun, 50 (2014) 11863–11866.

[97]. Deliomeroglu MK, Lynch VM, Sessler JL, Chem. Sci, 7 (2016) 3843–3850. [PubMed: 30155027]

[98]. Guo C, Sun S, He Q, Lynch VM, Sessler JL, Org. Lett, 20 (2018) 5414–5417. [PubMed: 30136850]

[99]. Oshchepkov AS, Shumilova TA, Namashivaya SR, Fedorova OA, Dorovatovskii PV, Khrustalev VN, Kataev EA, J. Org. Chem, 83 (2018) 2145–2153. [PubMed: 29378129]

[100]. Shumilova TA, Rüffer T, Lang H, Kataev EA, Chem. - Eur. J, 24 (2018) 1500–1504. [PubMed: 29027757]

[101]. Namashivaya SSR, Oshchepkov AS, Ding H, Förster S, Khrustalev VN, Kataev EA, Org. Lett, 21 (2019) 8746–8750. [PubMed: 31603329]

[102]. Oshchepkov AS, Shumilova TA, Zerson M, Magerle R, Khrustalev VN, Kataev EA, J. Org. Chem, 84 (2019) 9034–9043. [PubMed: 31117577]

[103]. Agafontsev AM, Shumilova TA, Rüffer T, Lang H, Kataev EA, Chem. - Eur. J, 25 (2019) 3541–3549. [PubMed: 30644598]

[104]. Morozov BS, Namashivaya SSR, Zakharko MA, Oshchepkov AS, Kataev EA, ChemistryOpen, 9 (2020) 171–175. [PubMed: 32025461]

[105]. Agafontsev AM, Shumilova TA, Oshchepkov AS, Hampel F, Kataev EA, Chem. - Eur. J, 26 (2020) 9991–9997. [PubMed: 32497327]

[106]. Kang SO, Llinares JM, Day VW, Bowman-James K, Chem. Soc. Rev, 39 (2010) 3980–4003. [PubMed: 20820597]

[107]. Rothman J, Int. J. Cancer Res. Ther, 2 (2017) 1–10.

[108]. Farshbaf S, Anzenbacher P, Chem. Commun, 55 (2019) 1770–1773.

[109]. Chua MH, Shah KW, Zhou H, Xu J, Molecules, 24 (2019) 2711.

[110]. Zhao J, Yang D, Zhao Y, Yang X-J, Wang Y-Y, Wu B, Angew. Chem., Int. Ed, 53 (2014) 6632–6636.

[111]. Yuan Y-X, Wang J-H, Zheng Y-S, Chem. - Asian J, 14 (2019) 760–764. [PubMed: 30556960]

[112]. Nelson DL, Cox MM, The Citric Acid Cycle, in: Lehninger Principles of Biochemistry, 6th edition, W. H. Freeman and Company, New York, 2013, pp. 633–665.

[113]. Curiel D, Más-Montoya M, Sánchez G, Coord. Chem. Rev, 284 (2015) 19–66.

[114]. Chen T-H, Popov I, Kaveevivitchai W, Chuang Y-C, Chen Y-S, Daugulis O, Jacobson AJ, Miljanić OŠ, Nat. Commun, 5 (2014) 5131. [PubMed: 25307413]

[115]. Zhang Z, Hashim MI, Wu C-H, Wu JI, Miljanić OŠ, Chem. Commun, 54 (2018) 11578–11581.

[116]. Yokoyama S, Ito A, Asahara H, Nishiwaki N, Bull. Chem. Soc. Jpn, 92 (2019) 1807–1815.

[117]. Yokoyama S, Nishiwaki N, J. Org. Chem, 84 (2019) 1192–1200. [PubMed: 30567431]

[118]. Maeda H, Bando Y, Chem. Commun, 49 (2013) 4100–4113.

[119]. Juwarker H, Jeong K-S, Chem. Soc. Rev, 39 (2010) 3664–3674. [PubMed: 20730154]

[120]. Zhai D, Xu W, Zhang L, Chang Y-T, Chem. Soc. Rev, 43 (2014) 2402–2411. [PubMed: 24514005]

[121]. Sessler JL, Davis JM, Kral V, Kimbrough T, Lynch V, Org. Biomol. Chem, 1 (2003) 4113–4123. [PubMed: 14664401]

[122]. Cheng H-B, Sun Z, Kwon N, Wang R, Cui Y, Park CO, Yoon J, Chem. - Eur. J, 25 (2019) 3501–3504. [PubMed: 30645046]

[123]. Yang J, Dong C-C, Chen X-L, Sun X, Wei J-Y, Xiang J-F, Sessler JL, Gong H-Y, J. Am. Chem. Soc, 141 (2019) 4597–4612. [PubMed: 30798593]

[124]. Gale PA, Lee C-H, Calix[n]pyrroles as Anion and Ion-Pair Complexants, in: Gale PA, Dehaen W (Eds.) Anion Recognition in Supramolecular Chemistry, Springer-Verlag, Berlin Heidelberg, 2010, pp. 39–73.

[125]. Kim SK, Sessler JL, Acc. Chem. Res, 47 (2014) 2525–2536. [PubMed: 24977935]

[126]. Rather IA, Wagay SA, Hasnain MS, Ali R, RSC Adv., 9 (2019) 38309–38344.

[127]. Kohnke FH, Eur. J. Org. Chem, 2020 (2020) 4261–4272.

[128]. Peng S, He Q, Vargas-Zúñiga GI, Qin L, Hwang I, Kim SK, Heo NJ, Lee C-H, Dutta R, Sessler JL, Chem. Soc. Rev, 49 (2020) 865–907. [PubMed: 31957756]

[129]. Miyaji H, Sato W, Sessler JL, Angew. Chem., Int. Ed, 39 (2000) 1777–1780.

[130]. Anzenbacher P, Jursíková K, Sessler JL, J. Am. Chem. Soc, 122 (2000) 9350–9351.

[131]. Nishiyabu R, Anzenbacher P, J. Am. Chem. Soc, 127 (2005) 8270–8271. [PubMed: 15941245]

[132]. Nishiyabu R, Palacios MA, Dehaen W, Anzenbacher P, J. Am. Chem. Soc, 128 (2006) 11496–11504. [PubMed: 16939273]

[133]. Palacios MA, Nishiyabu R, Marquez M, Anzenbacher P, J. Am. Chem. Soc, 129 (2007) 7538–7544. [PubMed: 17530846]

[134]. Pushina M, Koutnik P, Nishiyabu R, Minami T, Savechenkov P, Anzenbacher P Jr, Chem. - Eur. J, 24 (2018) 4879–4884. [PubMed: 29385284]

[135]. Zhang Z, Wu Y-S, Tang K-C, Chen C-L, Ho J-W, Su J, Tian H, Chou P-T, J. Am. Chem. Soc, 137 (2015) 8509–8520. [PubMed: 26075574]

[136]. Wang J, Yao X, Liu Y, Zhou H, Chen W, Sun G, Su J, Ma X, Tian H, Adv. Opt. Mater, 6 (2018) 1800074.

[137]. Zhang Z, Sun G, Chen W, Su J, Tian H, Chem. Sci, 11 (2020) 7525–7537. [PubMed: 32874525]

[138]. Chen W, Chen C-L, Zhang Z, Chen Y-A, Chao W-C, Su J, Tian H, Chou P-T, J. Am. Chem. Soc, 139 (2017) 1636–1644. [PubMed: 28072523]

[139]. Chen W, Guo C, He Q, Chi X, Lynch VM, Zhang Z, Su J, Tian H, Sessler JL, J. Am. Chem. Soc, 141 (2019) 14798–14806. [PubMed: 31437397]

[140]. Hamm LL, Nakhoul N, Hering-Smith KS, Clin. J. Am. Soc. Nephrol, 10 (2015) 2232–2242.

[141]. Mulugeta E, He Q, Sareen D, Hong S-J, Oh JH, Lynch VM, Sessler JL, Kim SK, Lee C-H, Chem, 3 (2017) 1008–1020.

[142]. Vargesson N, Birth Defects Res. C Embryo Today, 105 (2015) 140–156. [PubMed: 26043938]

[143]. Hembury GA, Borovkov VV, Inoue Y, Chem. Rev, 108 (2008) 1–73. [PubMed: 18095713]

[144]. Chen Z, Wang Q, Wu X, Li Z, Jiang Y-B, Chem. Soc. Rev, 44 (2015) 4249–4263. [PubMed: 25714523]

[145]. Jo HH, Lin C-Y, Anslyn EV, Acc. Chem. Res, 47 (2014) 2212–2221. [PubMed: 24892802]

[146]. Sheykhi S, Mosca L, Durgala JM, Anzenbacher P, Chem. Commun, 55 (2019) 7183–7186.

[147]. Sharma B, Kanwar SS, Semin. Cancer Biol, 52 (2018) 17–25. [PubMed: 28870843]

[148]. Langton MJ, Beer PD, Acc. Chem. Res, 47 (2014) 1935–1949. [PubMed: 24708030]

[149]. Hein R, Beer PD, Davis JJ, Chem. Rev, 120 (2020) 1888–1935. [PubMed: 31916758]

[150]. Knighton RC, Dapin S, Beer PD, Chem. - Eur. J, 26 (2020) 5288–5296. [PubMed: 32130744]

[151]. Denis M, Qin L, Turner P, Jolliffe KA, Goldup SM, Angew. Chem., Int. Ed, 57 (2018) 5315–5319.

[152]. Crowley JD, Goldup SM, Lee A-L, Leigh DA, McBurney RT, Chem. Soc. Rev, 38 (2009) 1530–1541. [PubMed: 19587949]

[153]. Denis M, Goldup SM, Nat. Rev. Chem, 1 (2017) 0061.
[154]. Kim HN, Guo Z, Zhu W, Yoon J, Tian H, Chem. Soc. Rev, 40 (2011) 79–93. [PubMed: 21107482]
[155]. Ji X, Chen W, Long L, Huang F, Sessler Jonathan L., Chem. Sci, 9 (2018) 7746–7752. [PubMed: 30429983]
[156]. Wang H, Ji X, Page ZA, Sessler JL, Mater. Chem. Front, 4 (2020) 1024–1039.
[157]. Teodorescu M, Bercea M, Polym. Plast. Technol. Eng, 54 (2015) 923–943.
[158]. Oh SH, Ryoo R, Jhon MS, Macromolecules, 23 (1990) 1671–1675.
[159]. Song JD, Ryoo R, Jhon MS, Macromolecules, 24 (1991) 1727–1730.
[160]. Song G, Lin Y, Zhu Z, Zheng H, Qiao J, He C, Wang H, Macromol. Rapid Commun,, 36 (2015) 278–285. [PubMed: 25420749]
[161]. Kam HC, Ranathunga DTS, Payne ER, Smaldone RA, Nielsen SO, Dodani SC, Supramol. Chem, 31 (2019) 514–522.
[162]. Zhang Y, Cremer PS, Curr. Opin. Chem. Biol, 10 (2006) 658–663. [PubMed: 17035073]
[163]. Cui Y, Yue Y, Qian G, Chen B, Chem. Rev, 112 (2012) 1126–1162. [PubMed: 21688849]
[164]. Kreno LE, Leong K, Farha OK, Allendorf M, Van Duyne RP, Hupp JT, Chem. Rev, 112 (2012) 1105–1125. [PubMed: 22070233]
[165]. Hu Z, Deibert BJ, Li J, Chem. Soc. Rev, 43 (2014) 5815–5840. [PubMed: 24577142]
[166]. Zhao D, Cui Y, Yang Y, Qian G, CrystEngComm, 18 (2016) 3746–3759.
[167]. Lustig WP, Mukherjee S, Rudd ND, Desai AV, Li J, Ghosh SK, Chem. Soc. Rev, 46 (2017) 3242–3285. [PubMed: 28462954]
[168]. Zhang Y, Yuan S, Day G, Wang X, Yang X, Zhou H-C, Coord. Chem. Rev, 354 (2018) 28–45.
[169]. Ding Y, Zhu W-H, Xie Y, Chem. Rev, 117 (2017) 2203–2256. [PubMed: 27078087]
[170]. Paolesse R, Nardis S, Monti D, Stefanelli M, Di Natale C, Chem. Rev, 117 (2017) 2517–2583. [PubMed: 28222604]
[171]. Lee H, Hong K-I, Jang W-D, Coord. Chem. Rev, 354 (2018) 46–73.
[172]. Masih D, Aly SM, Alarousu E, Mohammed OF, J. Mater. Chem. A, 3 (2015) 6733–6738.
[173]. Masih D, Chernikova V, Shekhah O, Eddaoudi M, Mohammed OF, ACS Appl. Mater. Interfaces, 10 (2018) 11399–11405. [PubMed: 29578682]
[174]. Aletti AB, Gillen DM, Gunnlaugsson T, Coord. Chem. Rev, 354 (2018) 98–120.
[175]. Zeng X, Hu J, Zhang M, Wang F, Wu L, Hou X, Anal. Chem, 92 (2020) 2097–2102. [PubMed: 31842541]
[176]. Li J, Yuan S, Qin J-S, Pang J, Zhang P, Zhang Y, Huang Y, Drake HF, Liu WR, Zhou H-C, Angew. Chem., Int. Ed, 59 (2020) 9319–9323.
[177]. Yuan S, Chen Y-P, Qin J-S, Lu W, Zou L, Zhang Q, Wang X, Sun X, Zhou H-C, J. Am. Chem. Soc, 138 (2016) 8912–8919. [PubMed: 27345035]
[178]. Dolgopolova EA, Rice AM, Martin CR, Shustova NB, Chem. Soc. Rev, 47 (2018) 4710–4728. [PubMed: 29546889]
[179]. Coleman AW, Jebors S, Cecillon S, Perret P, Garin D, Marti-Battle D, Moulin M, New J Chem., 32 (2008) 780–782.
[180]. Nimse SB, Kim T, Chem. Soc. Rev, 42 (2013) 366–386. [PubMed: 23032718]
[181]. Geng W-C, Jia S, Zheng Z, Li Z, Ding D, Guo D-S, Angew. Chem., Int. Ed, 58 (2019) 2377–2381.
[182]. Luo T-Y, Das P, White DL, Liu C, Star A, Rosi NL, J. Am. Chem. Soc, 142 (2020) 2897–2904. [PubMed: 31972094]
[183]. Sierra AF, Hernández-Alonso D, Romero MA, González-Delgado JA, Pischel U, Ballester P, J. Am. Chem. Soc, 142 (2020) 4276–4284. [PubMed: 32045249]
[184]. Wu L, Huang C, Emery BP, Sedgwick AC, Bull SD, He X-P, Tian H, Yoon J, Sessler JL, James TD, Chem. Soc. Rev, 49 (2020) 5110–5139. [PubMed: 32697225]
[185]. Liu Y, Perez L, Mettry M, Easley CJ, Hooley RJ, Zhong W, J. Am. Chem. Soc, 138 (2016) 10746–10749. [PubMed: 27500515]

[186]. Liu Y, Lee J, Perez L, Gill AD, Hooley RJ, Zhong W, J. Am. Chem. Soc, 140 (2018) 13869–13877. [PubMed: 30269482]

[187]. Gill AD, Hickey BL, Zhong W, Hooley RJ, Chem. Commun, 56 (2020) 4352–4355.

[188]. Hooley RJ, Van Anda HJ, Rebek J, J. Am. Chem. Soc, 129 (2007) 13464–13473. [PubMed: 17927175]

[189]. Lee J, Waggoner NW, Polanco L, You GR, Lynch VM, Kim SK, Humphrey SM, Sessler JL, Chem. Commun, 52 (2016) 8514–8517.

[190]. Aguilera-Sigalat J, Sáenz de Pipaón C, Hernández-Alonso D, Escudero-Adán EC, Galan-Mascarós JR, Ballester P, Cryst. Growth Des, 17 (2017) 1328–1338.

HIGHLIGHTS:

- Pioneering studies in the field of supramolecular fluorescent sensors are highlighted.
- Recent advances involving the development of supramolecular fluorescent sensors, particularly those rely on new sensing mechanisms or novel sensing platforms, are summarized.
- Considerations of how the field may evolve and opportunities for future growth are also articulated.

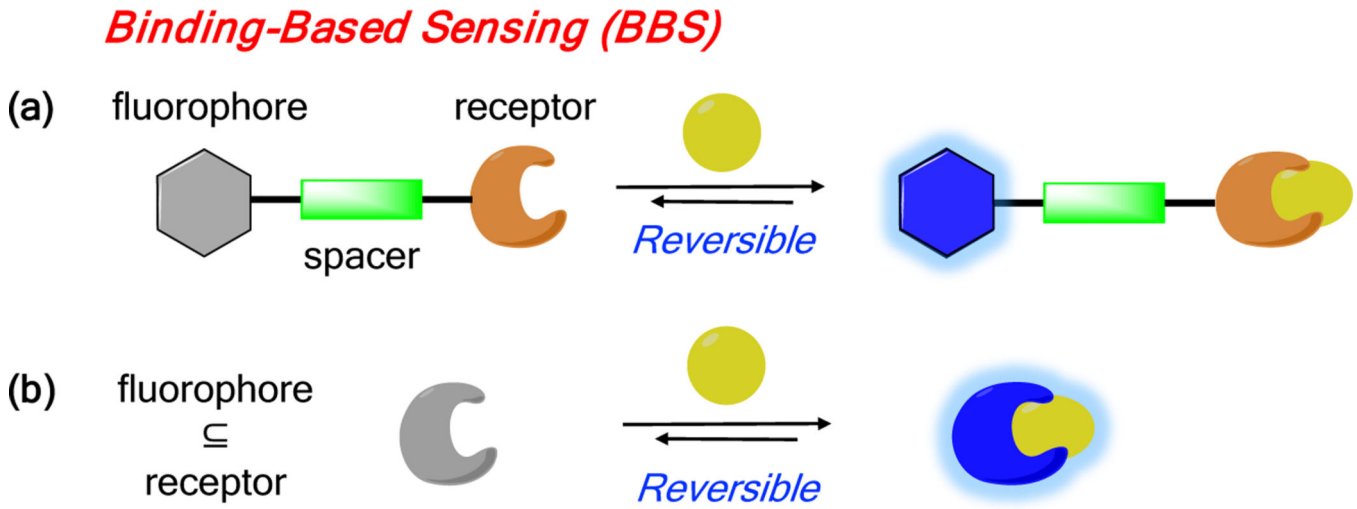

Scheme 1:

Schematic illustration of binding-based sensing (“BBS”). (a) The “fluorophore–spacer–receptor” paradigm. (b) A variation on the approach shown in (a) wherein the fluorophore and receptor are not discrete.

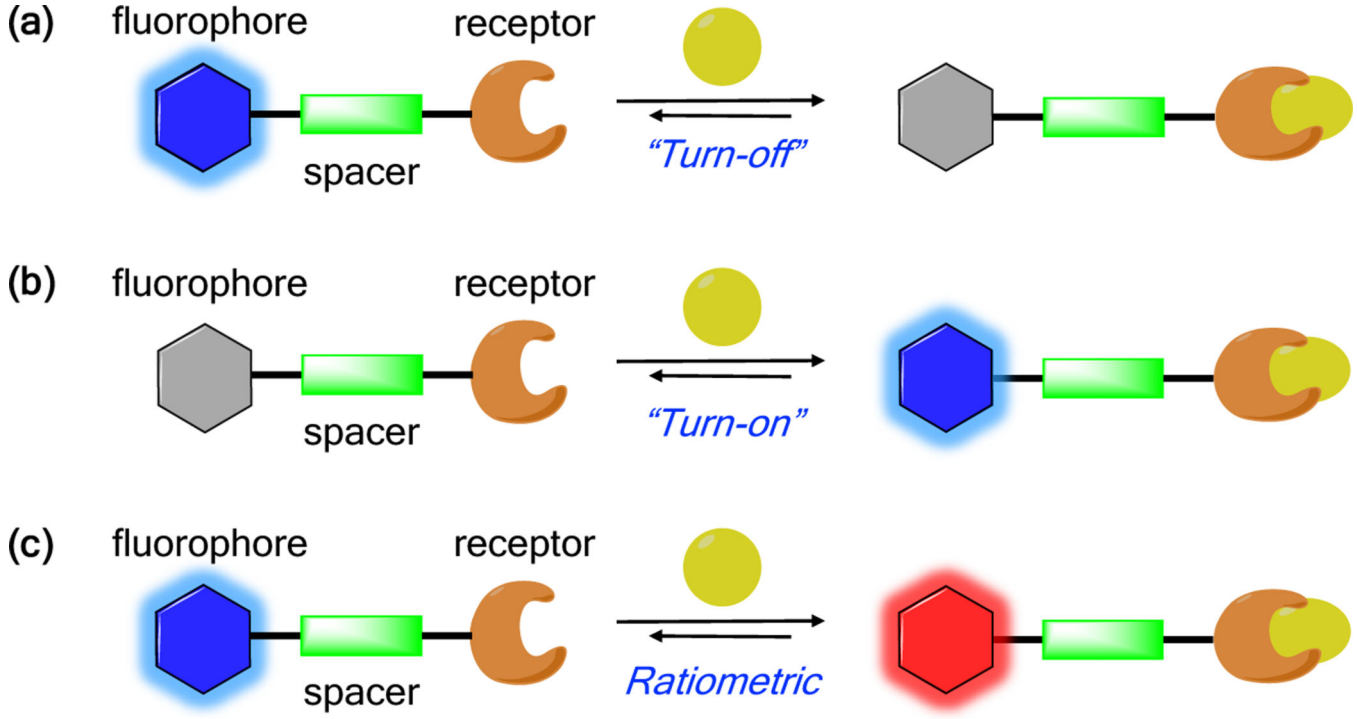

Scheme 2:
Schematic illustration of three limiting classes of sensors: (a) "turn-off"; (b) "turn-on"; (c) ratiometric.

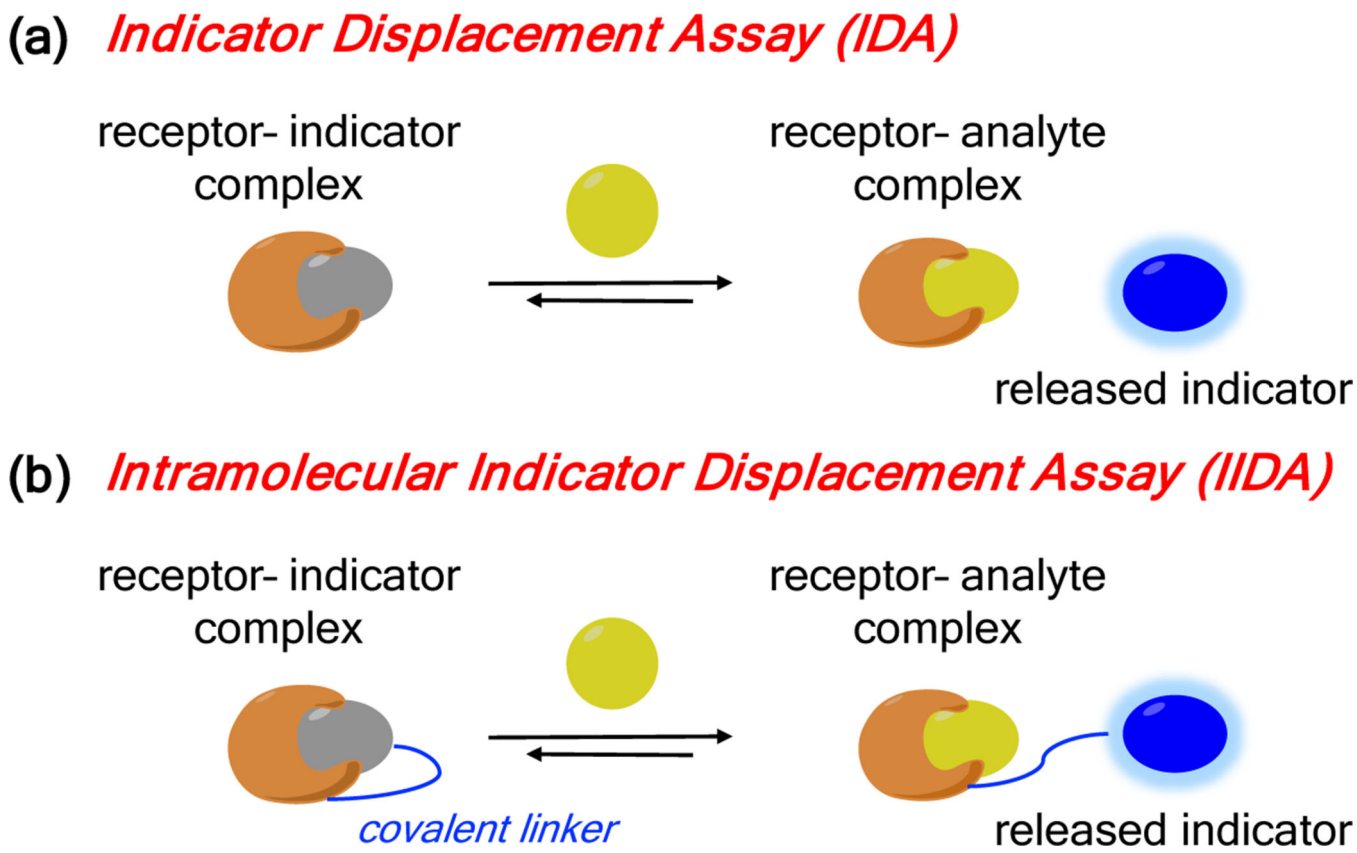

Scheme 3:
Schematic illustration of (a) an indicator displacement assay and (b) an intramolecular indicator displacement assay.

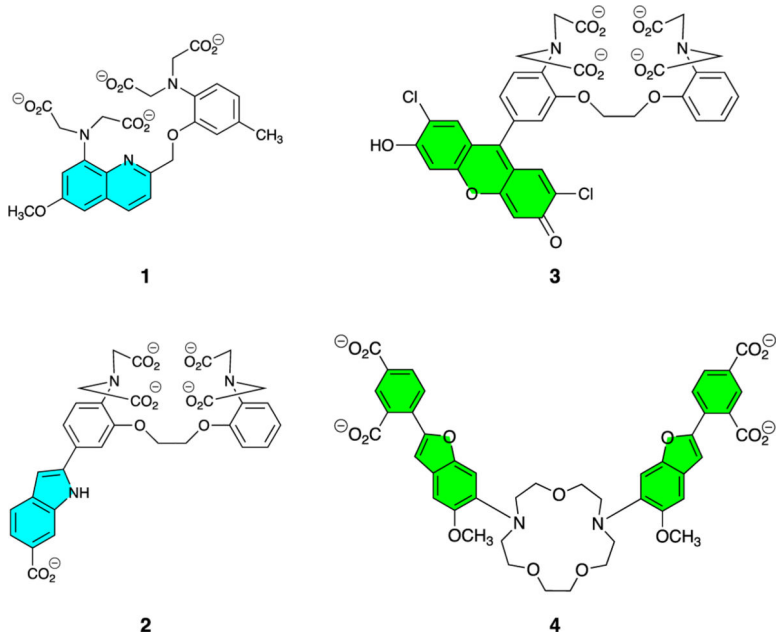

Figure 1:

Chemical structures of the fluorescent sensors for Ca^{2+} (**1–3**) and Na^{+} (**4**) developed by Tsien and co-workers.

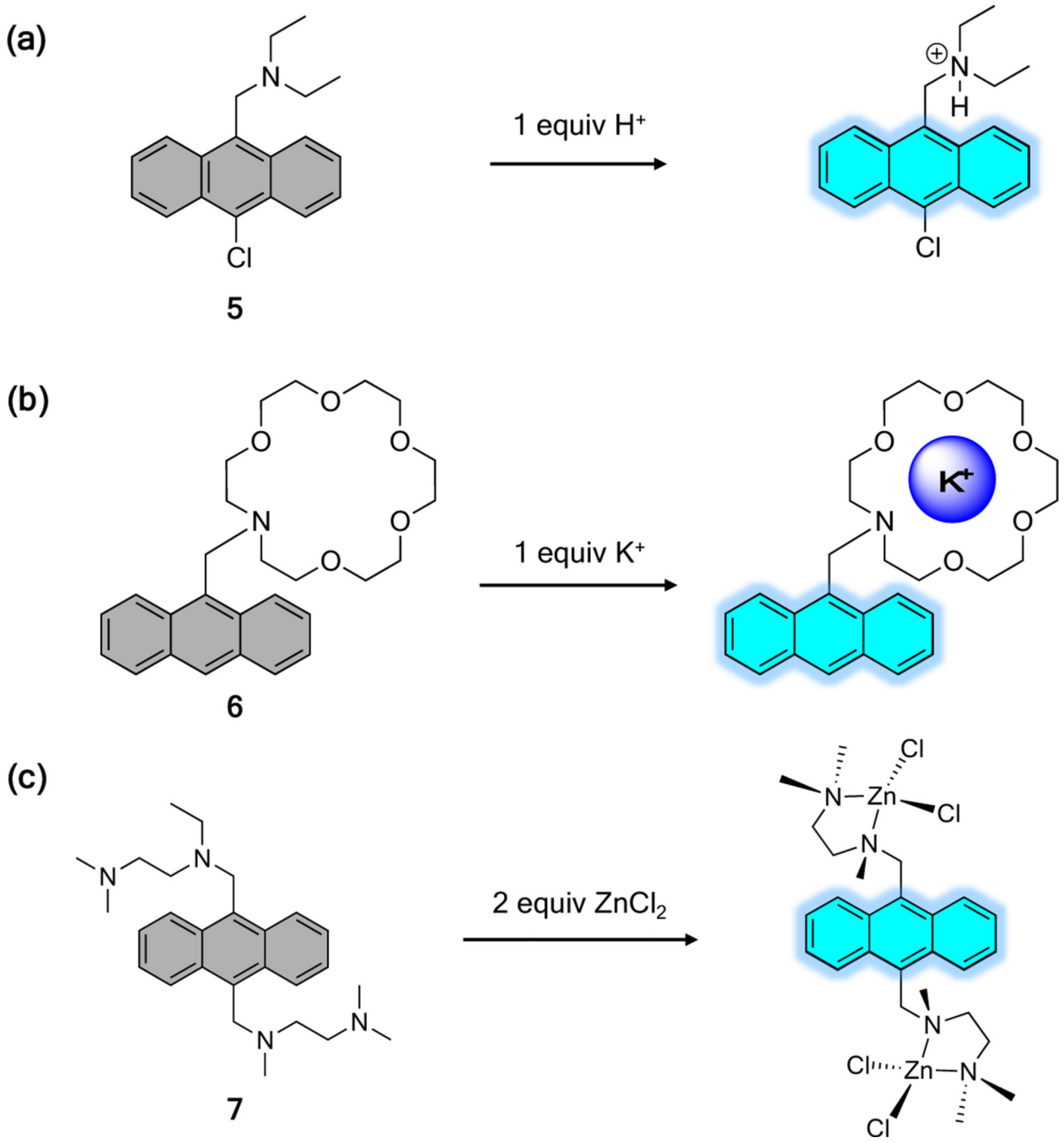

Figure 2:

Chemical structures of selected fluorescent PET sensors **5**–**7** showing schematically the "turn-on" response seen upon the addition of (a) H^+, (b) K^+, and (c) Zn^{2+}, respectively.

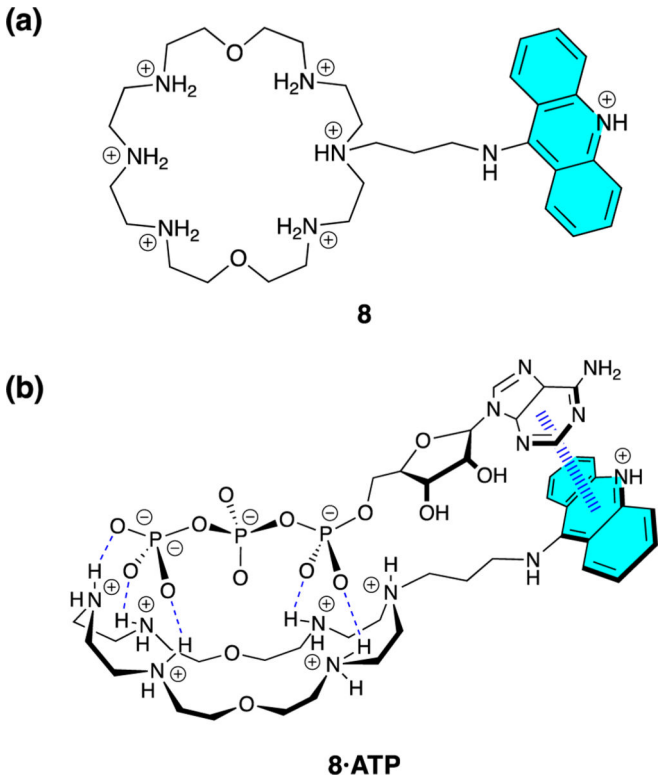

Figure 3:

(a) Chemical structure of the acridine-appended aza-crown ether **8** reported by Lehn and co-workers. (b) Presumed binding mode between **8** and ATP, where the hydrogen bonding and **π**–**π** interactions are highlighted by blue dashed lines. The counter anion (i.e., chloride) is omitted for clarity.

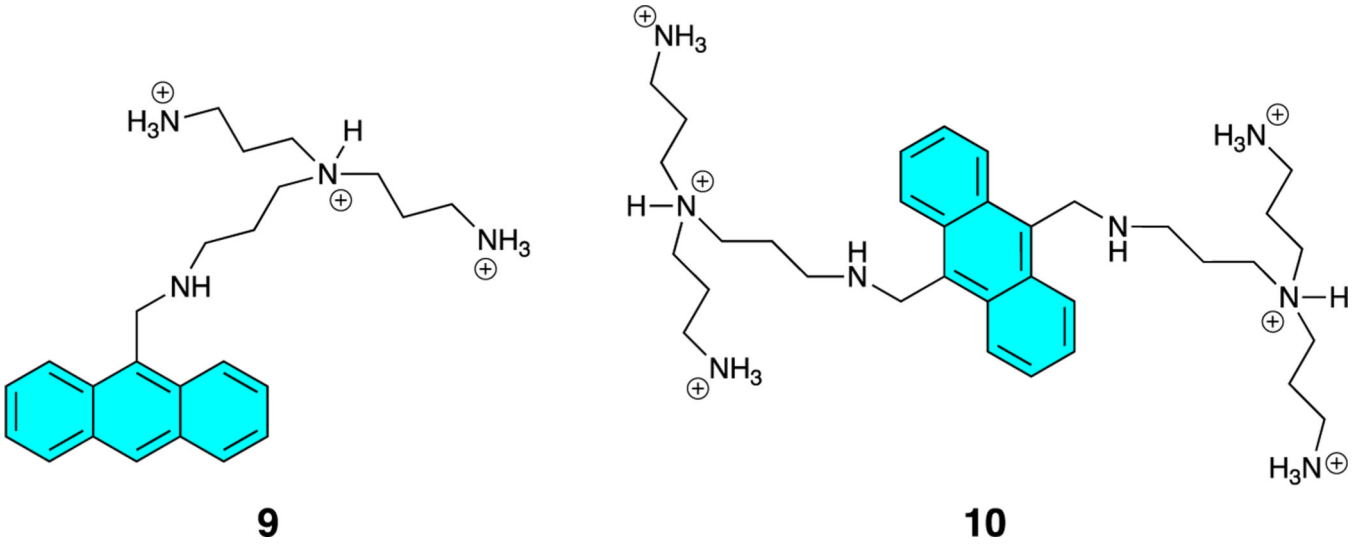

Figure 4:

Chemical structures of two protonated anthryl–polyamines **9** and **10** reported by Czarnik and co-workers. The counter anion (i.e., chloride) is omitted for clarity.

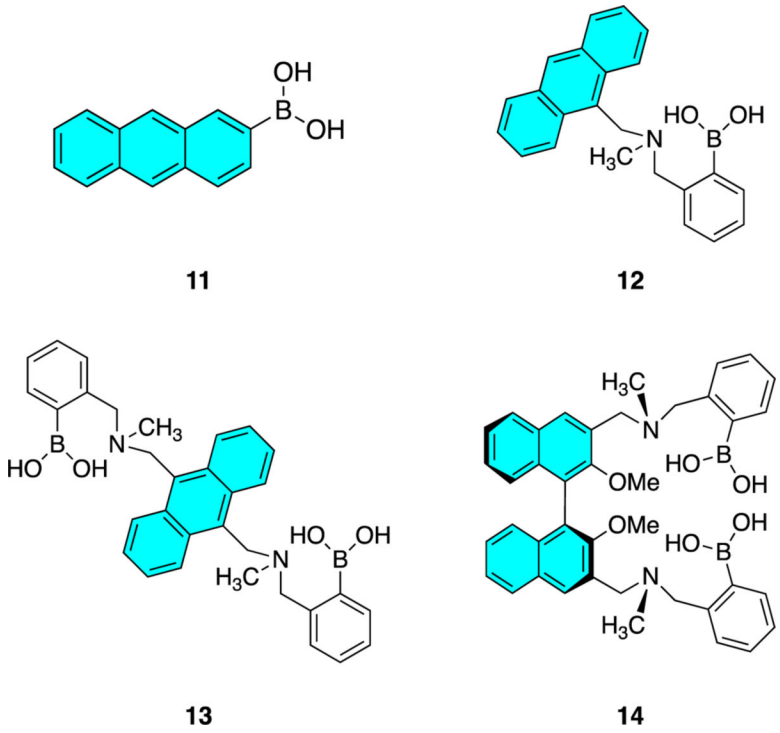

Figure 5:
Chemical structures of early PET sensors **11–14** for carbohydrates.

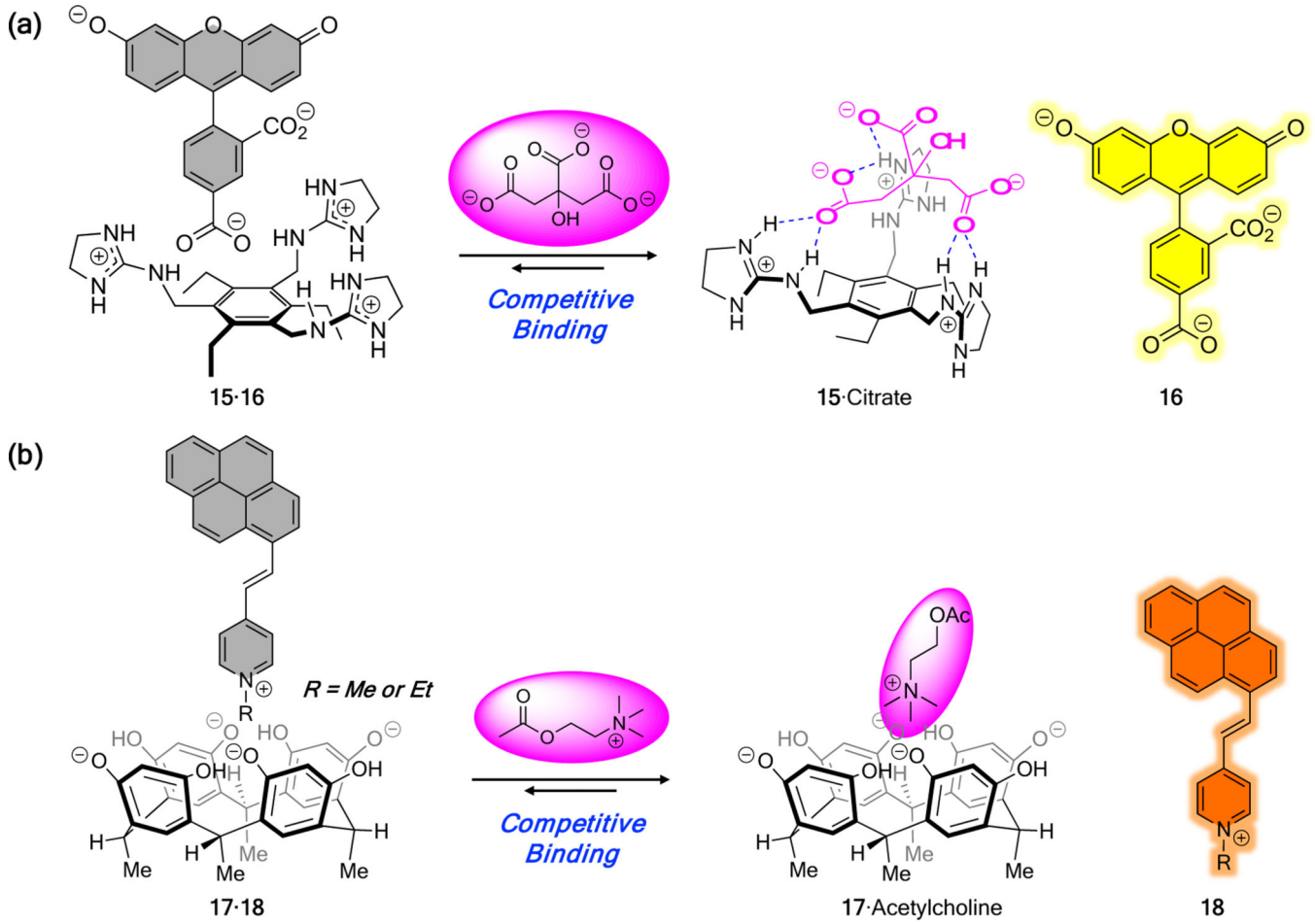

Figure 6:

Early examples of supramolecular fluorescent sensors based on indicator displacement assays. (a) Citrate sensor complex **15·16** developed by Anslyn and co-workers. (b) Acetylcholine sensor complex **17·18** developed by Inouye and co-workers.

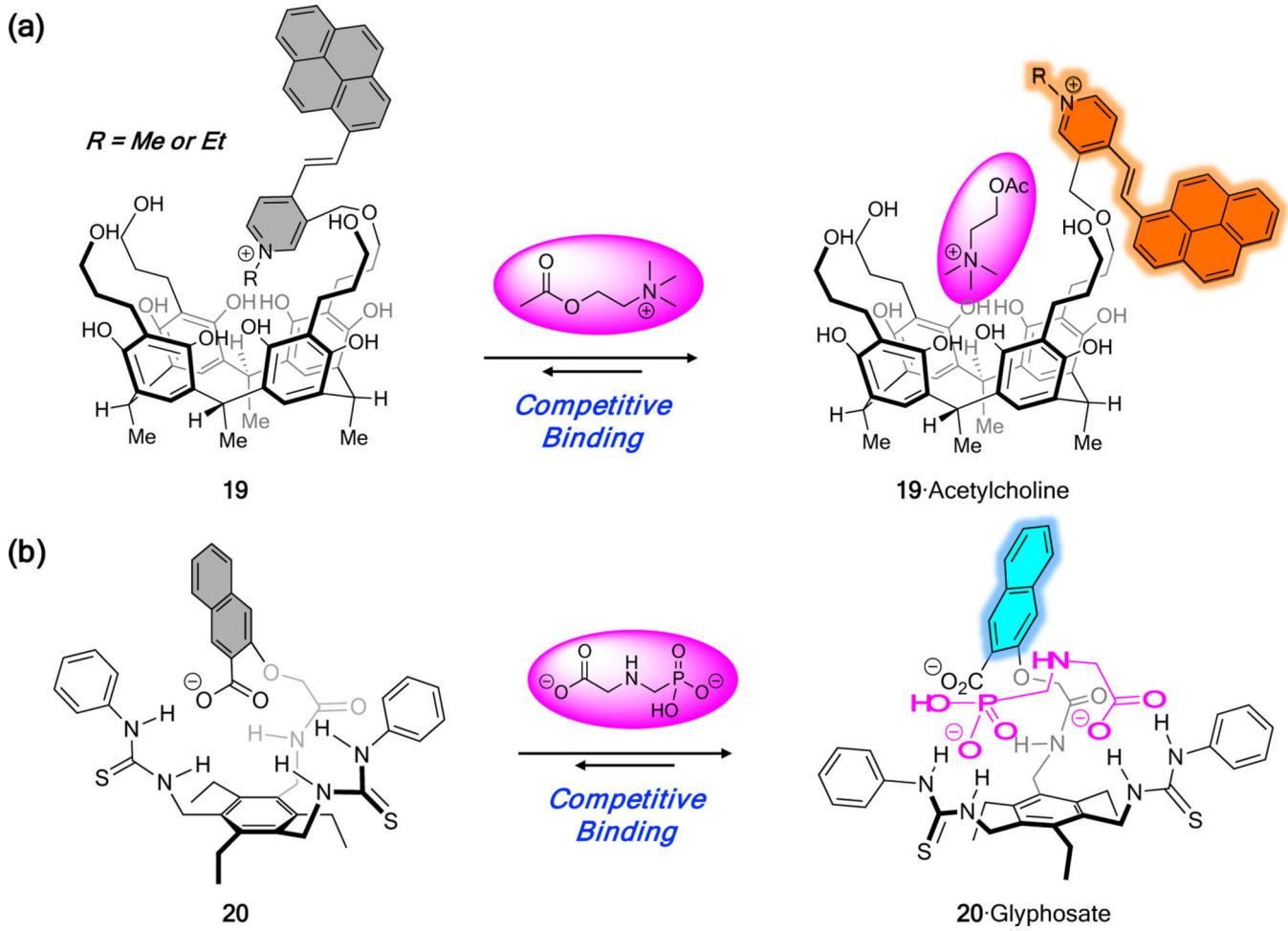

Figure 7:

Representative supramolecular fluorescent sensors based on intramolecular indicator displacement assays (IIDAs). (a) Acetylcholine sensor **19** developed by Inouye and co-workers. (b) Glyphosate sensor **20** developed by Anzenbacher, Kubo, and co-workers.

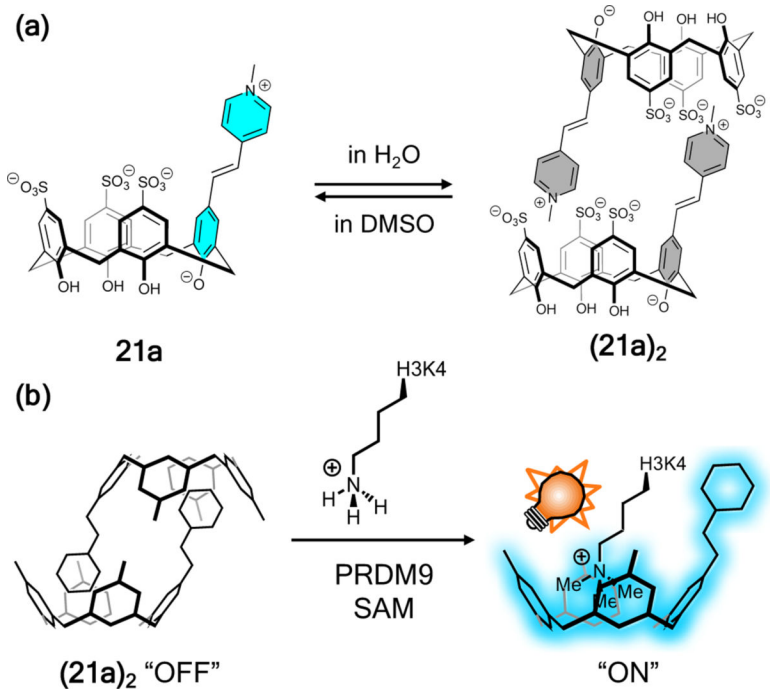

Figure 8:

DimerDye-disassembly assay (DDA) developed by Hof et al. (a) Solvent-dependent dimerization of the DimerDye **21a**. (b) Fluorescent "turn-on" response associated with the lysine methyltransferase reaction converting H3K4 to H3K4me3. Note: PRDM9 (positive-regulatory domain zinc finger protein 9) and SAM (S-adenyl-methionine) are the enzyme and the co-factor, respectively, required for the enzymatic conversion of H3K4 to H3K4me3.

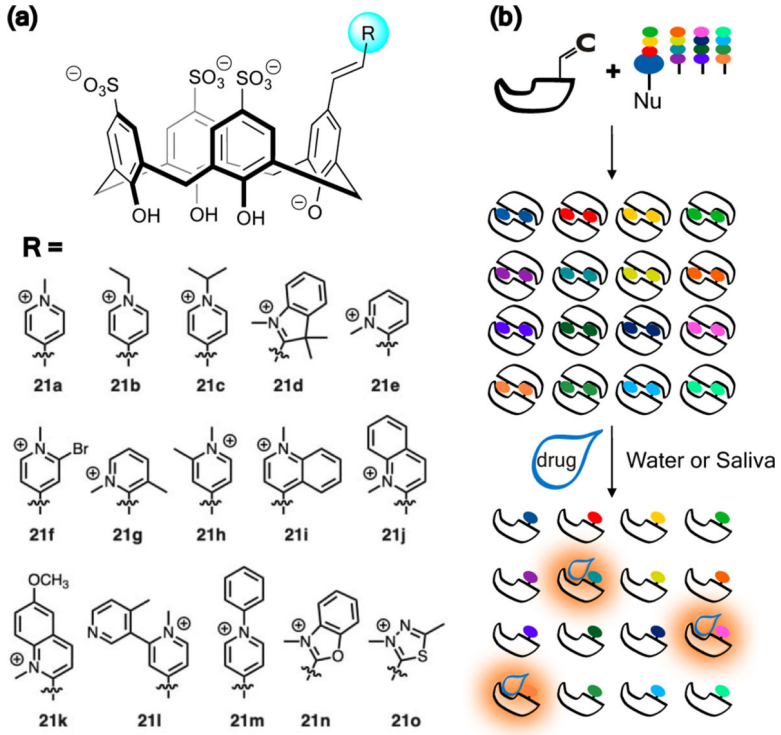

Figure 9.

Water-soluble calix[4]arene-dimers for illicit drug detection. (a) Chemical structures of the DimerDyes (DDs) subject to study. (b) Schematic view of the approach used to create a library of DDs that was used for the array-based sensing of drug molecules.

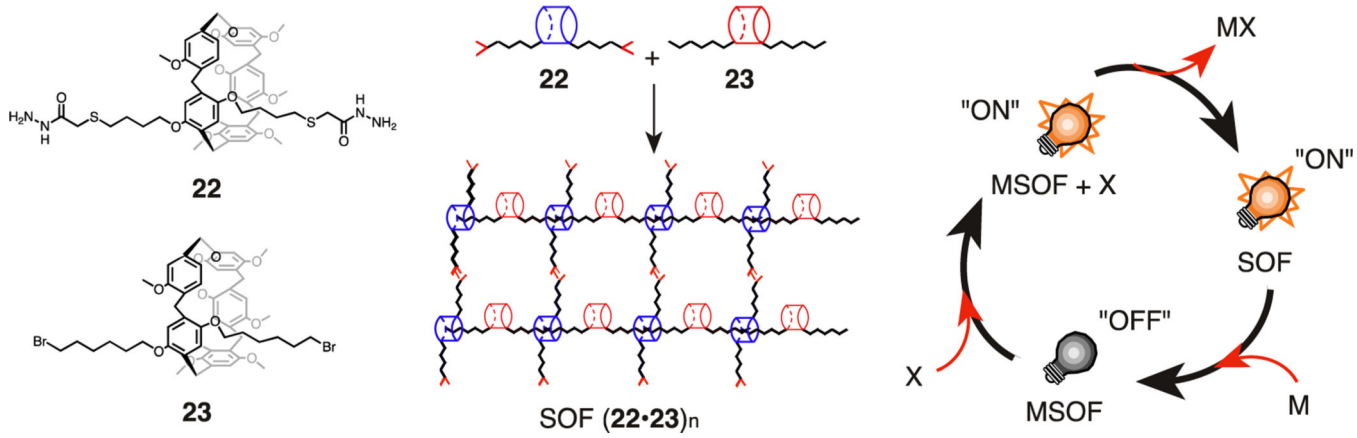

Figure 10.

Supramolecular organic framework (SOF) based on functionalized pillar[5]arenes **22** and **23** that allows for the detection and separation of various guests.

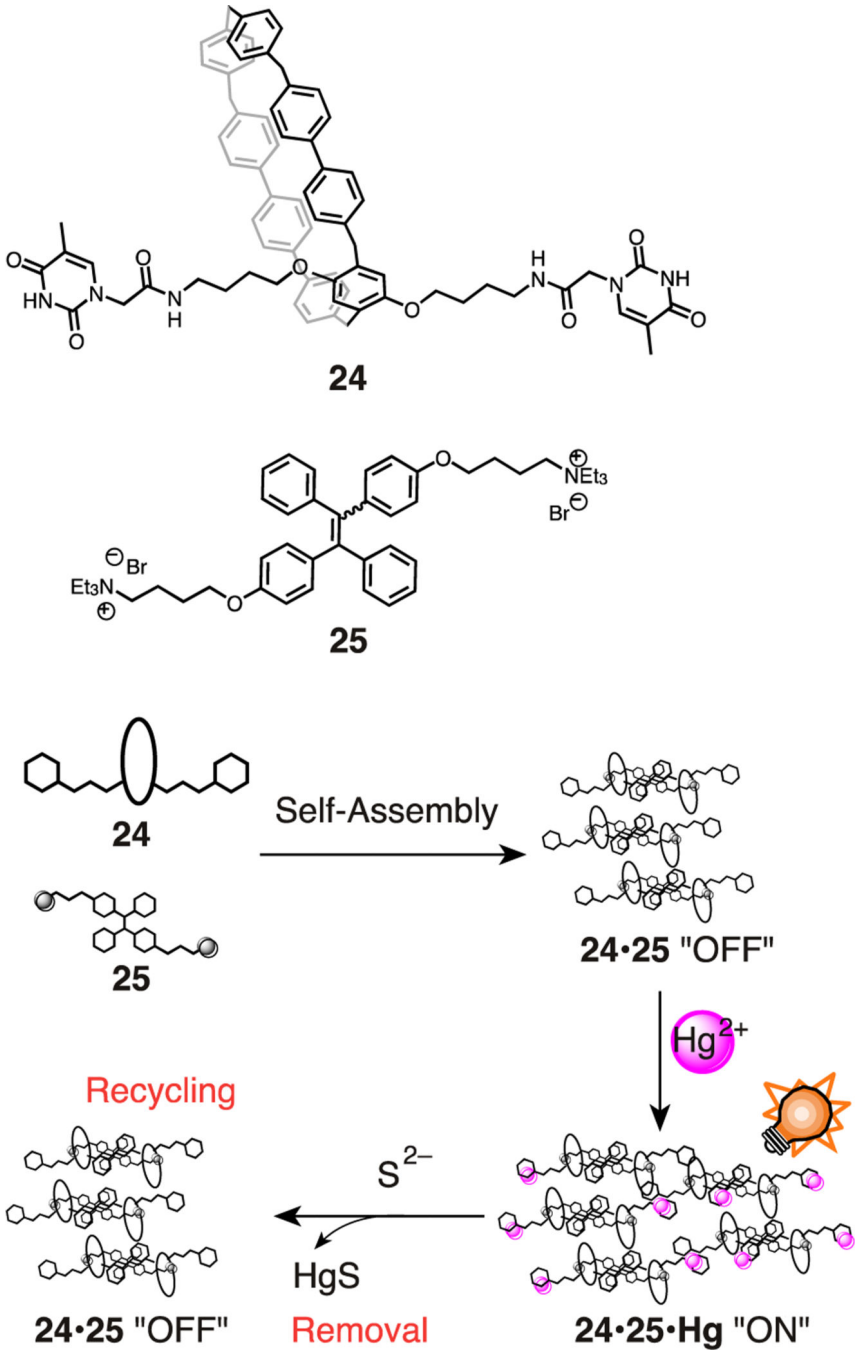

Figure 11.
Fluorescent supramolecular polymer that allows for efficient Hg^{2+} detection.

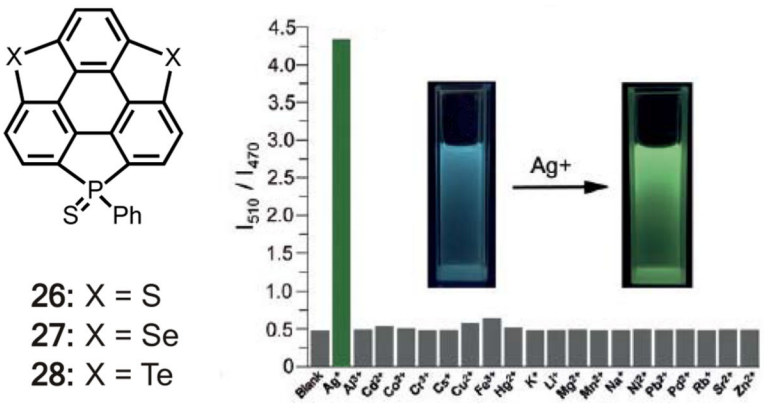

Figure 12.

Chemical structures of chalcogen- and phosphorus(V)-doped sumanenes **26**–**28** and the fluorescent "turn-on" response of **26** toward Ag^+. Reproduced with the permission from ref. 85. Copyright 2019 Wiley-VCH.

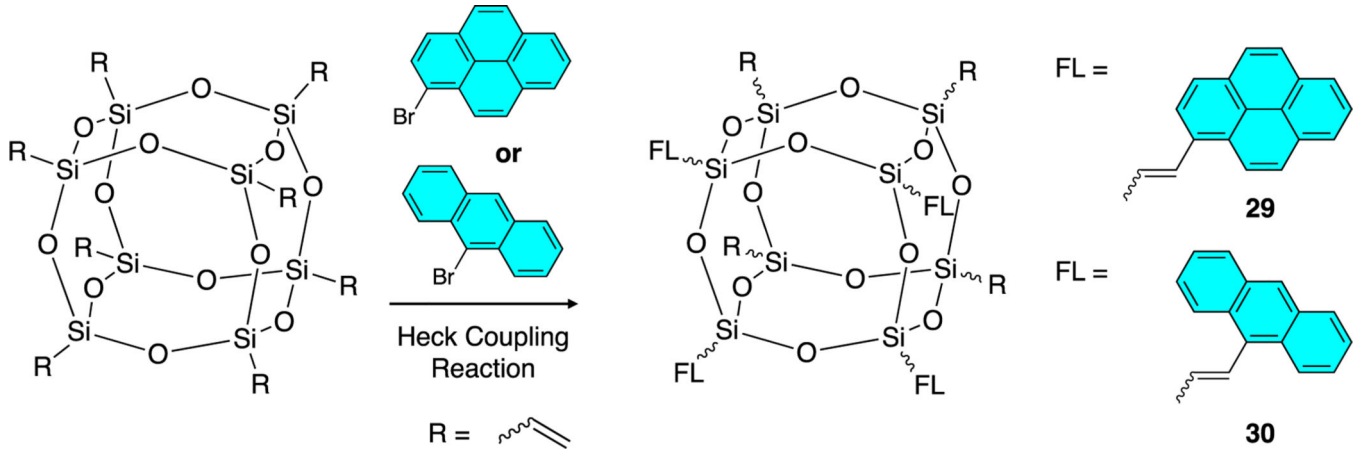

Figure 13.

Syntheses of two fluorescent sensors for the fluoride anion based on the pyrene-appended T_8 cage **29** and anthracene-appended T_8 cage **30**. Note: The cubic oligosilsesquioxanes **29** and **30** are the proposed structures of the most abundant species among all possible products inferred from mass spectrometric analyses.

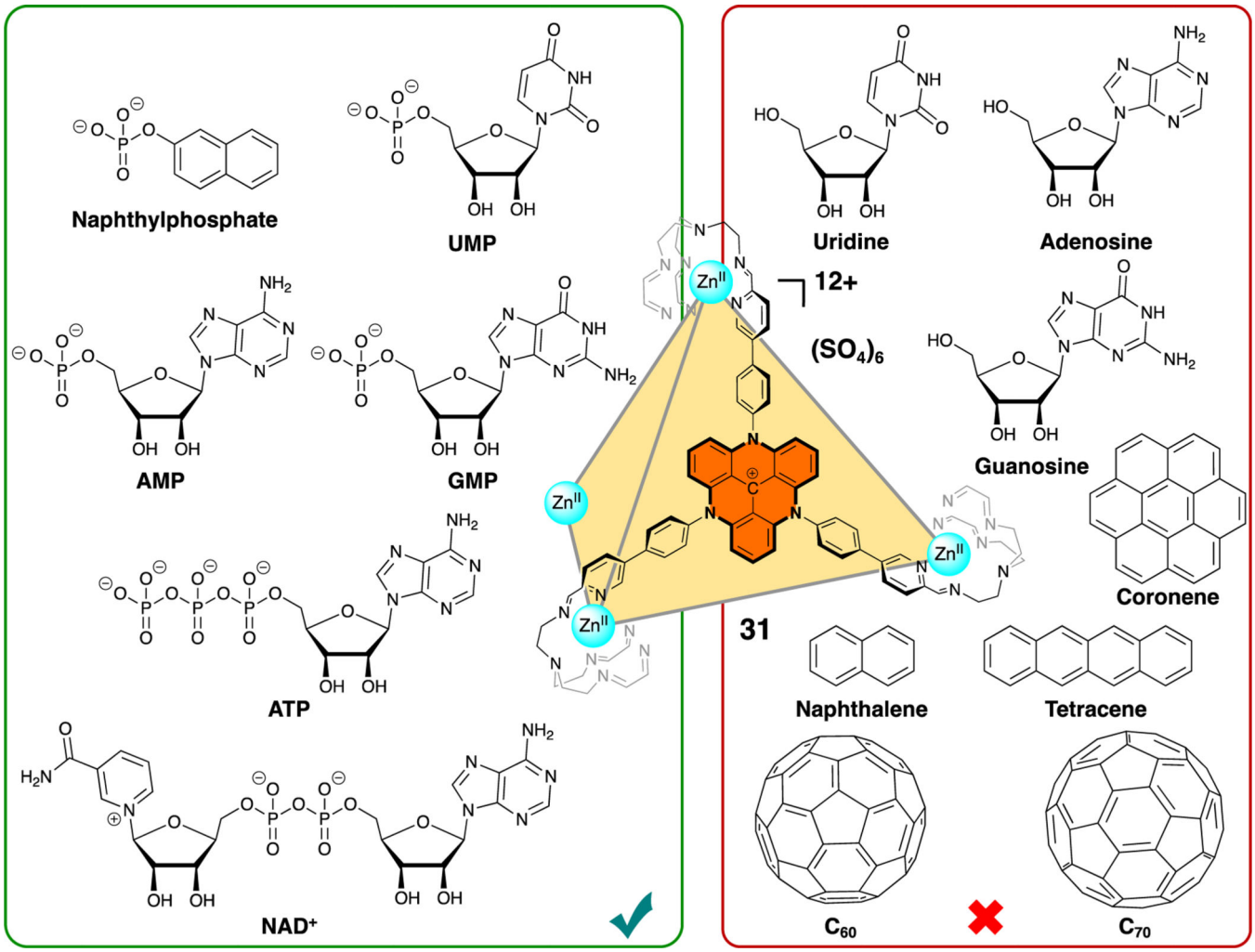

Figure 14.

Chemical structures of the subcomponent self-assembled cationic cage **31** and various test anionic and neutral guests. The guests shown in the green box can be encapsulated inside the interior cavity of cage **31**, whereas those shown in the red box are not encapsulated effectively within cage **31**. Reproduced with permission from ref. 95. Copyright 2019 Wiley-VCH.

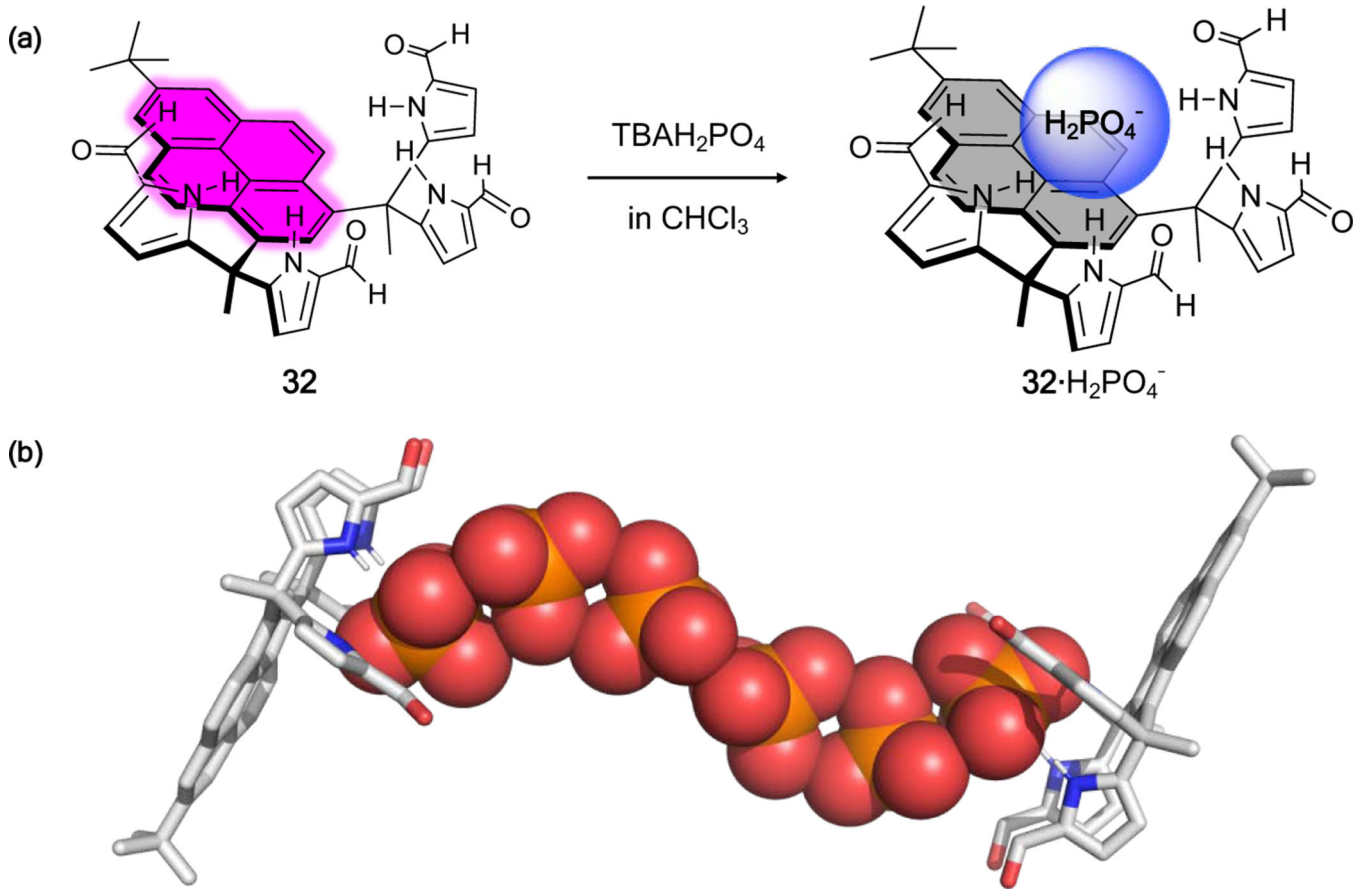

Figure 15:

(a) Fluorescent "turn-off" probe **32** used for the fluorescent sensing of dihydrogen phosphate. (b) Single crystal structure of the complex [**32**·3$H_2PO_4^-$]$_2$ (counter cation and solvent molecules are omitted for clarity). This figure was reproduced using data downloaded from the Cambridge Crystallographic Data Centre (CCDC: 1854747).

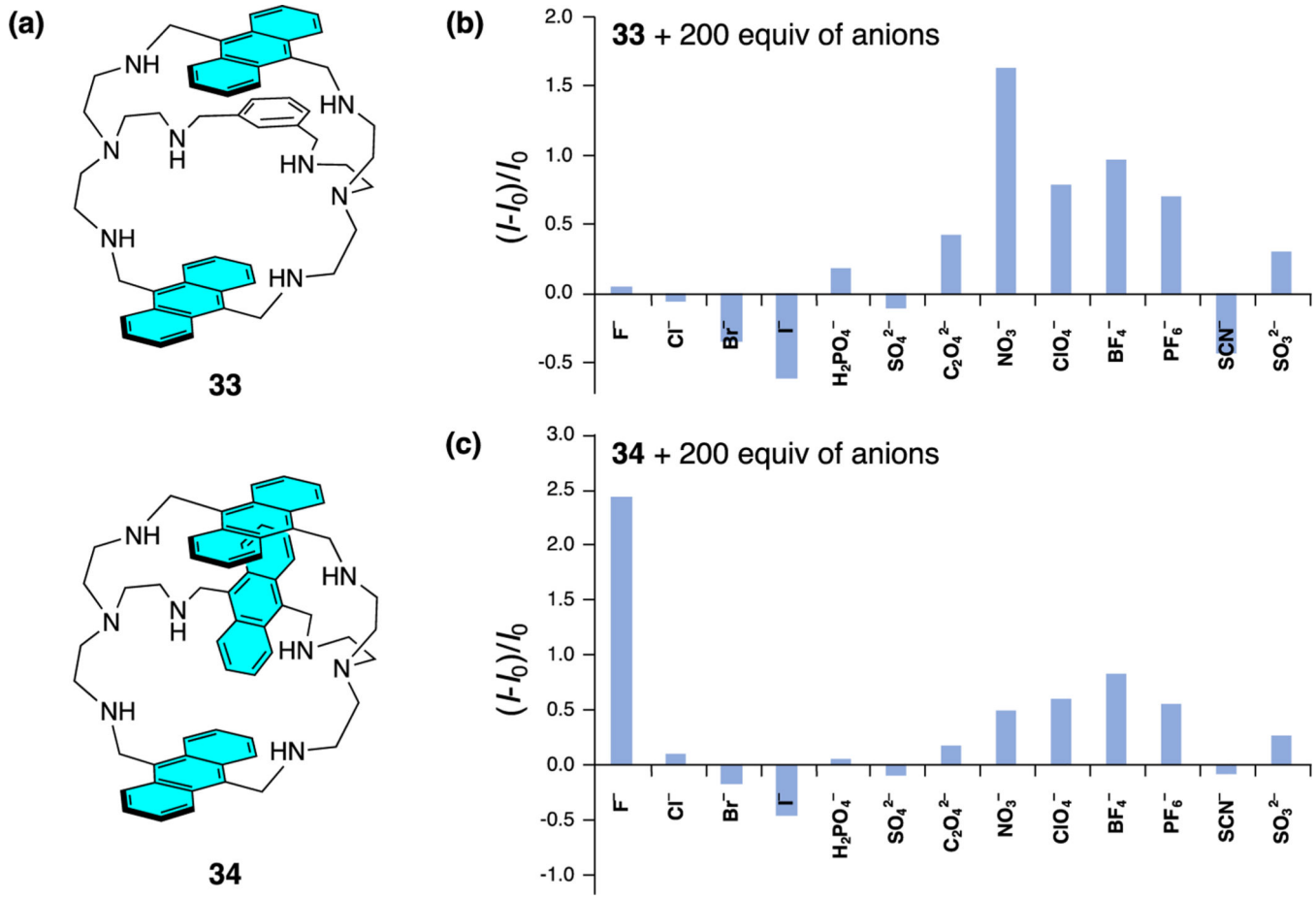

Figure 16:

Anthracene-modified azacryptands **33** and **34** and their respective saturated fluorescent response to various anions. Reproduced with the permission from ref. 101. Copyright 2019 American Chemical Society.

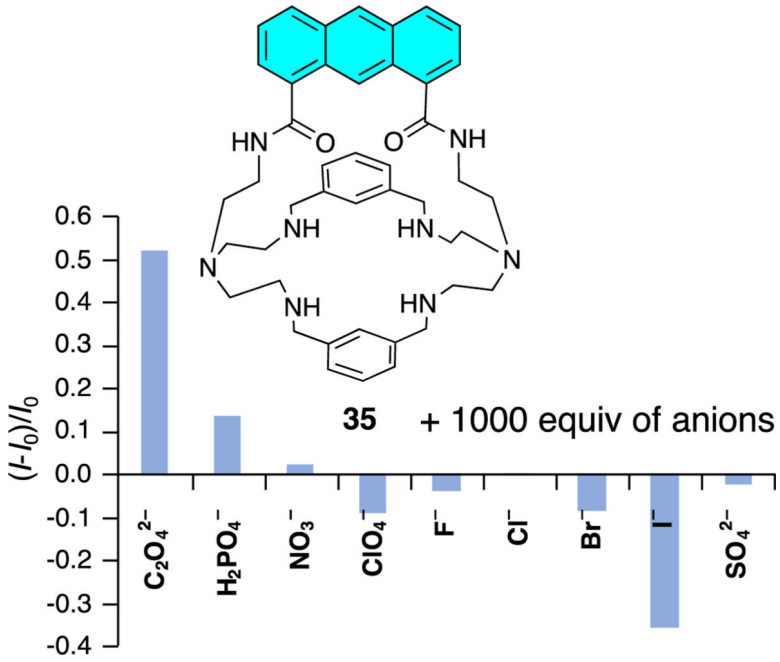

Figure 17:

Anthracene-modified azacryptand **35** and its fluorescent response to various anions under saturating conditions. Reproduced with the permission from ref. 104. Copyright 2020 Wiley-VCH.

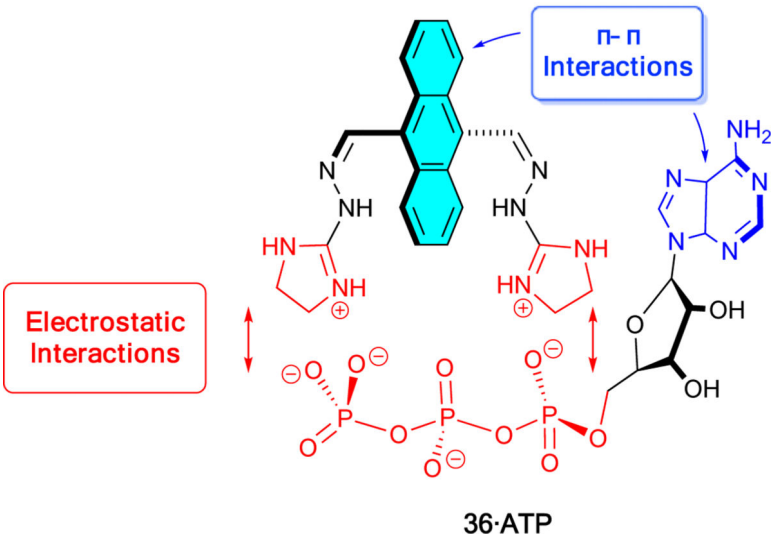

Figure 18:

Proposed mechanism underlying the fluorescent “turn-on” sensing of ATP in aqueous media provided by the bisantrene-derived sensor **36**.

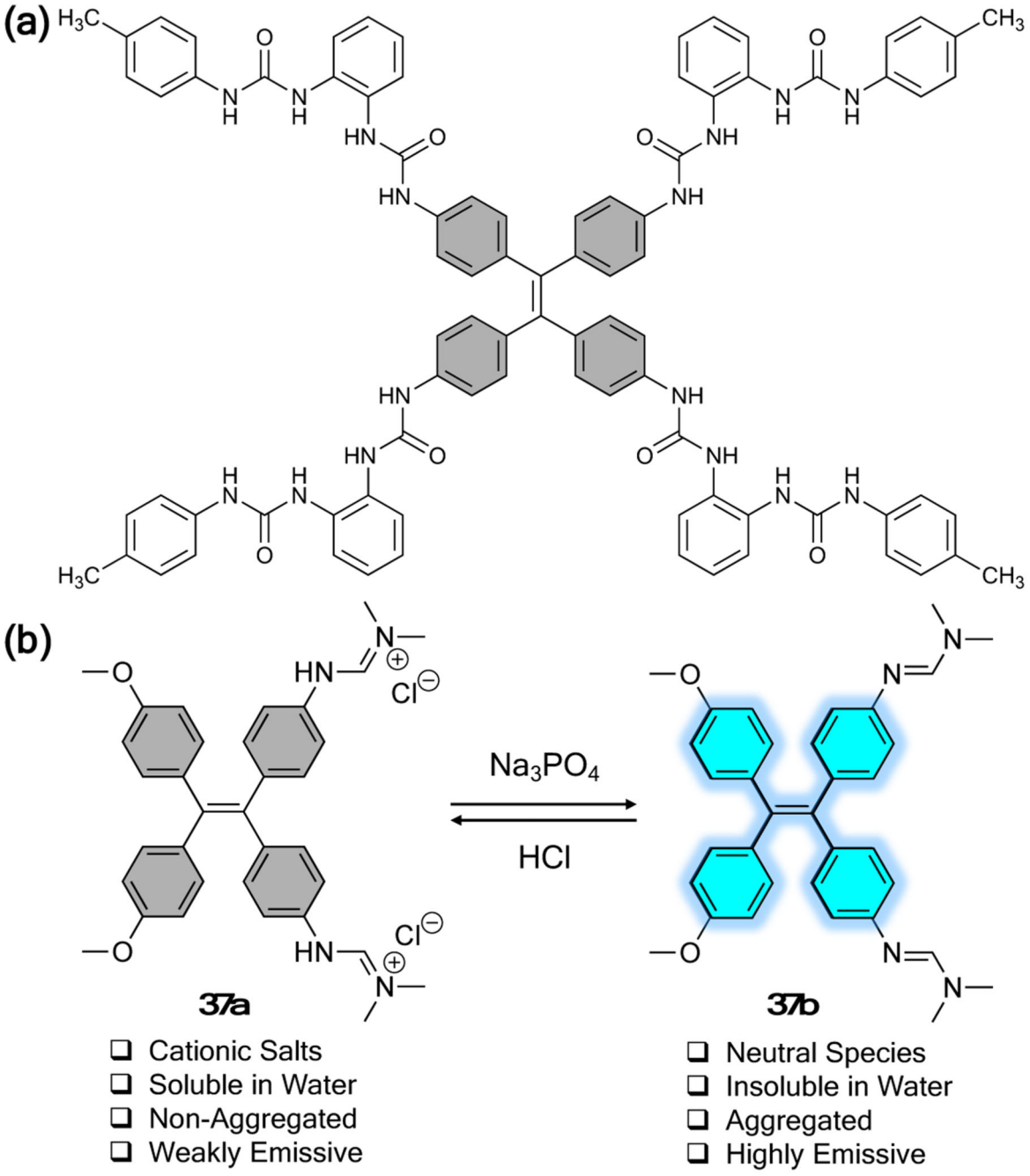

Figure 19:
(a) Chemical structure of a TPE-based anion sensor reported by Wu et al. in 2014. (b) A simplified TPE-based sensor that proved effective for sodium phosphate recognition in aqueous media.

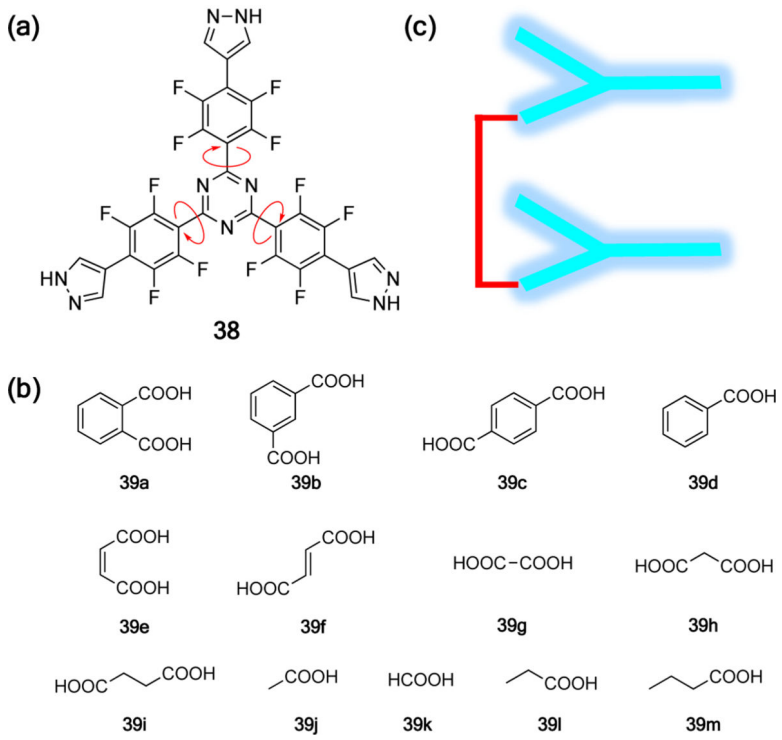

Figure 20:

Fluorescent sensor **38** that proved effective for sensing dicarboxylic acids **39a**–**39m** in a response-selective manner presumably as the result of a RIM mechanism. (a) Chemical structure of sensor **38**. Note: The red arrows indicate the presumed rotation of the single bonds in solution. (b) Chemical structures of various test carboxylate acids. (c) Cartoon illustration of the proposed rotationally restricted dimer.

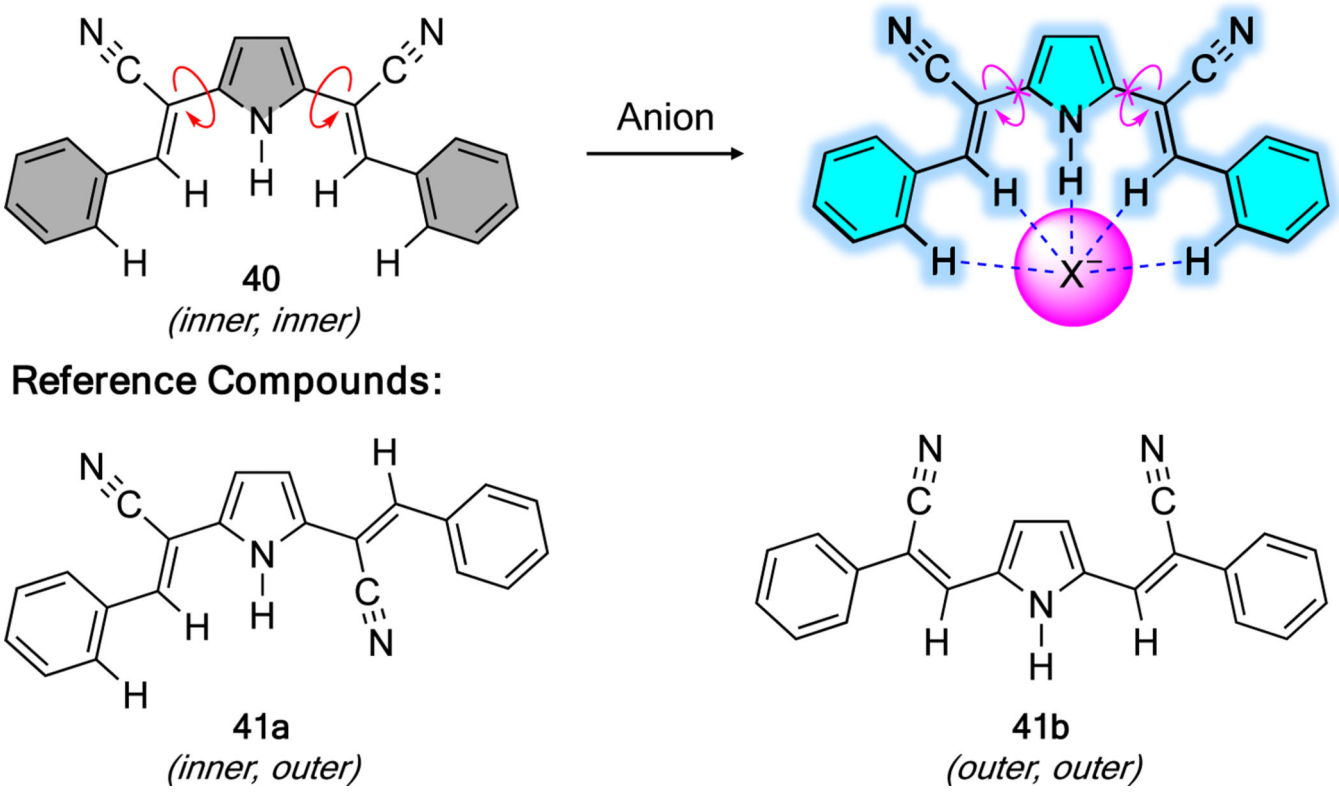

Figure 21:

Anion-coordination-induced emission (ACIE) of a bis(cyanostyryl)pyrrolic anion receptor **40** and its analogs **41a** and **41b**. Note: the “inner” and “outer” shown in the parentheses indicate the relative positions of the cyano groups.

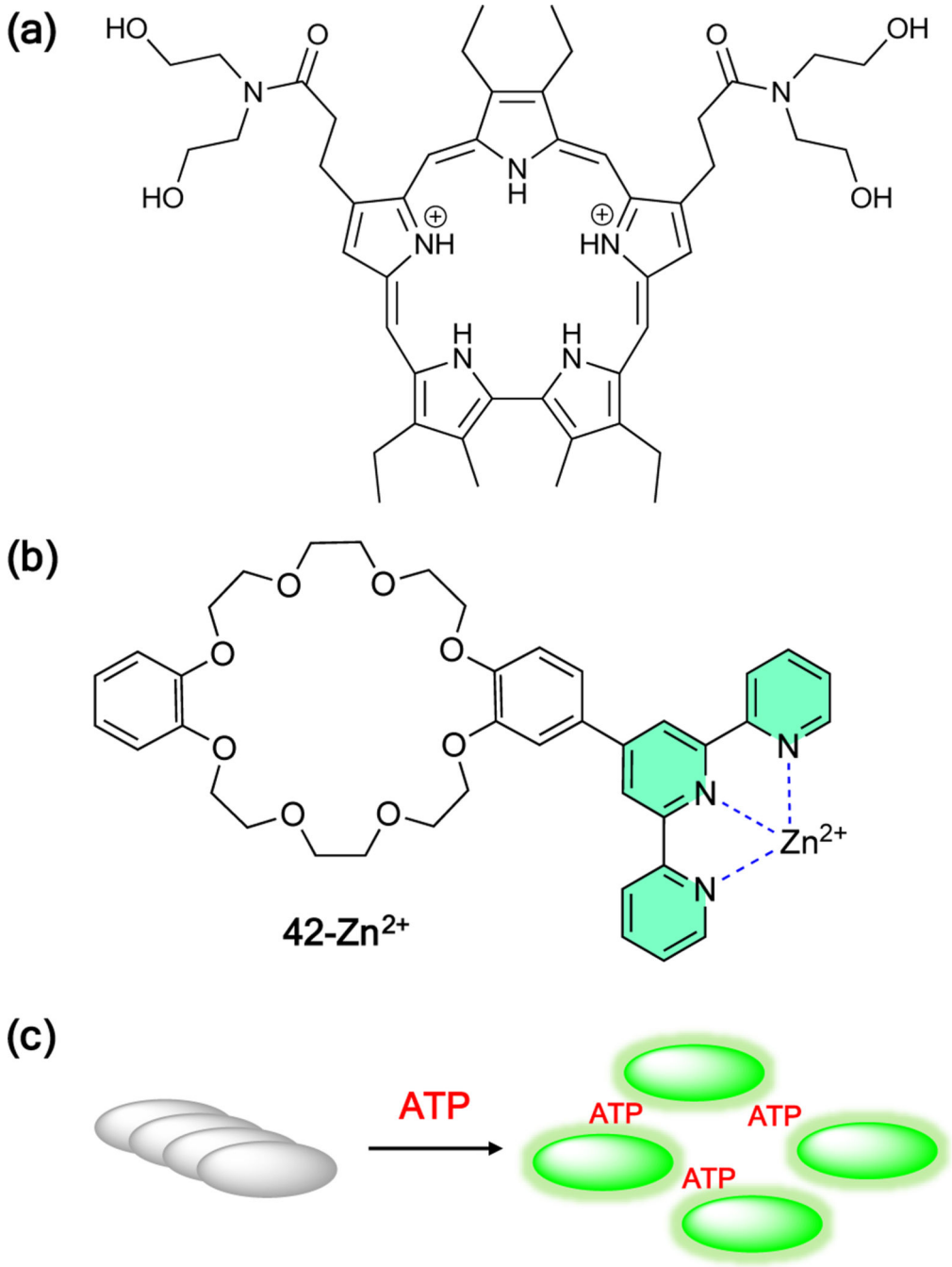

Figure 22:

(a) Chemical structure of a water-soluble sapphyrin capable of producing “turn-on” response to phosphate anions reported early on by Sessler et al. (b) Chemical structure of a DIE-based fluorescent “turn-on” sensor **42** for ATP. (c) Schematic representation of ATP-induced breakup of the aggregates of **42** formed in water.

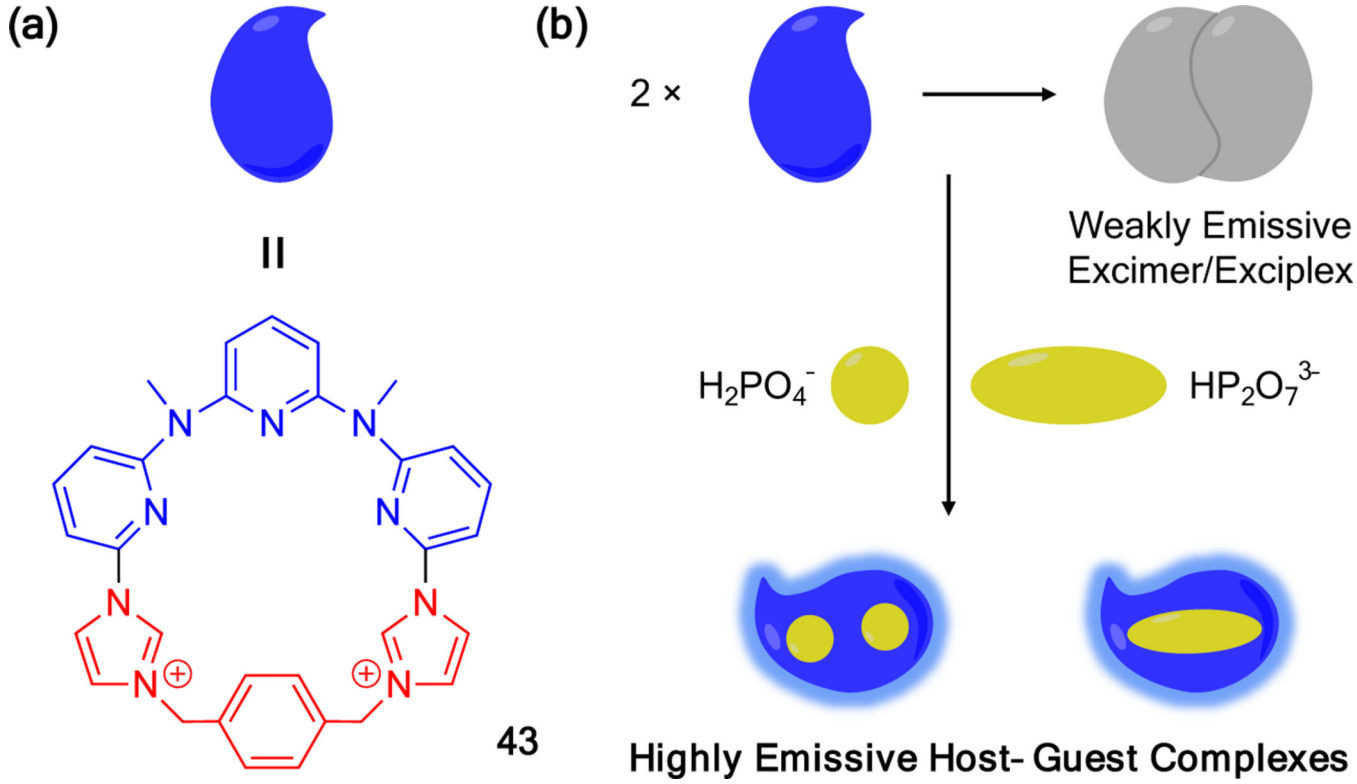

Figure 23:
A macrocyclic EDIE sensor for $H_2PO_4^{3-}$ and $HP_2O_7^{3-}$ oxyanions developed by Gong and Sessler et al.

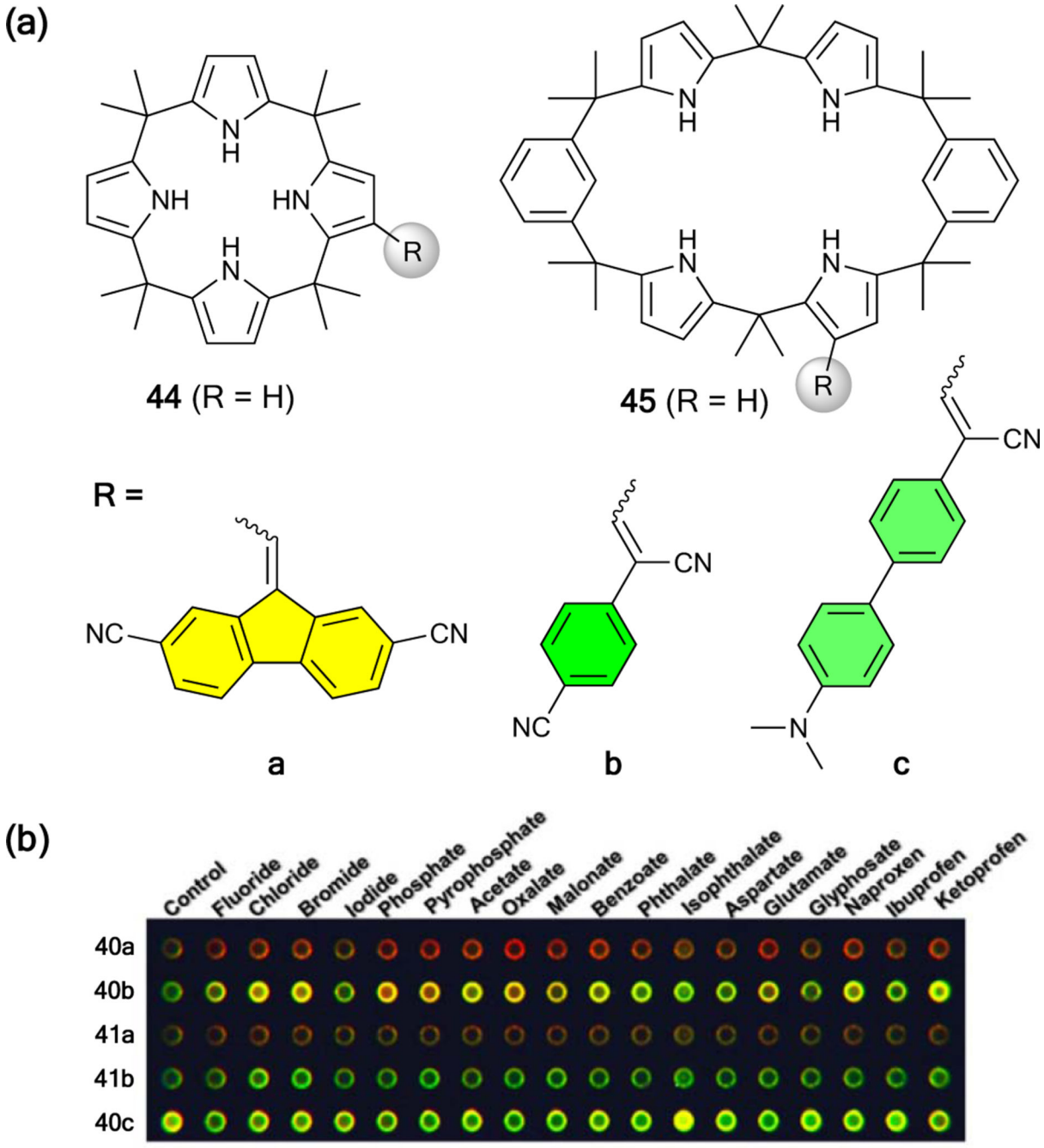

Figure 24:

(a) Chemical structures of the fluorophore-appended calix[4]pyrroles **44a**–**44c** and the fluorophore-appended calix[2]benzo[4]pyrroles **45a** and **45b**. (b) Photograph showing a polymer microchip array wherein sensors **41a**–**41c**, **45a**, and **45b** are embedded in a polyurethane matrix along with the optical response produced upon exposure to anions (as their TBA^+ salts in water/THF) under conditions of photoexcitation. Reproduced with the permission from ref. 134. Copyright 2018 Wiley-VCH.

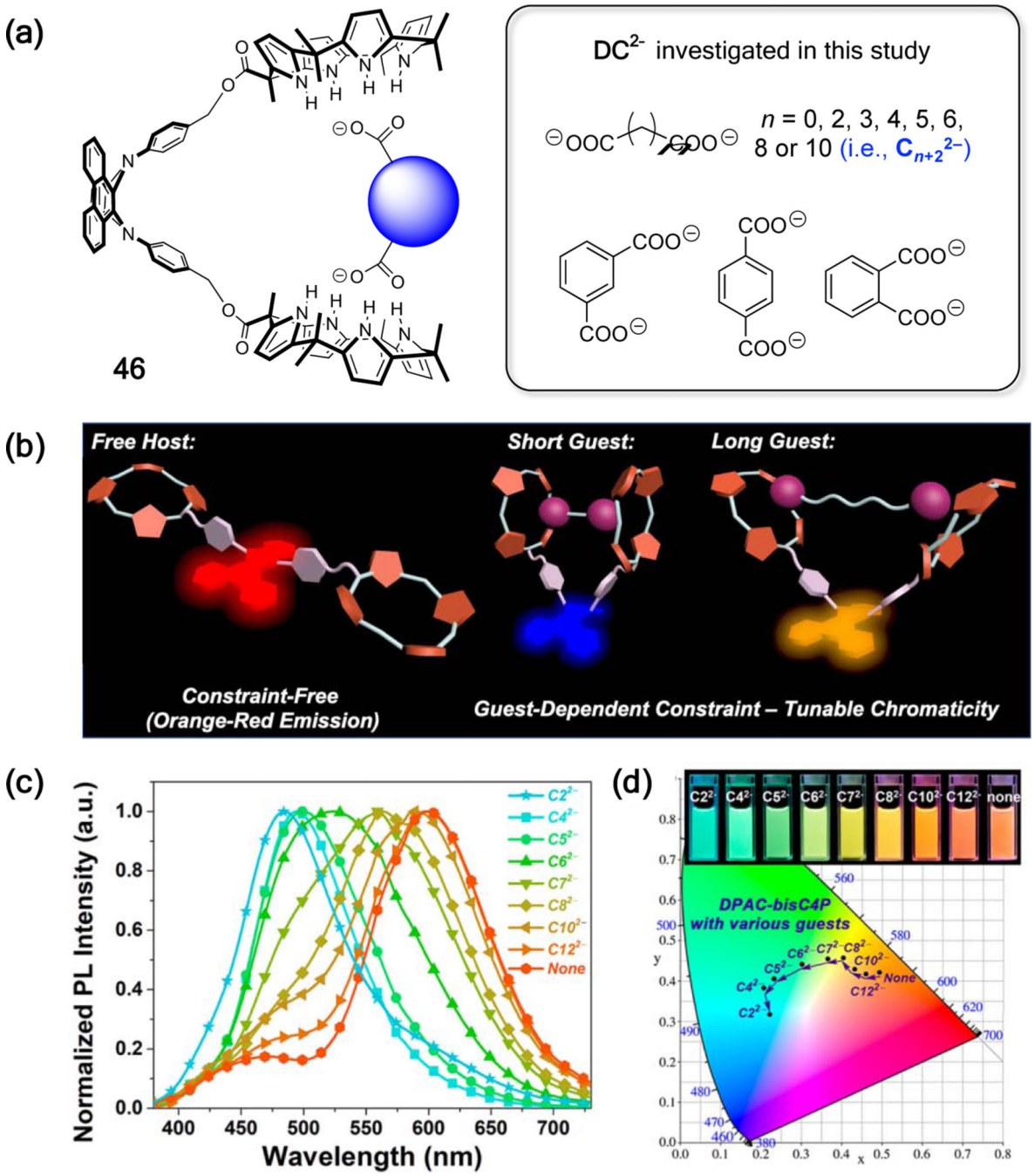

Figure 25:

(a) Chemical structures of sensor **46** and dicarboxylate anion guests tested as substrates. (b) Proposed working principle of the VIE-active dicarboxylate anion sensor based on **46**. (c) Normalized fluorescent emission spectra of the host–guest complexes. (d) Chromaticity coordinates (CIE) along with the photographs showing the respective emission colors of the host–guest complexes. Reproduced with the permission from ref. 139. Copyright 2019 American Chemical Society.

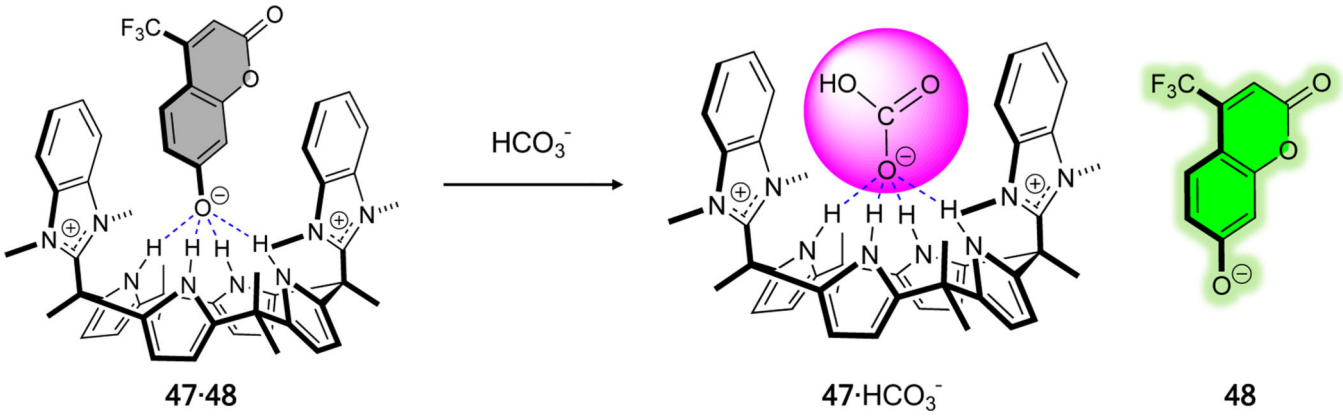

Figure 26:
IDA-based sensing of bicarbonate using a bis(imidazolium)-functionalized calix[4]pyrrole receptor **47** and coumarin-derived fluorescent dye **48**.

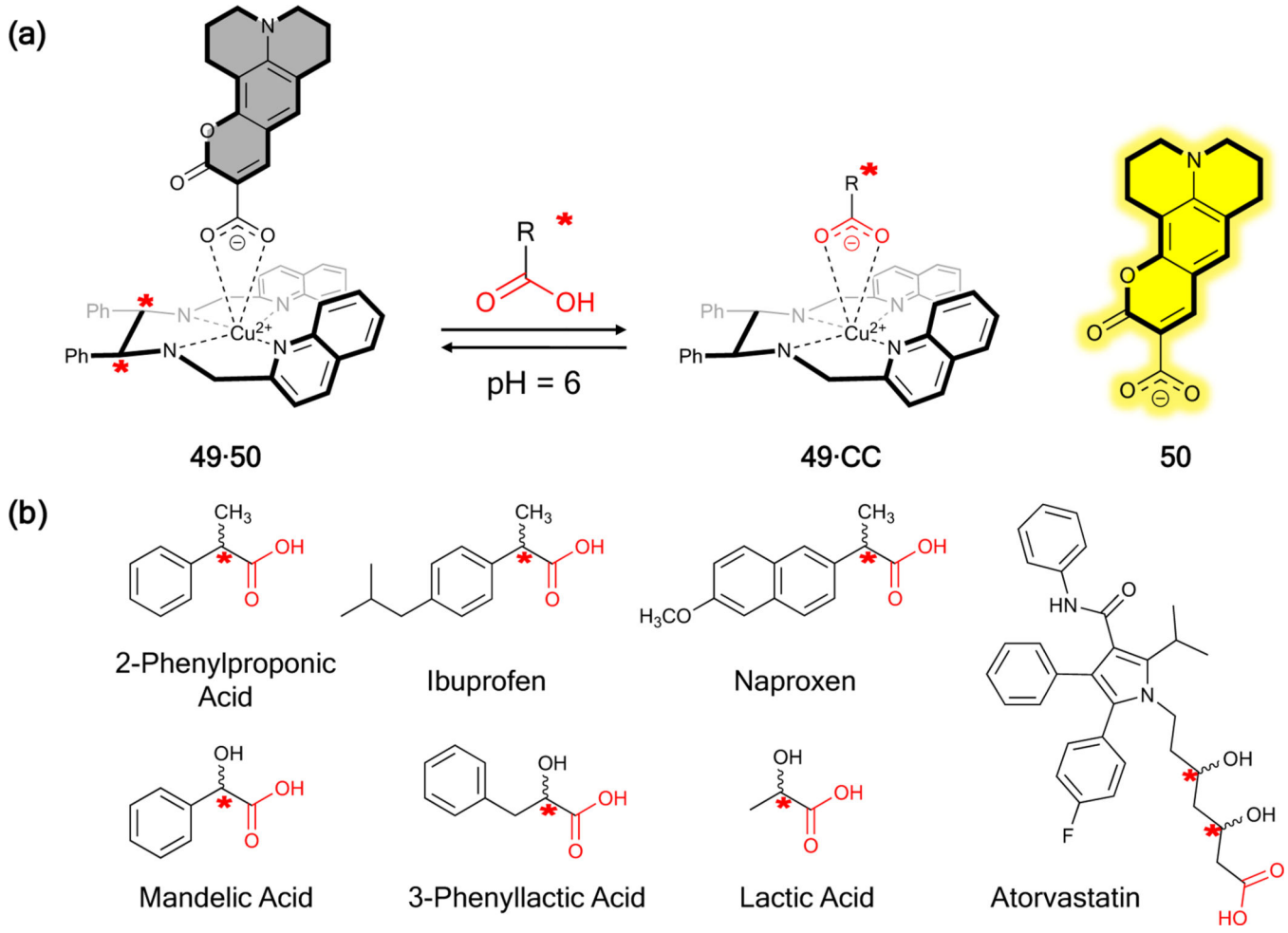

Figure 27:
(a) Chirality sensing of chiral carboxylates (CCs) based on eIDA. (b) All CCs investigated in this study.

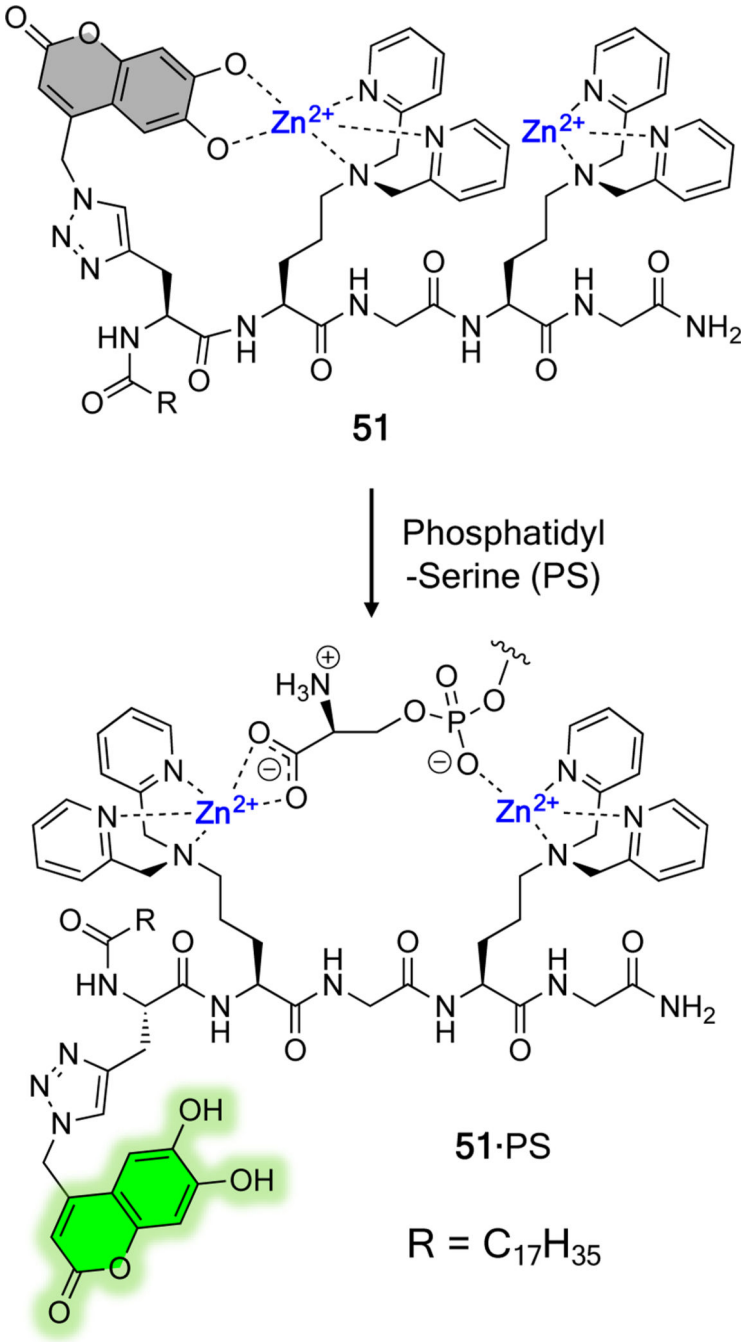

Figure 28:
IIDA-based fluorogenic probe **51** used to sense phosphatidylserine on the surface of cells.

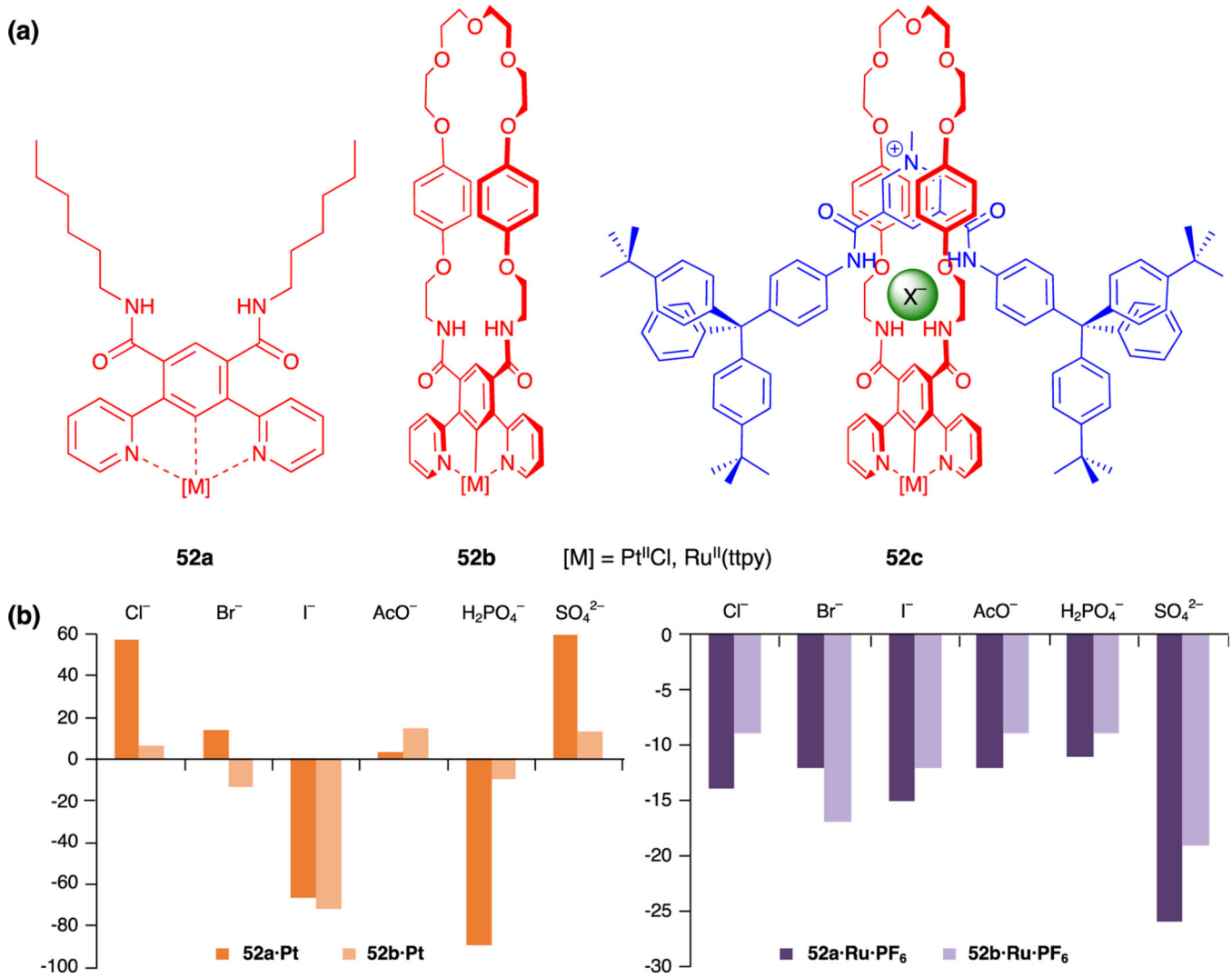

Figure 29:

(a) Chemical structures of the acyclic, macrocyclic, and interlocked anion sensors **52a**, **52b**, and **52c**, respectively, where ttpy = tolylterpyridine. (b) Fluorescent response of the hosts in question to anionic guests. Reproduced with the permission from ref. 150. Copyright 2019 Wiley-VCH.

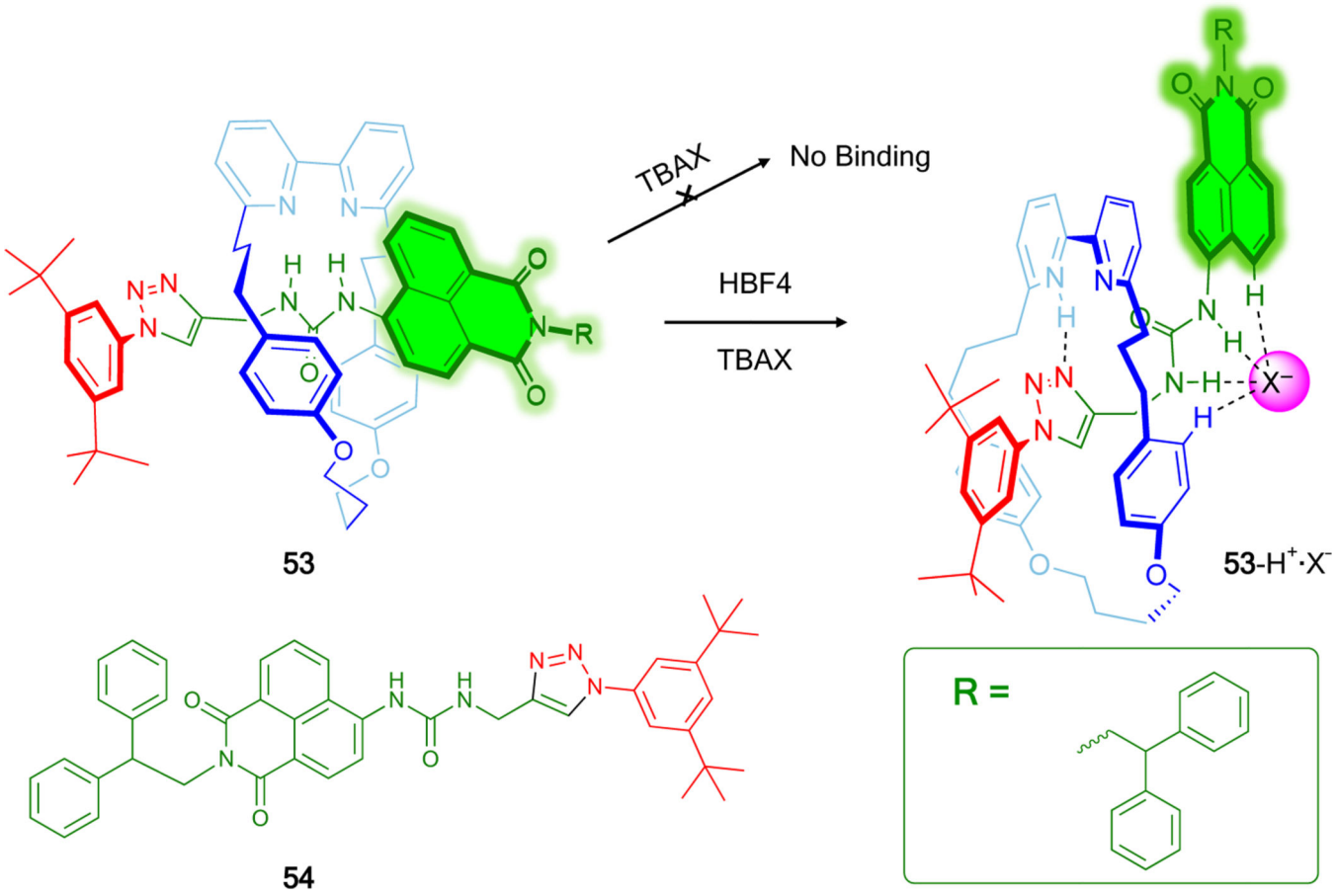

Figure 30:

Rotaxane-based ion pair receptor **53** and its sensing capability. The chemical structure of the control compound **54** is also shown.

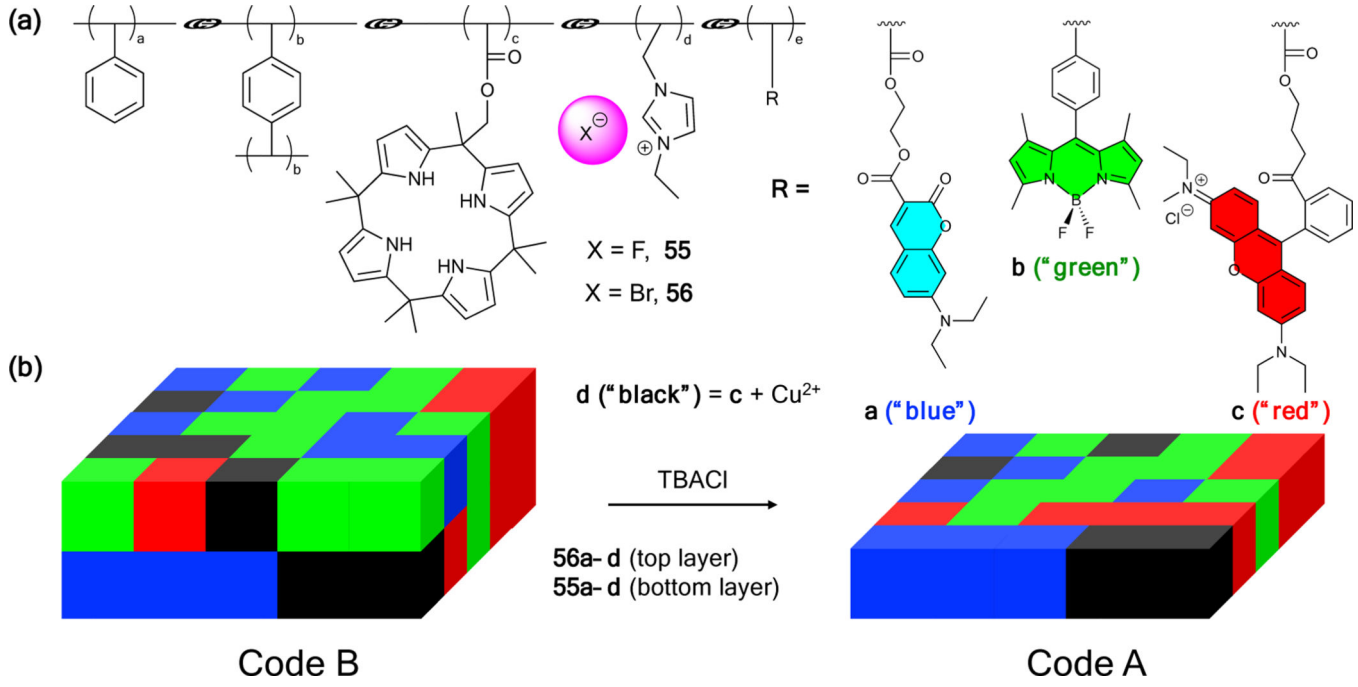

Figure 31:

Chloride sensing using fluorescent organogels based on 3D codes. (a) Chemical structures of the polymeric organogels **55a–d** and **56a–d**. (b) Sensing mechanism showing the delamination of the double-layered 3D codes that allows for chloride sensing.

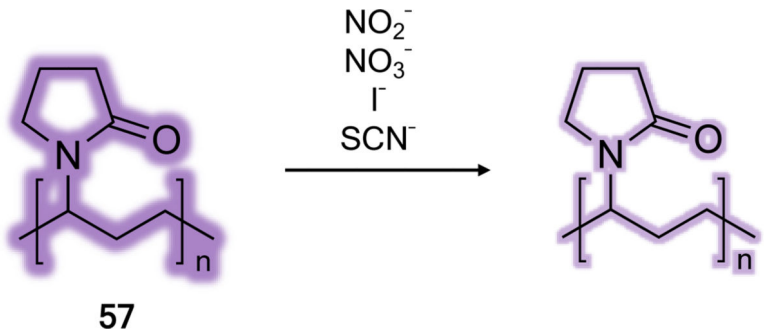

57

Figure 32:
Off-the-shelf polymer **57** that acts as a fluorescent “turn-off” anion sensor.

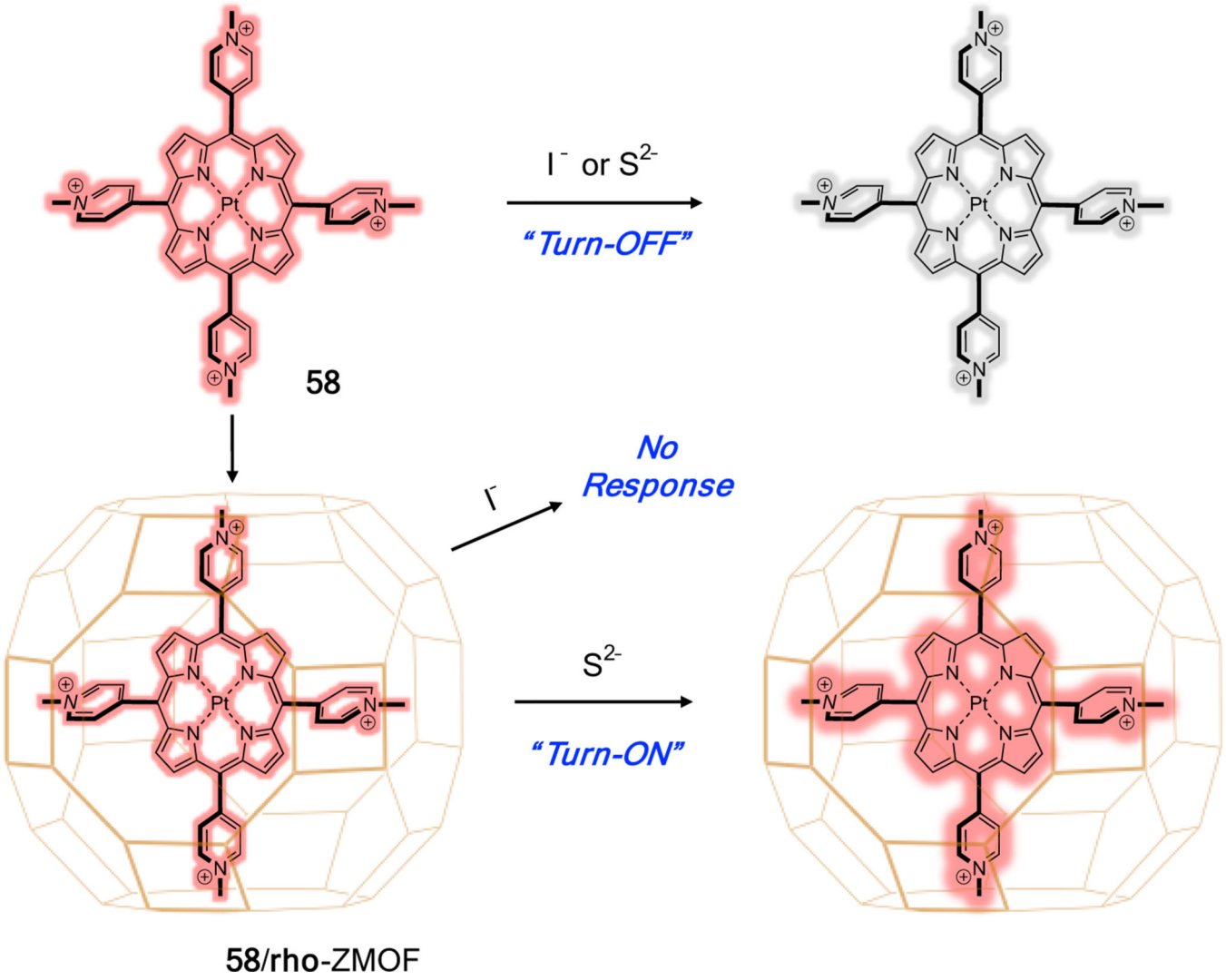

Figure 33:

Fluorescent "turn-off" anion sensor **58** and the associated MOF-based "turn-on" anion sensor **58**/**rho**-ZMOF. The anions were studied as their alkali metal (either Na^+ or K^+) salts.

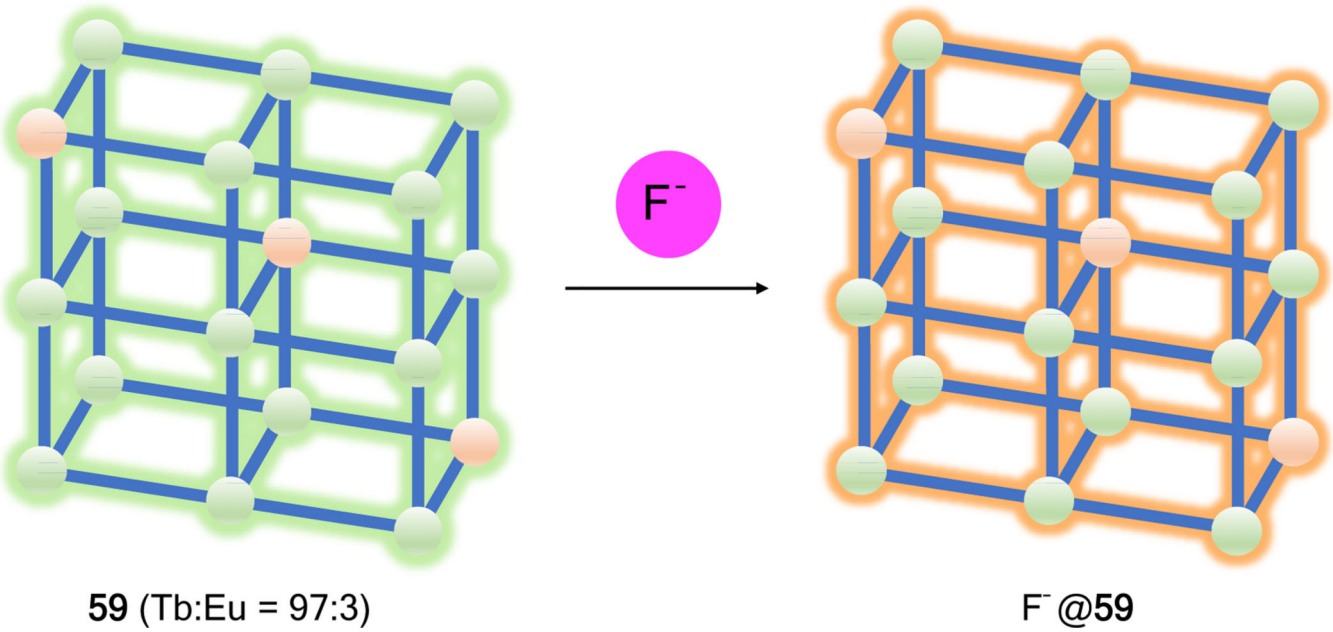

Figure 34:
MOF-based fluorescent sensor **59** for detecting fluoride.

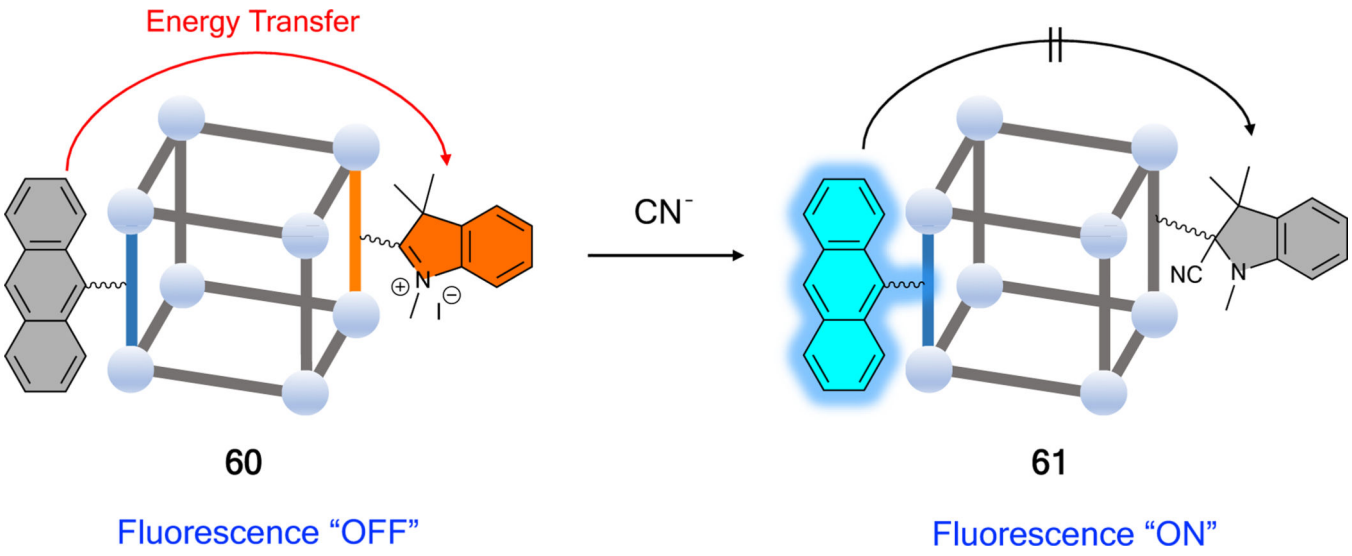

Figure 35.
Fluorescent “turn-on” cyanide sensor **60** based on a multicomponent MOF.

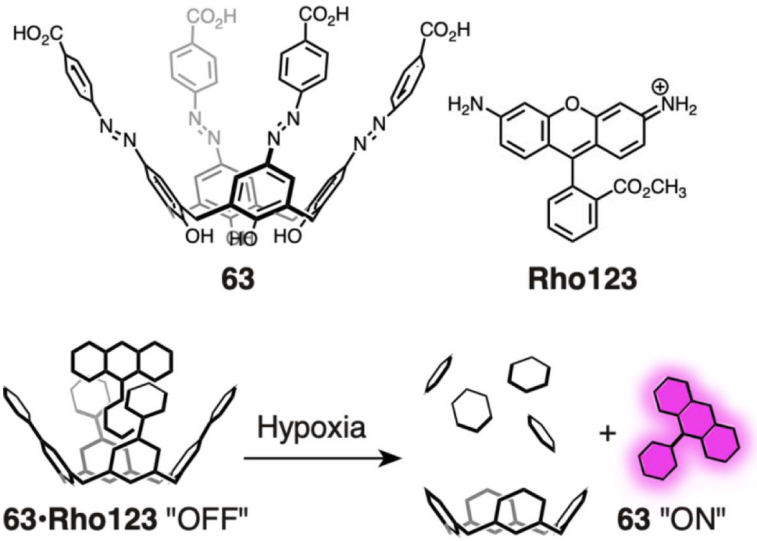

Figure 36.
A water-soluble calix[4]arene-based construct that allows for hypoxia-responsive sensing.

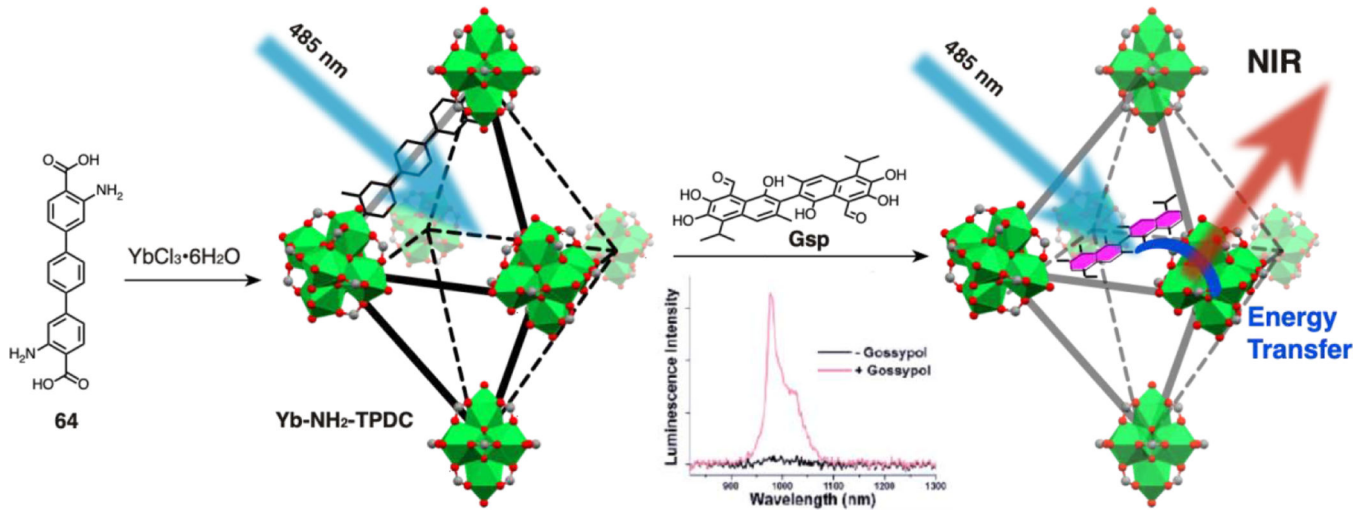

Figure 37.

MOF-based “turn-on” sensor for gossypol (**Gsp**). Reproduced with the permission from ref. 181. Copyright 2020 American Chemical Society.

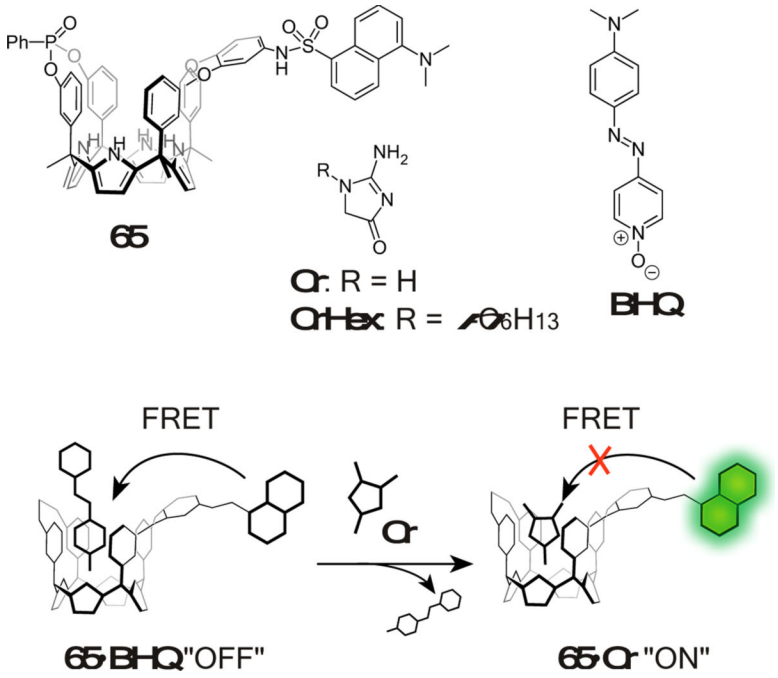

Figure 38.

Chemical structures and schematic representation of a calix[4]pyrrole-based “turn-on” sensor for creatinine.

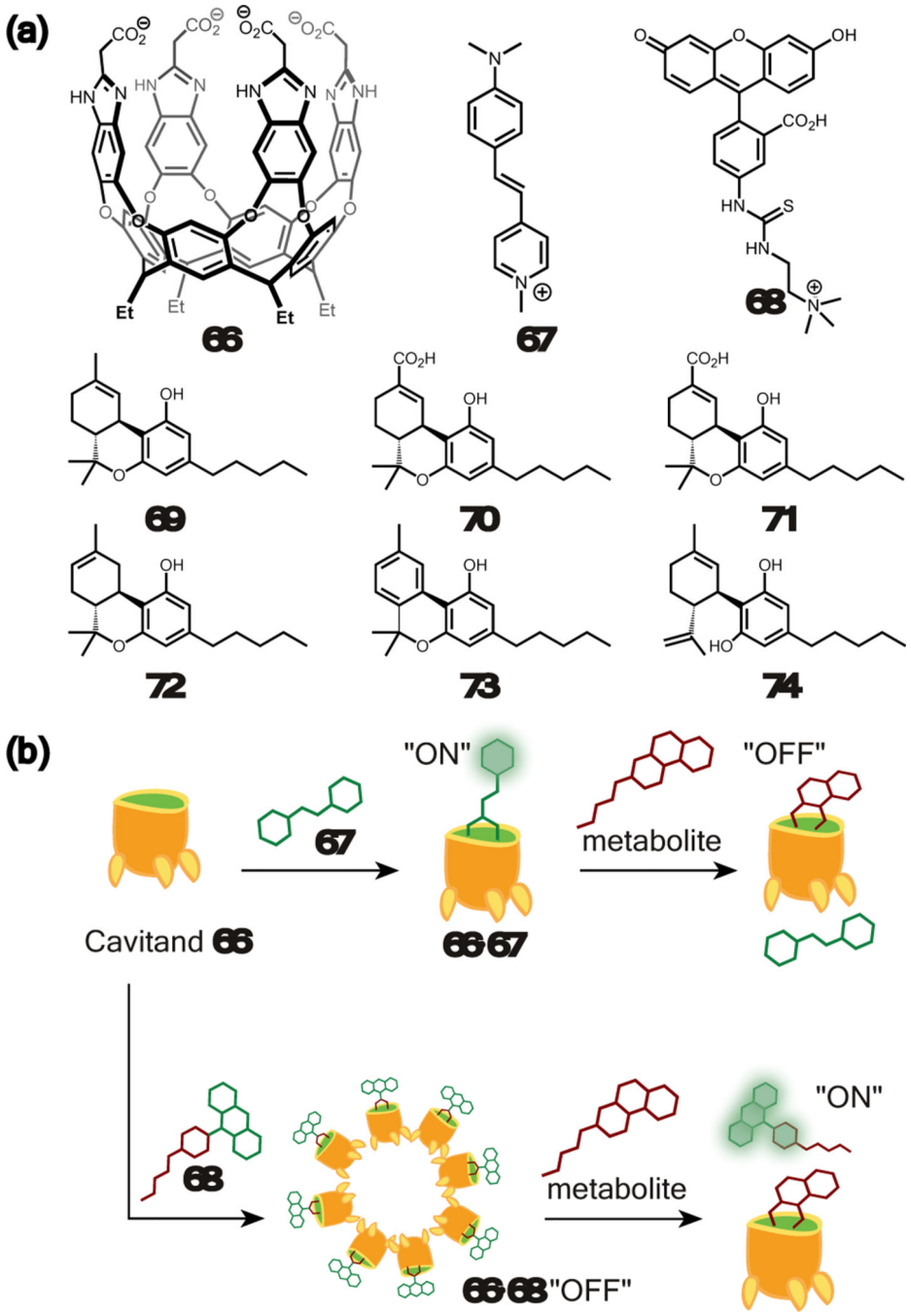

Figure 39.

(a) Chemical structures of the cavitand host **66**, fluorescent indicators **67** and **68**, and cannabinoids **69**–**74**. (b) Schematic representations of the mode of action proposed for the cavitand-based fluorescent sensor complexes **66·67** and **66·68** developed for cannabinoid detection.